PREPARATION OF ELECTROSPUN POLYVINYLIDENE FLUORIDE/NANOSILVER NANOFIBROUS MEMBRANE AND ITS ANTIMICROBIAL POTENTIAL

NORASIKIN BINTI AHMAD

FACULTY OF ENGINEERING
UNIVERSITY OF MALAYA
KUALA LUMPUR

2018

PREPARATION OF ELECTROSPUN POLYVINYLIDENE FLUORIDE/NANOSILVER NANOFIBROUS MEMBRANE AND ITS ANTIMICROBIAL POTENTIAL

NORASIKIN BINTI AHMAD

DISSERTATION SUBMITTED IN FULFILMENT OF THE REQUIREMENTS FOR THE DEGREE OF MASTER OF ENGINEERING SCIENCE

FACULTY OF ENGINEERING
UNIVERSITY OF MALAYA
KUALA LUMPUR

2018

UNIVERSITY OF MALAYA

ORIGINAL LITERARY WORK DECLARATION

Name of Candidate: Norasikin binti Ahmad

Matric No: KGA150017

Name of Degree: Master of Engineering Science

Title of Project Paper/Research Report/Dissertation/Thesis ("this Work"): Preparation of Electrospun Polyvinylidene Fluoride/Nanosilver Nanofibrous Membrane and Its Antimicrobial Potential

Field of Study: Advanced Materials

I do solemnly and sincerely declare that:

(1) I am the sole author/writer of this Work;
(2) This Work is original;
(3) Any use of any work in which copyright exists was done by way of fair dealing and for permitted purposes and any excerpt or extract from, or reference to or reproduction of any copyright work has been disclosed expressly and sufficiently and the title of the Work and its authorship have been acknowledged in this Work;
(4) I do not have any actual knowledge nor do I ought reasonably to know that the making of this work constitutes an infringement of any copyright work;
(5) I hereby assign all and every rights in the copyright to this Work to the University of Malaya ("UM"), who henceforth shall be owner of the copyright in this Work and that any reproduction or use in any form or by any means whatsoever is prohibited without the written consent of UM having been first had and obtained;
(6) I am fully aware that if in the course of making this Work I have infringed any copyright whether intentionally or otherwise, I may be subject to legal action or any other action as may be determined by UM.

Candidate's Signature Date:

Subscribed and solemnly declared before,

Witness's Signature Date:

Name:

Designation:

PREPARATION OF ELECTROSPUN POLYVINYLIDENE FLUORIDE/NANOSILVER NANOFIBROUS MEMBRANE AND ITS ANTIMICROBIAL POTENTIAL

ABSTRACT

In the current study, nanofibrous membrane (NFM) was produced through electrospinning and developed as a cost-effective membrane that able to improve the microbial quality of water, by removing *Escherichia coli* (*E. coli*), which is a type of fecal coliform bacteria, as well as fecal contamination indicator from the raw water. Electrospun NFM was prepared by incorporating as-synthesized nanosilver particles (NSPs) into polyvinylidene fluoride (PVDF). In phase I, an investigation was performed to obtain the smallest size of NSPs by varying precursor concentration (0.1 M, 0.5 M and 1.0 M) and reaction temperature (60 °C and 80 °C). At 60 °C, the size was increased as the precursor concentration increased from 0.1 M to 0.5 M. When the concentration further increased to 1.0 M, the size becomes smaller due to the fewer Ag^+ released upon the incomplete precursor reduction by the reducing agent. In contrast, at 80 °C, the size was gradually increased as the precursor concentration increases up to 1.0 M. In terms of controlled precursor concentration, the physical size and crystallite size become smaller as the temperature increases. In general, the hydrodynamic, physical and crystallite size of NSPs displayed similar trends. In this phase, S1T8 which have the smallest physical size and crystallite size was chosen to proceed to the next phase. The second phase was carried out to investigate the properties of electrospun PVDF/NSPs NFM. The morphological study revealed that the electrospun NFM form randomly oriented fibers, fewer beads as well as increasing average fiber diameter up to 311.2 nm when NSPs load increases from 0.5 wt% to 3.0 wt%. Through the elemental and microstructural study by energy dispersive spectrometer (EDS) and X-ray diffractometer (XRD), NSPs were detected in each membrane that verifies NSPs successfully incorporated into the

membrane. The XRD diffraction pattern exhibited that the PVDF crystalline phases kept constant after the incorporation of different NSPs loads, while, the NSPs crystallinity slightly changed which might due to the crystallite growth or increment of crystallinity degree. In nitrogen physisorption analysis, the electrospun NFM displayed type IV isotherm that proves they are the mesoporous membrane and has pore size range from 4.16 to 34.93 nm, which able to retain the bacteria cells from passing through the membrane. The last phase was related to the efficacy of electrospun NFM in removing *E. coli*. As a model of contaminated water, *E. coli* with standardized concentration was spiked into the sterile saline water and then was passed through the sterile electrospun NFM. The removal efficiency of the *E. coli* was determined by colony counts on the membrane. The colony counting results showed that the concentration of *E.coli* decreased as the NSPs loading increased. The highest *E. coli* removal effectiveness was achieved by a membrane that contains 3.0 wt% of NSPs. Leaching analysis by UV-vis spectrophotometer exposed the absence of the silver element in the filtrate which proves NSPs did not leach from the membrane. Overall, the electrospun PVDF/NSPs NFM capable to generate clean water, which is free from pathogens and also silver.

Keywords: *E. coli* removal, electrospun nanofibrous membrane, nanosilver particles.

PENYEDIAAN MEMBRAN NANOGENTIAN ELECTROSPUN POLYVINYLIDENE FLUORIDA/NANOARGENTUM DAN POTENSI ANTIMIKROB

ABSTRAK

Dalam kajian semasa, membran nanogentian dihasilkan melalui electrospinning dan dibangunkan sebagai membran efektif kos yang dapat memperbaiki kualiti mikrob air, dengan menyingkirkan *Escherichia coli* (*E. coli*), iaitu sejenis bakteria kolifom najis, serta penunjuk pencemaran najis dari air mentah. Elektrospun NFM telah disediakan dengan menggabungkan zarah nanoargentum yang disintesis (NSPs) ke dalam polyvinylidene fluorida (PVDF). Dalam fasa I, satu penyiasatan dilaksanakan bagi mendapatkan saiz NSPs yang paling kecil dengan mempelbagaikan kepekatan pelopor (0.1 M, 0.5 M dan 1.0 M) dan suhu tindak balas (60 °C dan 80 °C). Pada 60 °C, saiz meningkat apabila kepekatan pelopor meningkat dari 0.1 M ke 0.5 M. Apabila kepekatan terus meningkat kepada 1.0 M, saiz menjadi lebih kecil disebabkan kurang Ag^+ yang dibebaskan ke atas pengurangan pelopor yang tidak lengkap oleh agen pengurangan. Sebaliknya, pada 80 °C, saiz beransur-ansur meningkat apabila kepekatan pelopor meningkat sehingga 1.0 M. Dari segi kepekatan pelopor terkawal, saiz fizikal dan kristalit menjadi lebih kecil apabila suhu meningkat. Secara umum, saiz hidrodinamik, fizikal dan kristalit NSPs memaparkan trend yang sama. Dalam fasa ini, S1T8 yang mempunyai saiz fizikal dan saiz kristalit terkecil telah dipilih untuk meneruskan fasa berikutnya. Fasa kedua dijalankan untuk menyiasat sifat elektrospun PVDF/NSPs NFM. Kajian mofologikal menunjukkan bahawa elektrospun NFM membentuk gentian berorientasi secara rawak, sedikit manik serta purata garis pusat gentian meningkat sehingga 311.2 nm apabila muatan NSPs bertambah dari 0.5 wt% ke 3.0 wt%. Melalui kajian unsur dan mikrostruktur oleh spektrometer penyebaran tenaga (EDS) dan pembelau X-ray (XRD), NSPs telah dikesan dalam setiap membran yang mengesahkan NSPs berjaya dimasukkan

ke dalam membran. Corak belauan XRD menunjukkan bahawa fasa berhablur PVDF kekal selepas penggabungan beban NSPs yang berbeza, manakala, penghabluran NSPs berubah sedikit yang mungkin disebabkan oleh pertumbuhan kristalit atau kenaikan darjah penghabluran. Dalam analisis fizijerapan nitrogen, elektrospun NFM mempamerkan ciri isoterma IV yang membuktikan bahawa mereka adalah membran mesoporous dan mempunyai julat saiz liang dari 4.16 sehingga 34.93 nm, yang mampu menghalang sel-sel bakteria daripada melepasi membran. Fasa terakhir adalah berkaitan dengan keberkesanan elektrospun NFM dalam menyingkirkan *E. coli*. Sebagai model air tercemar, *E. coli* dengan keseragaman kepekatan disalurkan ke dalam air garam steril dan kemudian melalui elektrospun NFM steril. Keberkesanan penyingkiran *E. coli* ditentukan oleh pengiraan koloni di atas membran. Hasil pengiraan koloni menunjukkan bahawa kepekatan *E. coli* berkurangan apabila muatan NSPs semakin bertambah. Keberkesanan penyingkiran *E. coli* tertinggi dicapai oleh membran yang mengandungi 3 wt% NSPs. Analisis larut resap oleh spektrofotometer UV-vis mendedahkan ketiadaan unsur argentum dalam cecair turasan yang membuktikan NSPs tidak larut dari membran. Secara keseluruhan, elektrospun PVDF/NSPs NFM mampu menjana air bersih, yang bebas dari patogen dan argentum.

Kata kunci: penyingkiran *E. coli*, membrane nanogentian electrospun, zarah nanoargentum.

ACKNOWLEDGEMENTS

I would like to express my sincere gratitude for those who spare their time in helping and supporting me in various ways, directly and indirectly throughout the progression of this research.

Sincere indebtedness and gratitude are expressed to Assoc. Prof. Ir. Dr. Ang Bee Chin for her guidance, patience, understanding and most importantly, her endless support during my difficult time. I appreciate her generosity for giving me an opportunity to attend various conferences that expose me to the latest development in the engineering field and also a chance to build networks with other experts and academicians.

The deepest sense of my gratitude and respect towards Assoc. Prof. Dr. Amalina M. Afifi for her continuous advice, support, effort and precious time that been spent for me. My heartfelt appreciation goes to Dr. Bong Chui Wei and her team, especially Ms. Yvaine Thiang for their tremendous guidance, encouragement and valuable time that helps me a lot in understanding the microbiology field. I am extremely grateful for the input.

Special thanks go to Mr. Said, Mr. Zaharudin, Mrs. Pang Swee Ling, Mrs. Zubaidah, Mrs. Azura and other laboratory assistants for allowing me to use lab facilities and giving their cooperation and guidance during handling the equipment. For funding of my research, I would like to thank University of Malaya Postgraduate Research Fund, PPP Grant No. PG222-2015B.

Sincere and deepest gratitude also conveyed to my beloved family who always supports and encourages me from the beginning of my postgraduate life, and has faith and belief in me. I also would like to thank my colleagues for their great help, invaluable knowledge sharing, cooperation and continuous support during my hard time.

TABLE OF CONTENTS

LIST OF FIGURES

LIST OF TABLES

LIST OF SYMBOLS AND ABBREVIATIONS

°	:	Degree
°C	:	Degree Celsius
≈	:	Approximate
µl	:	Microliter
µm	:	Micrometer
Å	:	Angstrom
Ag	:	Silver
Ag^+	:	Silver ion
$AgNO_3$	:	Silver nitrate
Ag-$[PVP]^+$	:	Silver complex ion
Al	:	Aluminium
ATCC	:	American Type Culture Collection
$BaCl_2$	:	Barium chloride
BET	:	Brunauer-Emmett-Teller
BSA	:	Bovine Serum Albumin
C	:	Carbon
CFU/ml	:	Colony forming unit per milliliter
$C_6H_{12}O_6$	:	Glucose
cm	:	Centimeter
DC	:	Direct current
DLS	:	Dynamic light scattering
DMF	:	N,N-dimethylformamide
DNA	:	Deoxyribonucleic acid
E. coli	:	*Escherichia coli*

EDS	:	Energy-dispersive X-ray spectroscopy
etc	:	Etcetera
F	:	Fluoride
FESEM	:	Field emission scanning electron microscopy
FTIR	:	Fourier transform infrared
g	:	Gram
h	:	Hours
H^+	:	Hydrogen ions
Hc	:	Coercivity
$H\text{-}[PVP]^+$	:	Hydrogen complex ion
H_2O	:	Water
H_2SO_4	:	Sulphuric acid
JCPDS	:	Joint Committee on Powder Diffraction Standards
KBr	:	Potassium bromide
kV	:	Kilovolt
M	:	Molar
MAC	:	MacConkey
MB	:	Methylene blue
MDOE	:	Malaysia Department of Environment
mins	:	Minutes
ml	:	Milliliter
Ml/h	:	Milliliter per hour
Mr	:	Retentivity
Ms	:	Saturation magnetization
NA	:	Nutrient agar
NaCl	:	Sodium chloride

NaOH	:	Sodium hydroxide
NB	:	Nutrient Broth
NFM	:	Nanofibrous membrane
NIPS	:	Non-solvent induced phase separation
nm	:	Nanometer
NO_3^-	:	Nitrate ion
NSPs	:	Nanosilver particles
OH^-	:	Hydroxide ion
PVP	:	Polyvinyl pyrrolidone
PVDF	:	Polyvinylidene fluoride
PVDF/NSPs NFM	:	Polyvinylidene fluoride nanosilver nanofibrous membrane
RAS	:	Return activated sludge
RNA	:	Ribonucleic acid
ROS	:	Reactive oxygen species
rpm	:	Rotation per minutes
s	:	Seconds
SEM	:	Scanning emission microscopy
SER	:	Surface-enhanced Raman
SPR	:	Surface plasmon resonance
SRT	:	Solids retention time
TEM	:	Transmission electron microscopy
TIPS	:	Thermally induced phase separation
USFDA	:	The United States Food and Drug Administration
UV-vis	:	Ultraviolet visible
VSM	:	Vibrating-sample magnetometer
WAS	:	Waste activated sludge

wt%	:	Weight percentage
XRD	:	X-ray diffraction
Z*p*	:	Zetapotential

CHAPTER 1: INTRODUCTION

1.1 Background of the Study

Water, the most crucial substance for life on Earth, not only for human but also for other organisms such animals and plants to survive (Qu et al. 2013; Mohd Zainudin et al. 2018). The poor quality of water can cause the outbreaks of water-related diseases to a human being like diarrhea, cholera and gastroenteritis, which still a major cause of death in many parts of the world (WHO, 2013; Praveena et al. 2016). The World Health Organization (WHO) and the United Nations Children's Fund (UNICEF) (2017) reported that 844 million people lack a basic drinking water service, includes 159 million people who are dependent on surface water and globally, at least 2 billion people consumed fecally contaminated water. In emergency situations, a clean water is essential to save lives and consumption of contaminated water can lead to the tremendous risk to public health (Praveen et al. 2016). In order to reduce the water scarcity problem and demand for clean water, a proper approach needs to be developed for the water treatment.

Membrane technology is a competent strategy for water treatment due to its simplicity, cost-effective, high productivity, high removal capacity and easy scaling up (Zahid et al. 2018). Nowadays, polyvinylidene fluoride (PVDF) nanofibrous membrane widely used for water treatment due to its outstanding characteristics such as mechanical properties, chemical resistance, thermal stability and aging resistance (Sundaray, 2013; Kang & Cao, 2014; Moradi et al. 2016; Sheikh et al, 2016; Lalia et al. 2017; Obaid et al. 2017). Even though the membrane has unique properties, modification still needed to further enhance its performance. The common membrane modification for water treatment is by adding nanoparticles into the membrane (Tiwari et al. 2008; Qu et al. 2013; Esakkimuthu et al. 2014).

Silver nanoparticle is the most effective antimicrobial agent that extensively employed in water treatment due to its excellent properties such as high surface area to volume ratio, strong and broad spectrum of antimicrobial activities and low toxicity to humans and animals (Qu et al. 2013; Amin et al. 2014; Dizaj et al. 2014; Beyth et al. 2015; Praveena et al. 2016; Zhang et al. 2016). The antimicrobial effect of silver nanoparticles is size dependent, where the finer particles are more effective than the larger particles (Amin et al. 2014; Sarma, 2014; Beyth et al. 2015). The smaller silver nanoparticles able to release more silver ions during the filtration (Sarma, 2014) and allows better contact with microorganisms of bacteria and fungus (Zhang et al. 2016). Besides that, the effectiveness of silver nanoparticles depends on its aggregation state. The formation of aggregation may result in the loss of their antimicrobial ability (Zhang, 2013; Beyth et al. 2015).

1.2 Problem Statement of the Study

Numerous studies have been conducted on the application of nanoparticles in water treatment. Among the nanoparticles, silver is the most promising material due to its outstanding properties. However, the size-controlled and agglomeration of particles still a major issue because larger particles and agglomeration will reduce their antimicrobial ability.

Various research has been carried out to fabricate and investigate the antimicrobial properties of the silver-incorporated filter. However, an investigation of the capability of this filtration membrane in removing bacteria from various sources of water has not been fully explored. Besides that, even though the current fabricated membrane able to remove bacterial up to 100 % but the filtrate contains silver that leached from the membrane.

In this research, an evaluation was conducted on the performance of electrospun nanofibrous membrane as an antibacterial membrane in removing *E. coli* from various source of water. Silver nanoparticles were synthesized to obtain the smallest size prior to

the fabrication of electrospun nanofibrous membrane. The polyvinylidene fluoride (PVDF) nanofibrous membranes with a different weight percent of as-synthesized silver nanoparticles incorporation were fabricated using the electrospinning technique.

1.3 Objectives of the Study

The objectives of this study are:

i. To synthesis nanosilver particles (NSPs) by chemical reduction method and to study the influence of synthesis parameters on the size and formation of NSPs.
ii. To fabricate polyvinylidene fluoride/nanosilver nanofibrous membrane (PVDF/NSPs NFM) using the electrospinning process.
iii. To investigate the physicochemical and structural properties as well as *E. coli* removal efficacy of electrospun PVDF/NSPs NFM.

1.4 Scope of the Study

The ultimate goal of this study is to provide an alternative way of improving water quality especially microbial quality during emergency situations. To achieve this ultimate goal, this research is divided into 3 phases: a) Synthesis of nanosilver particles, b) Fabrication of electrospun PVDF/NSPs NFM and c) Investigate the effectiveness in removing *E. coli* (ATCC 25922) for PVDF/NSPs NFM.

In the first phase, NSPs was synthesized using a chemical approach called chemical reduction. Two important parameters were investigated which are silver nitrate concentration (0.1 M, 0.5 M and 1.0 M) and reaction temperature (60 °C and 80 °C). The effect of these synthesizing parameters was studied by a series of characterization using UV-vis, TEM, DLS, XRD, VSM and FTIR, and the smallest nanoparticles were chosen for the phase 2.

The second phase has mainly involved the fabrication and incorporation of various NSPs weight percent (0.5 wt%, 1.0 wt% and 3.0 wt%) into polymer via an electrospinning process. The main focus of this phase was to study the properties of the electrospun nanofibrous membrane which includes the physicochemical properties such as diameter size, pore size and elemental, and the structural properties such as morphology. All the properties contributed a great deal to the effectiveness of the membrane towards *E.coli* removal.

The final phase focused on the application of electrospun membrane in water purification. The capability of electrospun PVDF/NSPs NFM in eliminating *E. coli* was evaluated based on the number of viable *E. coli* on the NFM after the filtration process. Leaching test was performed to check the presence of NSPs in the filtrate after filtration process.

1.5 Outline of the Thesis

Chapter 1 briefly introduces water contaminants that cause the shortage of clean water, the technologies in treating the contaminated water and the advancement of current technology. Meanwhile, a short description of the research goals as well as a brief overview of the research will be discussed.

Chapter 2 presents the previous studies on the water contamination, water treatment technologies, improvement on the current technology as well as the incorporation of nanoparticles as filler into the membrane filtration.

Chapter 3 describes the list of raw material and the experimental work of the study including the synthesis and optimization of NSPs formation, the fabrication of electrospun PVDF/NSPs nanofibrous membrane and the removal of *E. coli*. A brief description of the characterization will be included in this chapter.

Chapter 4 presents the results and data interpretation from a series of characterization, analysis and observation that involved in this study. In phase 1, NSPs are characterized using UV-vis, TEM, DLS, XRD, VSM and FTIR. In phase 2, electrospun PVDF/NSPs NFM are analyzed using FESEM, EDS, XRD and BET. In phase 3, the NFM performance on *E. coli* removal is checked by the colony counting.

Chapter 5 provides a summary and conclusion of the research finding.

CHAPTER 2: LITERATURE REVIEW

2.1 Contamination of Water

Water, an essential element in life and a valuable natural resource for human activities from the simple household task to the very complex industrial and agricultural processes (Dhakras, 2011). However, in this century the world is facing a great problem which is the shortage of clean water and basic sanitation due to contamination that resulted from various sources.

2.1.1 Sources of Water Contamination

There are a number of possible sources resulting water contaminations and most of it results from human activities such as ocean dumping, atmospheric deposition, domestic, industrial and agricultural routines (Nasreen et al. 2013). The possible source of water contamination as illustrates in Figure 2.1.

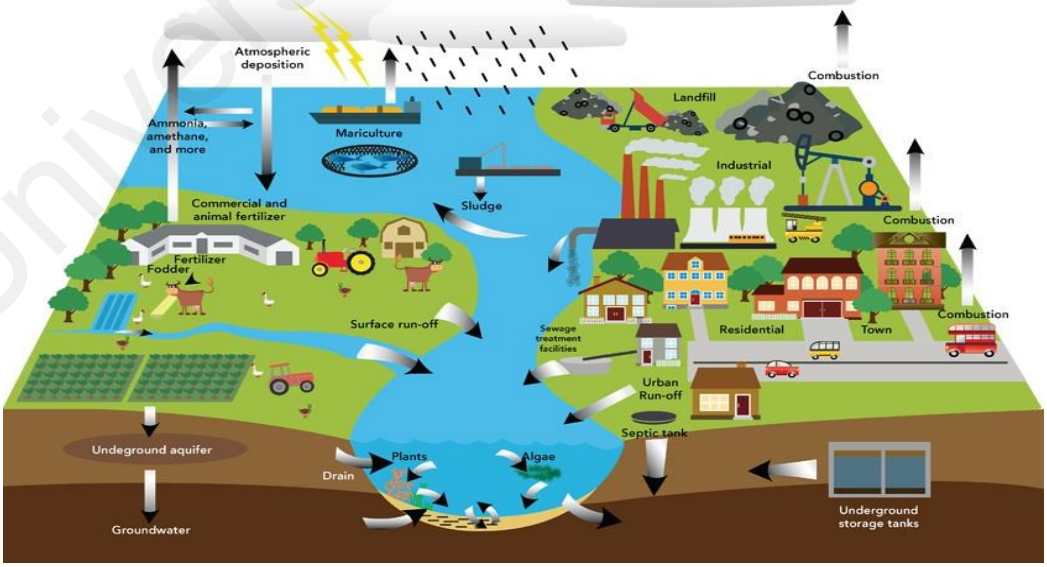

Figure 2.1: Possible source of water contamination (Internet reference, 20/8/2018)

In Malaysia, there are 5 major sources that contribute to water pollution, which is sewage treatment, piggery, manufacturing industries, wet market and agricultural industries (DOE, 2016). According to Malaysian environment quality report 2016, the discharge of waste from these sources into waterbodies caused the impaired beneficial use of water and hazardous to health, safety or welfare, animals, fishes as well as aquatic life.

2.1.2 Types of Water Contamination

2.1.2.1 Physical Contamination

Physical contamination refers to the contamination that affects the physical appearance and the physical properties of water. The issue related to the physical properties of water are color contamination, offensive odor and turbidity (Inamori & Fujimoto, 2009).

Color contamination is caused by dye pollution, soil particles and by the incidence of water bloom caused by eutrophication. The discharge of wastewater from textile dyeing industry into water sources can induce dye pollution because it is heavily polluted with dyes, textiles auxiliaries and chemical (Muralimohan et al. 2014). The soil particles normally enter water bodies during rain falls, where the rainwater carrying soil into water bodies and causes the water to become turbid due to the sediment (Inamori & Fujimoto, 2009). The occurrence of water bloom related to the algae species such as Cyanobacteria, Chlorophyceae, Bacillariophyceae and Flagellates. When these algae form a bloom, the water body is colored by their pigments.

Unpleasant odor and taste in drinking water is the common issue encountered by the residents. The earthy-musty odor is normally caused by the metals such as iron and copper due to the effects of corrosion problem (Burlingame et al. 2017). In addition, the bloom

of microorganisms such as Cyanobacteria, *Oscillatoria*, *Phormidium* and Actinomycetes *Streptomyces* (Inamori & Fujimoto, 2009; Sun et al. 2013; Lee et al. 2017) in water sources also produced an offensive odor.

Turbidity, the other element that affects the physical properties of water. A murky or cloudy appearance of water is due to the presence of solids residing inside the water. For instance, silt, clay, soluble colored organic and soluble fluorescent organic matter, inorganic materials, algae, plankton and other microscopic organisms. Turbidity is commonly used as an indicator to measure the quality of water based on its transparency and the total suspended solids (Lijesh & Malhotra, 2016). The more total suspended solids in water, the cloudier it seem, the more light scattered, therefore, the higher will be the turbidity.

2.1.2.2 Chemical Contamination

Chemical contaminants are the elements or compounds that may naturally occur or may derive from human-related activities, such as housework, agriculture, mining and industry (Barrett, 2014). Goel and Kaur (2012) revealed that powder detergent plays a major role in water contamination as compared to the liquid detergent. The composition of powder detergent that contains various chemical elements such as surfactants, builders, fillers, bleaches and anti-redeposition agent, can cause contamination, health problems and disturbing drainage system. Typical categories of this contaminants are heavy metals, inorganic compounds, agricultural chemicals and organic compounds (Inamori & Fujimoto, 2009).

Heavy metals include arsenic, mercury, cadmium and lead, and inorganic compounds such as nitrate and cyanide are extremely toxic and some of them are acutely toxic and carcinogenic (Inamori & Fujimoto, 2009). According to Fawell and Nieuwenhuijsen

(2003), an exposure to arsenic through drinking water brings an adverse effect to human health. For instance, cancers (skin, lung, bladder and liver), hyperkeratosis and peripheral vascular disease. Contamination by inorganic compound like nitrate in groundwater due to the enormous usage of chemical fertilizers, seepage of domestic wastewater into the ground and inappropriate control of waste material from animal husbandry can cause infants contract methemoglobinaemia (Fawell & Nieuwenhuijsen, 2003; Inamori & Fujimoto, 2009).

Agricultural chemicals are organic chemicals that extremely toxic and when human expose to them, they can suffer from internal and neurological diseases. Due to high solubility, agricultural chemicals contaminate the environment by seeping into the ground with rainwater, while those on the ground's surface can be transported into the river by rainwater. Organochlorine compounds are one of the substances in agricultural chemicals and it has been confirmed to be carcinogens through animal testing and is suspected of acting as carcinogens on the human body (Inamori & Fujimoto, 2009).

Organic chemicals especially dioxins have been reported to be teratogenic, carcinogenic and immunotoxic, and to have toxic effects in reproduction. Ninety-five percent of dioxins are produced by incineration plants and approximately half the dioxins discharged into the atmosphere fall to the ground with soot, in which they contaminate the soil and water bodies. They cause cancer and damage nervous and reproductive systems, kidney, stomach as well as liver. In general, chemical contaminations enter water through leaching, accidental spills, runoff and atmospheric deposition and will cause long-term effects.

2.1.2.3 Microbial Contamination

Microbial contamination is often linked to the water-related diseases, which still a major cause of death in the most regions of the world. Water-related diseases that normally connected to the microbial contamination are waterborne diseases, water-washed diseases, water-based diseases and water-related disease (Table 2.1). The presence of pathogenic organisms such as bacteria, cholera, helminths, scabies and typhoid are contaminating the water sources and spreading the water-related diseases, which lead to the death. There are many possible sources of microorganisms in water such as human and animal feces, domesticated animals and discharges of water treatment plants, decontamination stations, hospitals, industries, etc. (Jung et al. 2014).

Table 2.1: Water-related diseases (Gleick, 2002)

Diseases	Cause	Microorganisms
Waterborne	Ingestion of water contaminated by human or animal feces or urine containing pathogenic bacteria or viruses	▪ Cholera ▪ Typhoid ▪ Amoebic ▪ Bacillary dysentery
Water-washed	Poor personal hygiene and skin or eye contact with contaminated water	▪ Scabies ▪ Trachoma and flea ▪ Lice
Water-based	Parasites found in intermediate organisms living in the contaminated water	▪ Dracunculiasis ▪ Schitosomiasis ▪ Helminths
Water-related	Insect vectors	▪ Dengue ▪ Malaria ▪ Trypanosomiasis

Fecal contamination of water, a typical microbial pollution that correlates with the outbreak of numerous diseases and can risk the consumer health. The assessment of fecal pollution depends on the indicator bacteria like *Escherichia coli* (*E. coli*), coliforms and *Pseudomonas aeruginosa* (Praveena et al. 2016). The national water quality standards for Malaysia and World Health Organization (WHO) have used total coliform and *E. coli* as

the main indicator to monitor the quality of water as their presence in water directly related to the fecal contamination. A total coliform is a group of different types of bacteria that typically found in the environment, including soil, vegetation, untreated surface water and human or animal waste. While, *E. coli* is a subgroup of fecal coliform which exist in great quantities in the human and warm-blooded animal intestines (Varkey, 2010) and can enter water bodies from human and animal wastes (Hamzah & Hattasrul, 2007).

E. coli is considered as a more specific indicator of fecal contamination than fecal coliforms due to the detection of the thermotolerant non-fecal coliform bacteria by the general test for fecal coliforms (Odonkor & Ampofo, 2013). The detection of *E. coli* in water does not indicate directly the presence of pathogenic microorganisms, but it may indicate a greater risk of the occurrence of fecal contamination and the presence of other fecal-borne bacteria and viruses that could be even more pathogenic to human and both domestic and wild animals (Sousa, 2006; Odonkor & Ampofo, 2013). The concentration or level of *E. coli* plays a major role in the sanitary and safety of water for the consumption. Table 2.2 outlines the acceptable value of *E. coli* concentration in water based on the purpose of water consumption.

Table 2.2: Malaysia water quality standard (DOE, 2016)

Purpose	**Acceptable limit (CFU/100ml)**
Drinking water	Must be not detected
Preservation, Marine Protected Areas, Marine Parks	70
Marine Life, Fisheries, Coral Reefs, Recreational and Mariculture	100
Ports, Oil & Gas Fields	200
Mangroves Estuarine & River-mouth Water	100

E. coli is a gram negative rod shaped bacteria that have dimension approximately 0.25 – 1 µm in diameter and 2 µm long (Figure 2.2), with a cell volume of 0.6 – 0.7 µm and commonly found in the intestine of warm-blooded organisms (endotherms). Most of *E. coli* strains are harmless, which are part of the normal flora of the gastrointestinal tract of human and animals. These strains can benefit their host by producing vitamin K2 or by preventing the establishment of pathogenic bacteria within the intestine (Lim et al. 2010; Odonkor & Ampofo, 2013). At the same time, there are some *E.coli* strains which are pathogenic and can cause serious food poisoning in humans. The harmless *E. coli* can transform into deadly bacteria through evolution that involves mutation and horizontal transfer. According to Johnson (2002), mutation involves the sporadic introduction of single-nucleotide substitutions or deletions of various sizes throughout the genome. While, horizontal transfer involves the en bloc exchange of substantial amounts of DNA between different *E. coli* lineages or between another species and *E. coli*. The combination of mutation and horizontal transfer has shaped the overall phylogenetic structure of *E. coli*. In addition, some strains evolved the ability to cause disease in healthy individuals in their own right (Grande, 2015). The more virulent strains cause serious illness or death in the elderly, the very young or the immunocompromised (Odonkor & Ampofo, 2013).

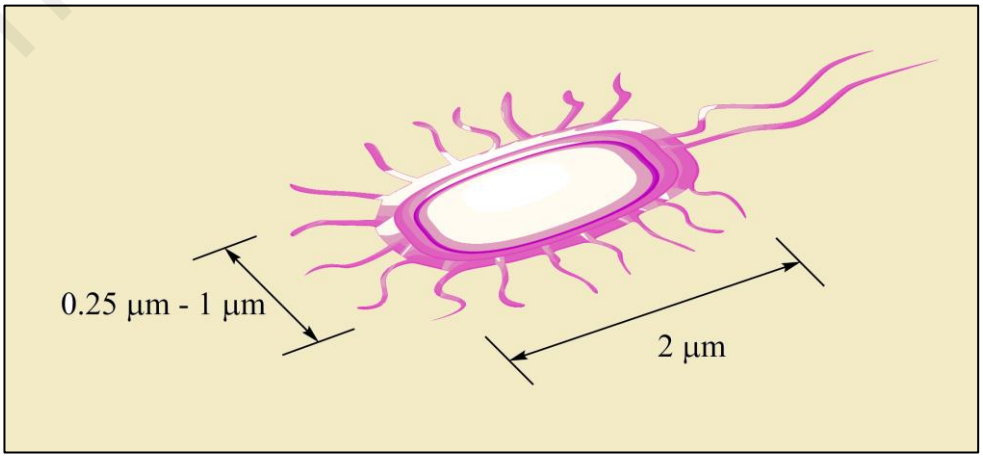

Figure 2.2: *Escherichia coli* cell

2.2 Water Treatment Technologies

Water treatment is a process of making waster suitable for its application or returning its natural state (Internet reference, 7/12/2017). All water treatments involve the removal of bacteria, solids, inorganic compounds, organic compounds and algae. Water treatment technologies can be divided into 3 main categories; physical method, chemical treatment and biological method.

2.2.1 Physical Method

The physical method typically consists of filtration techniques that involve the use of screens, sand filtration and filtration membrane (Internet reference, 7/12/2017). Screens typically used to remove larger suspended materials and sand filtration commonly used to filter suspended solids, however, smaller suspended solids and dissolved solids are often able to pass through these filters. While, membrane filtration a thin layer of semi-permeable material, which is used to separate unwanted constituents up to a certain size, shape and character from the fluid. The effectivity of membrane are determined through selectivity (retention or separation factor) and productivity (flux) of the membrane which refers to the surface properties of membrane that discriminates the type of species that can pass through and the rate at which species are transported across the membrane, respectively (Gopal et al. 2006).

2.2.2 Chemical Treatment

Chemical treatment in water treatment involves chlorination and ozonation. In another word, a chemical treatment known as disinfection process. According to Templeton and Butler (2011), chlorination involves the addition of an adequate amount of chlorine gas or sodium hypochlorite solution into the wastewater in order to overcome the chlorine

demand of the wastewater and then allowing the chlorine residual to remain in contact with the water for a certain period in a chlorine contact tank. Elimination of residual chlorine normally occurs in the de-chlorination step prior to discharge of the effluent, to prevent chlorine release into the aquatic environment. Even though chlorination is effective on a large scale, but it becomes expensive for smaller towns and villages (Boutilier et al. 2014) and it forms toxic chemical by-products due to the reaction of the chlorine with the organic compounds in the wastewater (Templeton & Butler, 2011). Ozonation is the transforming process of oxygen into ozone, which carried out by corona discharge or by ultraviolet radiation. In water treatment application, an ozone generator combined with a compact air preparation unit and a venture injector, in order to transfer the ozone into the water safely. A schematic diagram of an ozonation process setup is shown in Figure 2.3. Ozone able to remove water contaminants due to its properties in which it is very effective in disinfecting bacteria and viruses. Besides that, ozone can reduce the concentration of iron, manganese and sulfur in water to form insoluble metal oxides or elemental sulfur.

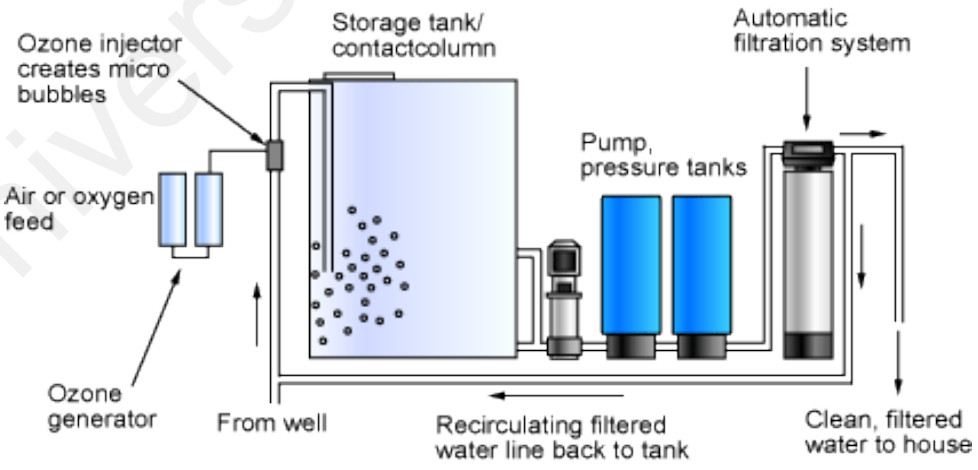

Figure 2.3: Ozonation process setup in water treatment application (Internet reference, 20/8/2018)

2.2.3 Biological Treatment

Biological treatment is actually a secondary treatment in water treatment technologies that using aerobic activated sludge process (Mittal, 2013). Activated sludge process is a process where microorganisms are used to consume the organic contaminants in the pre-treated sewage. The microorganism involved in the activated sludge are mainly bacteria (≈ 95%) and organisms such as protozoa, rotifiers and invertebrate (5%). In general, activated sludge consists of three main components which are aeration tank, clarifier tank and return activated sludge (RAS) or waste activated sludge (WAS) equipment. In this process, the pre-treated sewage is delivered into an aeration tank at which it is mixed with anaerobic microorganisms. After a specific time, the mixed liquor flows into the clarifier tank, where the sludge is allowed to settle. The liquid that discharged from the process is known as treated effluent and the resulting settled activated sludge is recirculated to the aeration tank called as return sludge or removed from the system as excess (waste sludge).

2.2.4 Comparison between Water Treatment Technologies

Table 2.3 shows the advantages and disadvantages of the water treatment technologies. Physical treatment is the best choice to treat contaminated water due to its capability to separate suspended solids from larger solids to the smallest element such as mineral ions. The nanofibrous membrane is a type of filtration membrane that categorized as physical treatment gain much attention due to the high surface area to volume ratio, large porosity, good mechanical properties and good water permeability which provides a major contribution towards water filtration.

Table 2.3: Summary of advantage and disadvantage of water treatment technologies

Treatment	Advantage	Disadvantage
Physical	▪ Cost effective (Gopal et al. 2006) ▪ Good water permeability (Nasreen et al. 2013) ▪ Flexible design (Qu et al. 2013) ▪ Good mechanical properties (Nasreen et al. 2013)	▪ Membrane fouling (Deegan et al. 2011; Luo et al. 2014) ▪ Not fully effective in removing organic contaminants as pore sizes vary from 100 to 1000 times larger than the micropollutants (Deegan et al. 2011; Luo et al. 2014; Ahmed et al. 2017)
Chemical	▪ Effective on large scale (Boutilier et al. 2014) ▪ Reduced turbidity arising from suspended particles (Ahmed et al. 2017)	▪ Expensive (Boutilier et al. 2014) ▪ Forms of toxic chemical by-product (Templeton & Butler, 2011)
Biological	▪ Cost effective (Sreekanth et al. 2009; Luo et al. 2014) ▪ Environmental friendly (Deegan et al. 2011; Luo et al. 2014) ▪ A wide range of organic contaminants removal (Ahmed et al. 2017)	▪ Regeneration and disposal issues of high sludge (Deegan et al. 2011; Luo et al. 2014) ▪ A large amount of sludge contains organic contaminants (Luo et al. 2014; Ahmed et al. 2017)

2.3 Advancement of Membrane Technology in Water Treatment

The current development in water treatment system is the application of nanotechnologies like nanoparticles and nanomembrane. Nanotechnology, the intentional manipulation of materials at size scales of less than 100 nm (Tiwari et al. 2008; Qu et al. 2013). Application of nanofibrous membrane in water treatment not only effective in separating solids or particles but it also efficient for the removal of contaminants such as microbial and heavy metals, depending on the selectivity of nanoparticles.

2.3.1 Electrospun Nanofibrous Membrane

In the filtration applications, the nanofibrous membrane normally has a large surface area to volume ratio, high porosity, small pore size to trap tiny particles, turnable morphology and interconnected pore structure (Ahmed et al. 2014; Dong et al. 2014; Huang et al. 2016; Sheikh et al. 2016; Obaid et al, 2017) . These nanofibrous membranes are commonly fabricated through a simple, versatile and low-cost technique called electrospinning (Sundaray et al. 2013; Ahmed et al. 2014; Kang & Kang, 2016; Sheikh et al. 2016; Obaid et al. 2017). This process involves a set of syringe and needle filled with a polymer solution, a syringe pump, a DC voltage supply in the kV range and a collector. Figure 2.4 shows the setup of electrospinning process in the laboratory. In electrospinning, a high voltage is applied to a syringe filled with the polymer solution that is held at the needle of the syringe via surface tension. The voltage is applied gradually and a Taylor cone forms when the hemispherical surface of the solution at the needle tip elongates. As the voltage increases and reaches a critical value where the repulsive force overcomes the surface tension, a charged jet of solution is discharged from the cone tip. The discharged polymer solution undergoes an instability and elongation process, which allows the jet to become very long, uniform and thin fibers (Nasreen et al. 2013).

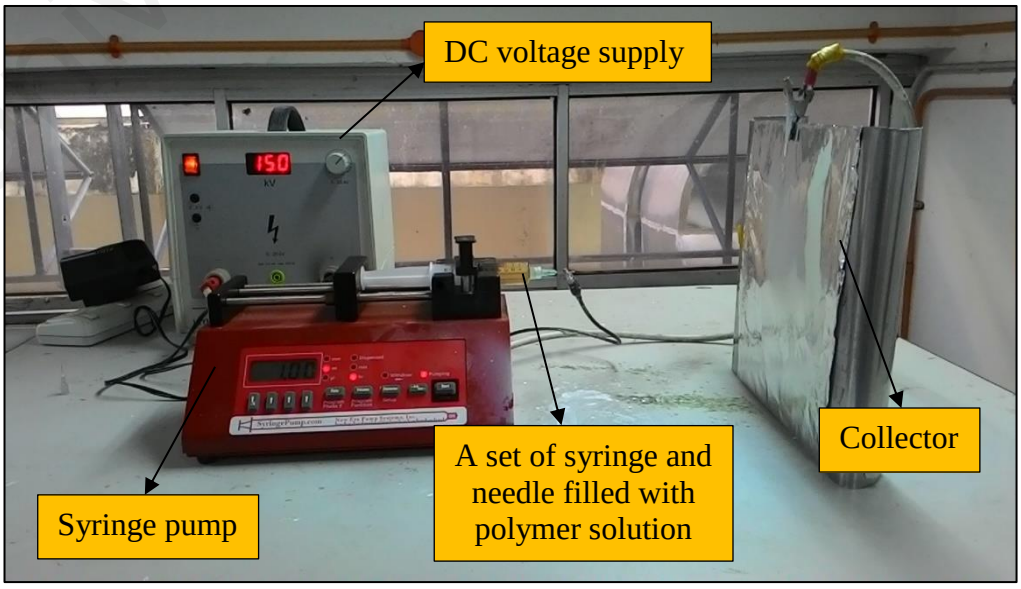

Figure 2.4: Electrospinning set up

During fabrication of electrospun nanofibrous membrane, several important parameters must be considered such as solution parameters (polymer concentration, molecular weight of polymer, viscosity, surface tension and conductivity density), processing parameters (voltage, flow rate, collectors and distance between needle tip to collector) and ambient parameters (humidity and temperature) in order to produce electrospun nanofibrous membrane with desired properties. Basically, all the mentioned parameters can influence the properties and performance of electrospun nanofibrous membrane and it is possible to produce nanofibers with different morphology, pore size, thickness and etc. by varying these parameters (Kwankhao, 2013). The increase of polymer solution viscosity, applied voltage, flow rate and humidity will produce smooth fibers with large diameter size. While, a small fibers diameter can be obtained when the polymer solution conductivity and working distance (needle to collector distance) increases. If the rate of evaporation of solvents higher, there will be a higher number of beaded fibers as well as the number of beads. The influences of parameters in the electrospinning process on the fiber morphology are summarized in Table 2.4.

Table 2.4: Influences of parameters in electrospinning process on the fiber morphology (Kwankhao, 2013)

Parameter	Effect on fiber morphology	Reference
Viscosity increase	▪ Fiber diameter increase ▪ Smooth fibers	▪ Fong et al. 1999 ▪ Megelski et al. 2002 ▪ Mit-uppatham et al. 2004 ▪ Li et al. 2006 ▪ Tan & Obendorf, 2007 ▪ Nakata et al. 2007 ▪ Yao et al. 2008
Surface tension increase	▪ Number of beaded fibers increase ▪ Number of beads increase	▪ Fong et al. 1999
Solution conductivity increase	▪ Fibers diameter decrease	▪ Fong et al. 1999 ▪ Megelski et al. 2002 ▪ Zong et al. 2002 ▪ Zeng et al. 2003
Evaporation of solvents increase	▪ Pores on fiber surfaces	▪ Megelski et al. 2002
Applied voltage increase	▪ Fiber diameter increase	▪ Megelski et al. 2002 ▪ Zong et al. 2002
Needle to collector distance increase	▪ Fiber diameter decrease ▪ Smooth fibers	▪ Megelski et al. 2002
Humidity increase	▪ Fiber diameter increase	▪ Wang et al. 2006 ▪ Tang et al. 2009
Flow rate increase	▪ Fiber diameter increase	▪ Megelski et al. 2002 ▪ Zong et al. 2002 ▪ Nakata et al. 2007

2.3.1.1 Polymeric Nanofibrous Membrane

There are several materials usually employed to fabricate polymeric nanofibrous membrane such as polyamine (PA), polyamide (PI), poly(ether sulfone) (PES), polysulfone (PSF), polyacrylonitrile (PAN), polyvinylidene fluoride (PVDF), polytetrafluoroethylene (PTFE), polypropylene (PP) (Dong et al. 2014; Heydari Beni, 2014; Kang & Cao, 2014), polyvinyl alcohol (PVA), polyvinyl chloride (PVC),

polyethylene (PE), cellulose acetate (CA) and chitosan (Zahid et al. 2018). According to Park (2005), the electrospinning of polymeric membrane usually involves two phases. In the first phase, a polymer jet formed on the needle and is accelerated and stretched smoothly by electrostatic forces. In the second stage, a bending instability occurs further downstream when the jet gets sufficiently thin and fiber spirals vigorously. Polymeric nanofibrous membrane is typically cost-effective, flexible, good film-forming property, good mechanical strength, high perm-selectivity, chemically stable and widely used in the water industry (Lai et al. 2014; Zahid et al. 2018)

2.3.1.2 Inorganic Nanofibrous Membrane

The majority of the inorganic membranes are made up of ceramics or metals oxide such as alumina, titania, zirconia, silica, zeolites, silicon carbide and microporous carbon (Park, 2005; Heydari Beni, 2014; Lai et al. 2014; Baji & Mai, 2017; Warsinger et al. 2018; Zahid et al. 2018). Ceramic or inorganic membrane normally combined with the polymeric membrane to accomplish the desired filtration mode and achievement and to carry out microfiltration and ultrafiltration (Lai et al. 2014; Warsinger et al. 2018). The first ceramic membranes were produced in 2002 by using electrospinning. The electrospinning of ceramic membranes is slightly different from the polymeric membranes, which includes the preparation of electrospinning solution, the electrospinning of the prepared inorganic fibers and the calcination of the composite fibers (Park, 2005). Ceramic membranes reportedly have excellent thermal stability and chemical resistance than the polymeric membrane, where they can be cleaned at high temperatures with strong acids and bases to recover the permeated flux of the fouled ceramic membrane (Heydari Beni, 2014; Lai et al. 2014). Besides that, they displayed high structural and mechanical strength (Zahid et al. 2018). However, ceramic

membranes are expensive, mostly have larger pores and less permeable, as compared to the polymeric membranes.

2.3.1.3 Consideration of PVDF as Membrane Material

PVDF, a fluoropolymer consisting of $-CF_2-CH_2-$ monomer units is a semi-crystalline polymer that shows four different crystal phases known as α, β, γ and δ at different processing conditions (Costa et al. 2010; Liu et al. 2011; Liu et al. 2013; Wang et al. 2014; Tarasova et al. 2015). It has been extensively exploited in membrane applications due to its outstanding properties such as thermal stability, chemical resistance and mechanical properties (Sundaray, 2013; Kang & Cao, 2014; Moradi et al. 2016; Sheikh et al, 2016; Lalia et al. 2017; Obaid et al. 2017). The thermal stability of PVDF is basically depended on the electronegativity of fluorine atoms and the C–F bond dissociation energy, where the high electronegativity of fluorine atoms on the chain and the high bond dissociation energy of C–F bond provide the high stability of PVDF (Liu et al. 2011). Benzinger et al. (1980) reported that PVDF demonstrates excellent resistance to the high concentration of strong oxidants and long-term stability in mineral acids and in dilute alkaline solutions. This proves that PVDF has good resistance towards harsh chemicals including acids, oxidants, halogens and alkaline (Rabuni et al. 2013). Mechanical properties of PVDF are mainly depended on the crystallinity of the polymer, where the high percentage of α phase crystallites contributes to the excellent mechanical properties and this crystallization can be controlled by various parameters such as molecular weight, molecular distribution, polymerization method, thermal history and cooling rates (Liu et al. 2011; Liu et al, 2013).

2.3.2 Incorporation of Nanomaterial as Antimicrobial Agent

A significant number of studies have been carried out on the application of nanomaterials into polymeric or inorganic membranes in order to improve the membrane performance. Several nanomaterials have received great attention due to their potential for water and wastewater treatment such as metal nanoparticles and metal oxide nanoparticles and photocatalytic nanoparticles.

2.3.2.1 Metal Nanoparticles

Metal nanoparticles such as silver and copper, play an important role in removing the contamination because of its unique properties such as small particle size and larger specific surface area (surface/volume). These metal nanoparticles have improved the capability of membranes to disinfect waterborne disease-causing microbes. According to Amin et al. (2014), they possess antibacterial properties due to their charge capacity. The mechanisms of antimicrobial activity of these metal nanoparticles are illustrated in Figure 2.5. In general, the antimicrobial activities of nanoparticles depends on two main factors which are physicochemical properties of nanoparticles and the bacterial species. Nanoparticles and ions can form free radical which resulting in the production of reactive oxygen species (ROS). These ROS destroy the bacteria cell by disrupting the cell membrane and by damaging the mitochondria, DNA and RNA (Hajipour et al. 2012).

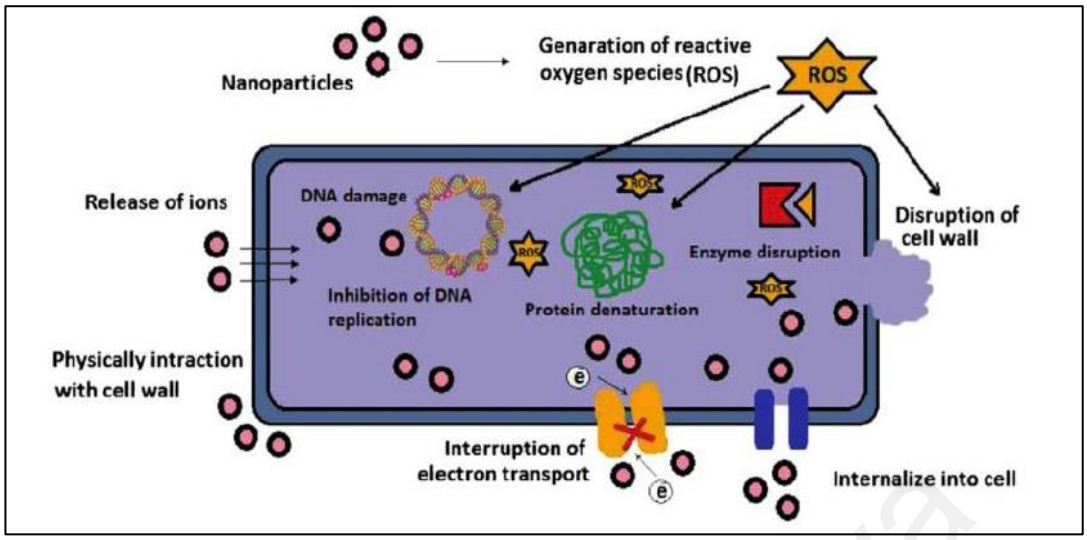

Figure 2.5: Mechanisms of antimicrobial activity of the metal nanoparticles (Dizaj et al. 2014)

Nanosilver has been incorporated into polysulfone (Zodrow et al. 2009; Mollahosseini et al. 2012; Koseoglu-Imer et al. 2013), polyvinylidene fluoride (Li et al. 2011) and polyvinyl alcohol (Sarma, 2014). Ultrafiltration polysulfone membrane with improved bio-fouling and antiviral properties was successfully fabricated by incorporating nanosilver particles (Zodrow et al. 2009). The fabricated membranes exhibited antimicrobial properties towards a variety of bacteria such as *E.coli* K12, *Pseudomonas Mendocina* KR1, and MS2 bacteriophage. Besides that, incorporation of nanosilver increased membrane hydrophilicity, reducing the potential for other types of membrane fouling. Mollahosseini et al. (2013) have fabricated a polysulfone ultrafiltration membrane with the addition of different size of nanosilver particles. From their studies, the incorporation of smaller size of nanosilver (30 nm) have produced membrane with better antibacterial performance, smoother surfaces, high hydrophilic surface, high flux of pure water and bovine serum albumin protein (BSA) solution and high rejection of BSA as compared to membrane that produced with incorporation of large nanosilver particles (70 nm).

Copper, the other nanoparticle that gains attention in the modification of filtration membrane due to their unique biological, chemical and physical properties, antimicrobial

activities as well as the low cost of preparation (Dizaj et al. 2014). According to Varkey (2010), copper has the faster reaction rates in destroying the coliforms as compared to the metals nanoparticles from another group. He observed the reaction rate depends on the surface area, where the larger area can eliminate the bacteria in a shorter time, and he concluded that copper could eliminate total coliform and *E. coli* completely (100 %) within a few hours. Sheikh et al. (2011), who fabricate polyurethane membrane with the addition of copper nanoparticles using electrospinning, found a well oriented and smooth nanofibers can be produced through electrospinning and the pure copper particles are evenly dispersed on the membrane surface. They obtained the highest diameter for the zone of inhibition when there is the highest copper content on the membrane. The zone of inhibition is clearer in the case of *E. coli* than *B. subtilis*, which concluded that the obtained nanofibers can be used as an antimicrobial membrane.

2.3.2.2 Metal Oxide Nanoparticles

Metal oxide nanoparticles have a great potential in pressure-driven membranes because they can degrade both biological and chemical contaminants, and enhance the physical properties of the membranes by increasing the hydrophilicity, leading to reducing of biofouling. According to Tiwari et al. (2008), zinc oxide nanoparticles able to remove arsenic from water, even though bulk zinc oxide cannot absorb arsenic. At the same time, zinc oxide nanorods could effectively degrade dyes such as methylene blue and methyl orange as chemical test contaminants and for the inactivation of Gram negative and Gram-positive bacteria as biological test contaminations (Baruah et al. 2012). The influence of nanosized zinc oxide on the performance of PVDF microfiltration membranes was studied by Hong and He (2012) and they revealed that the fabricated membrane showed better membrane hydrophilicity, mechanical and thermal stability with the addition of nanosized zinc oxide.

2.3.2.3 Photocatalytic Nanoparticles

Photocatalytic nanoparticle incorporated membranes which also known as reactive membranes combine their physical separation function and the reactivity of a catalyst toward contaminant degradation (Qu et al. 2013). Titanium dioxide is the common material related to the photocatalytic nanoparticles. The photocatalytic properties of titanium dioxide help them to decompose organic chemicals as well as kill bacteria (Ng et al. 2013). Loeb et al. (2015) have compared the performance of different configuration of titanium dioxide coated foam support as photocatalytic in an enhanced disinfection system for drinking water treatment. The performance was evaluated using the reduction of methylene blue (MB) as a probe compound, 1,4-dioxane as a common environmental pollutant and *E.coli* as an indicator of biological contaminants. They found that the reactors with immobilized catalysts were able to match out or surpass the performance of a suspension configuration due to effective mass transport and association between the analyte and the foam.

2.4 Nanosilver Particles (NSPs)

Nanosilver particles are defined as fine particles that have at least one dimension less than 100 nm. Nanosilver is not a new discovery, in which it has been known for over 100 years (USFDA, 2010; Varner et al. 2010). Nanosilver has unique properties which mainly attributed to the high surface area to volume ratio, leading many industrial sectors (Varner et al. 2010).

2.4.1 Synthesis Methods

Recently, there are various methods have been discovered to synthesis silver nanoparticles. Different kinds of approaches have been studied and applied to produce silver nanoparticles such as chemical, physical and biological approaches. The general

idea to synthesize silver nanoparticles through chemical or biological approaches is by reduction of silver ions in aqueous or non-aqueous solution by different reducing agents. Whereas, by the physical approach, silver particles can be size-reduced to nanoscale by arc-discharge, milling and other physical approaches. The most frequent synthesis method in chemical and biological approaches is chemical reduction and fungal-based synthesis, respectively.

2.4.1.1 Chemical Reduction

Generally, chemical reduction method involved the reduction of metal precursor with a reducing agent in the present/absence of the stabilizing agent. A reducing agent which can be classified into different categories whether strong, medium and weak, is used to reduce the silver ions in aqueous or non-aqueous solutions (Iravani et al. 2014). Meanwhile, the stabilizer is used to obtain stable, monodispersed nanoparticles and to protect the particles from aggregation (Malina et al. 2012). Even though this method is simple, great care must be exercised to produce a stable and reproducible colloid (Bell & Myrick, 2001; Šileikaitė et al. 2006; Amany et al. 2012) and numerous parameters need to be considered because they will influence the properties of nanoparticles particularly particles size. For instance, chemicals used (reducer, stabilizer and accelerator) and reaction conditions (metal salt concentration, temperature, reaction time, etc.).

2.4.1.2 Arc-discharge

Arc-discharge, a physical method for synthesis of nanoparticles that involves a DC system (Figure 2.6) which consist of four main parts; i) two electrodes, ii) a servo control system that maintains a constant distance between the electrodes, iii) a power supply system that controls the DC arc-discharge parameters, iv) a glass tank containing the deionized water with an electrode holder to collect the colloidal. Tien et al. (2008) have

developed a novel method for synthesis of silver nanoparticles by using a DC arc discharge system. Without any usage of surfactants or stabilizers, the silver suspension can be produced in pure water. In their experiments, they have utilized silver wires as positive and negative electrodes and etched in pure water. During the discharge, the surface layer of the silver wires was evaporated and condensed in the water, thus, stable, round in shape and well-dispersed silver nanoparticles of 20-30 nm in size were obtained.

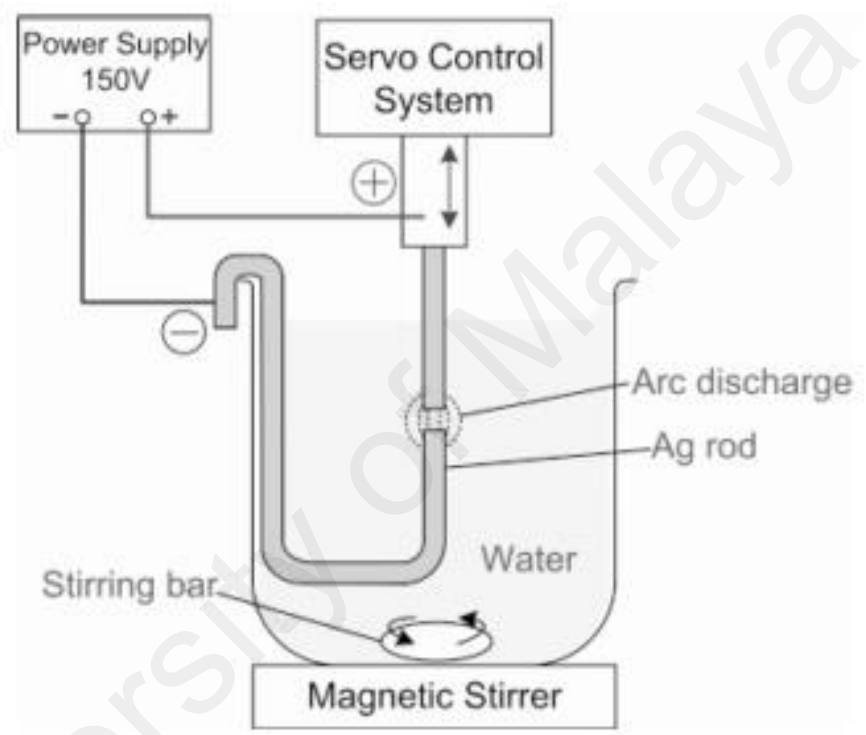

Figure 2.6: DC arc-discharge (Tien et al. 2008)

2.4.1.3 Fungal Based Synthesis

Fungal based synthesis is one of the biological approach, which normally involves living organisms such as bacteria, fungi and plants for the preparation of nanoparticles. According to Li et al. (2011), nanoparticles are biosynthesized when the microorganisms grab target ions from their environment and then turn the metal ions into the element metal through enzymes generated by the cell activities. Fungus-mediated synthesis of silver nanoparticles has been reported by Maliszewska et al. (2009) in their paper entitled

"Biological synthesis of silver nanoparticles". Silver nanoparticles with the size of 10-100 nm successfully synthesized using *Penicillium sp.* J3 strain isolated from soil. The reduction of the metal ions that occurs on the surface of the cells leads to the formation of nanosilver. From the morphological studies by using SEM and TEM, they revealed that protein might play an important role in the formation and stabilization of silver nanoparticles.

2.4.1.4 Comparison Between Synthesis Method

After studying the methods of producing NSPs, several main factors needed to be considered, which are the production cost, ease of conducting, time consumption and the quality of the final product. The summary of comparison is shown in Table 2.5. Based on the comparison table, the chemical reduction is the most preferable in obtaining nanoscale size powders and a colloidal dispersion of silver due to its low production cost, simple experimental procedure, relatively less time consumption and good quality product.

Table 2.5: Comparison of different NSPs synthesis method in regard to production cost, ease of conducting, time consumption and the quality of product

Synthesis method	Production cost	Ease of conducting	Time consumption	Quality of product	References
Chemical reduction	Low	Simple	1 day	▪ Spherical particles with a small average size ▪ Low aggregation	▪ Mavani & Shah, 2013 ▪ Iravani et al. 2014 ▪ Agnihotri et al. 2014
Arc-discharge	High	Simple	1 day	▪ Spherical particles with a size range from 20 nm to 40 nm	▪ Tien et al. 2010 ▪ Rashed, 2016 ▪ Zhang et al. 2017
Fungal based synthesis	Low	Simple	Up to 4 days	▪ Spherical particles with a size range from 10 nm to 100 nm	▪ Muhammed Fayaz et al. 2009 ▪ Ghorbani et al. 2011 ▪ Pantidos & Horsfall, 2014

2.4.1 Chemical Reduction as Synthesis Method

Among the synthesis methods, the chemical reduction is the best method to synthesis nanoparticles due to its simplicity, cost-effective, convenient operation, systematic and efficient procedure for synthesis without decreasing the production rate and ease of control (Lanje et al. 2010; Lah & Johan, 2011; Raza et al. 2016). Chemical reduction typically employs three major elements such as metal precursor, reducer and stabilizer, and these components have a strong influence on the physicochemical properties of the nanoparticles such as size, morphology, agglomeration and stability (Ghorbani et al. 2011; Zhang et al. 2016). Table 2.6 shows the influence of parameters in chemical reduction method on the NSPs physicochemical properties.

Table 2.6: Influence of parameters in chemical reduction method on the NSPs physicochemical properties

Parameters	Effect on physicochemical properties	References
Strong reducing agent	▪ Spherical particles with a size range from 1 nm to 3 nm ▪ High aggregation	▪ Dong et al. 2009 ▪ Khan et al. 2011 ▪ Amany et al. 2012 ▪ Basavaraj et al. 2012 ▪ Alahmad. 2014
Mild reducing agent	▪ Rod and spherical particles with a size range from 20 nm to 65 nm ▪ Low aggregation	
Weak reducing agent	▪ Spherical particles with a size range from 7 nm to 30 nm ▪ Low agglomeration	
Presence of stabilizing agent	▪ well dispersed non-aggregated spherical particles ▪ Particles size range from 50 nm to 100 nm	▪ Oliveira et al. 2005 ▪ Guzmán et al. 2009 ▪ Kumar et al. 2014
Concentration of metal precursor increase	▪ Spherical particles with larger mean particles size ▪ Low agglomeration	▪ Ajitha et al. 2013
Reaction temperature increase	▪ Spherical particles with larger size ▪ Formation of larger particles	▪ Nurul Akma et al. 2016 ▪ Piñero et al. 2017

2.4.1.1 Stabilization of NSPs by Polyvinylpyrrolidone (PVP)

In the synthesis of nanoparticles, agglomeration and aggregation issue remains a great challenge to the researchers. The terms agglomeration and aggregation is distinctly defined as weakly bonded particles and strong bonded or coalesced particles, respectively. This issue is predicted to affect the NSPs toxicity by reducing the effective specific surface area to decrease metal ion release and reactive oxygen species generation and influencing the cellular uptake (Zook et al. 2011). Therefore, numerous studies have stressed the use of stabilizing agent/capping agent/protecting agent in nanoparticles synthesis in order to reduce the formation of agglomeration and aggregation.

Various types of stabilizer have been used previously and PVP is one of stabilizer that commonly used to cap the particles surface and reduce the agglomeration (Pulit et al. 2011; Ahmad et al. 2017). PVP which is a non-ionic polymer with C=O, C-N and CH_2 functional groups not only used in the synthesis of silver nanoparticles but also other metallic nanoparticles such as copper (Dang et al. 2011; Ghorbani. 2014), gold (Chili et al. 2011; Nalawade et al. 2013) and nickel (Neiva et al. 2014; Liu et al. 2016). PVP is a great protecting agent which prevent the agglomeration of nanoparticles via repulsive forces that raise from its hydrophobic carbon chains that extend into solvents and interact with each other (steric hindrance effect) (Koczkur et al. 2015). The solvent-chain interaction increases the free energy of the system and generates an energy barrier to the closest approach of nanoparticles. When the nanoparticles come into closer contact with each other, the chains movement extending into the solvent become restricted and create an entropic effect (Lei. 2007). Besides acting as a stabilizer or protecting agent, PVP also act as a shape-control agent that promote the growth of specific crystal faces while hindering others (Koczkur et al. 2015).

2.4.2 The significance of Nanosized Silver Particles

The toxicity of silver to the microorganisms has been known for centuries and have debated among the researchers, where they stated that the toxicity of the nanoparticles differs from the release of free ions. Several researchers claimed that the main toxicity mechanism of NSPs is from the released Ag^{+} upon the dissolution of nanoparticles (Kittler et al. 2010; Marambio-Jones & Hoek, 2010; Chernousova & Epple, 2013; Ivask et al. 2014), while, the other researchers stated that the nanoparticles itself very toxic to the bacterial cells. The toxicity of nanoparticles depends on its physicochemical properties such as size and surface characteristics (Ivask et al. 2014; Lindgren, 2014; Tajkarimi et al. 2014). However, the primary factor of the toxicity of the nanoparticles or the free ions is actually related to the size of the nanoparticles (Ivask et al. 2014; Gatoo et al. 2014. In general, particles in nanoscale size which typically smaller than 100 nm often possess novel size-dependent properties from their large counterparts and due to this factor, nanosized silver particles are compulsory in this research as compared to bulk silver.

The nanosized particles are found to be reactive due to the extremely large surface area, leading to the higher bacterial cell in contact with the metal surface (Farkas et al. 2011; Lindgren. 2014; Franci et al. 2015). When NSPs in contact with microorganisms, the cellular metabolism of the electron transfer systems and the transport of substrate in the microbial cell membrane are adversely affected (Varner et al. 2010). In addition, the smaller particles will facilitate the particles uptake by the microorganisms (Sloan & Farnsworth, 2006). A higher volume-surface ratio leads to a lot of binding sites that allows metal and other compounds to easily enter cell membrane and accumulate inside the cell and cause damages (Lindgren. 2014). Ivask et al. (2014) observed a significant decrease in NSPs toxicity with an increase of the particles size, in which, with a 2-fold increase in silver particle size, the antibacterial activity decreased by a factor 2.5. The

smaller particles displayed excellent antibacterial activity due to high particles penetration and the particles easy to diffuse than the larger particles (Monores et al. 2005; Mohan et al. 2007; Durán et al. 2010).

Smaller-sized particles that have a high surface to volume ratio lead to the faster dissolution rate of nanoparticles, resulting in more released ionic silver. These silver cations cause the release of K^+ ions from bacteria; thus, the cytoplasmic membrane or bacterial plasma, which is associated with many important enzymes, is an important target site for silver cations (Jung et al. 2008; Kim et al. 2011). Silver ions may bind to thiol groups and form reactive oxygen species (ROS), resulting in the damage of enzyme. Besides that, Ag^+ can inhibit DNA replication by destroying DNA & RNA, leading to the death of bacterial cells (Dhakras, 2011; Qu et al. 2013; Tajkarimi et al. 2014).

In summary, the nanosized particles played a crucial role in the toxicity of NSPs. Generally, NSPs become toxic to the microorganisms through the direct attachment to the bacteria surface, penetrate into the cell as well as the release of free Ag^+. The nanoparticles and Ag cations that penetrated inside the bacteria be a soft acid, interact and damage the complexes such as DNA, and even disrupt the morphology of the membrane, resulting in the cell death (Raza et al. 2016).

CHAPTER 3: METHODOLOGY

This chapter describes the materials used and the experimental work that divided into 3 phases. Phase I includes the synthesis of nanosilver particles (NSPs) and follow by the characterization of NSPs, phase II contains the fabrication and characterization of electrospun PVDF/NSPs NFM and phase III is related to the membrane performance in water treatment. The overview of this study is shown in Figure 3.1.

3.1 Raw Materials

3.1.1 Phase I: Synthesis of NSPs by Chemical Reduction Method

All the chemicals used to synthesize NSPs were analytical reagents which is used without further purification. Silver nitrate, $AgNO_3$ (Systerm, China) was used as a silver precursor. D(+) glucose, $C_6H_{12}O_6$ (R&M Chemicals, UK) was utilized as a reducing agent. Sodium hydroxide pellets, NaOH (Merck KGaA, Germany) and poly(vinyl pyrrolidone) (PVP, average molecular weight 58,000; Alfa Aesar, Great Britain) were used as reaction enhancer and stabilizing agent, respectively.

3.1.2 Phase II: Fabrication of Electrospun PVDF/NSPs NFM via Electrospinning

Polyvinylidene fluoride (PVDF) with average molecular weight 534,000 was purchased from Sigma Aldrich (USA). Two solvents were used to dissolve the polymer which are N,N-dimethylformamide (DMF) from Ajax Finechem (Australia) and acetone from R&M Chemicals (UK). All the chemicals were analytical grade and used without further modification.

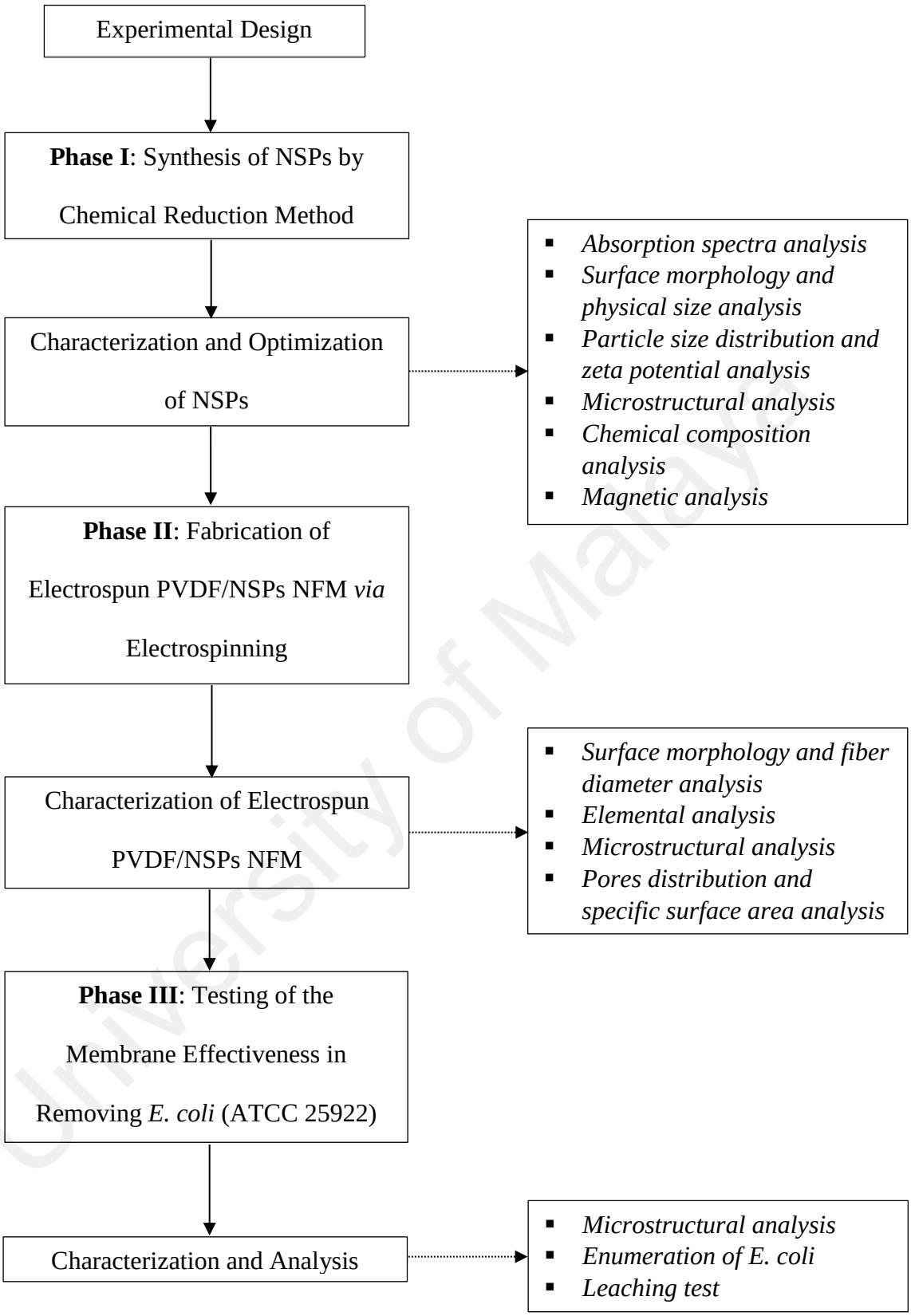

Figure 3.1: Overview of research methodology

3.1.3 Phase III: Testing of the Membrane Effectiveness in Removing *E. coli* (ATCC 25922)

Nutrient broth (NB), nutrient agar (NA) and MacConkey agar (MAC) from Merck KGaA (Germany) were utilized to culture the *E. coli* (ATCC 25922). Sodium chloride (NaCl) was used to prepare saline water. All the chemical reagents were used without further purification.

3.2 Experimental Procedure

3.2.1 Phase I: Synthesis of NSPs by Chemical Reduction Method

In this phase, NSPs were produced by the reduction of $AgNO_3$ using glucose as a reducing agent, PVP as stabilizing agent and NaOH as reaction enhancer. The concentration of precursor ($AgNO_3$) and the reaction temperature was varied to investigate the formation, size and agglomeration state of NSPs, through a series of characterization. The particles with the smallest size will be selected to proceed to the next phase.

3.2.1.1 Synthesis of NSPs

The experimental was started with the preparation of the polymer solution and silver precursor solution as solution A and solution B, respectively. Solution A was prepared by dissolving glucose, PVP and NaOH in distilled water. The solution was heated up to a temperature (60 °C and 80 °C) with continuous stirring for an hour. Meanwhile, solution B was prepared by dissolving $AgNO_3$ in distilled water. For this solution, three different concentration was prepared which is 0.1 M, 0.5 M and 1.0 M. Solution B was added drop by drop into solution A and as soon as all the solution B was used up, stirring and the heating process was stopped immediately. The mixture was cooled down at room temperature before centrifugation was carried out at 6000 rpm for 1 hour to separate the

particles. The separated particles were washed several times with distilled water until no NO_3^- could be traced using a centrifuge. The supernatant was discarded and the separated particles were dispersed in distilled water. The dispersion of particles was stored in a vial for the characterization in colloidal form. Finally, the particles were dried at 40 °C for 24 hours before undergoing a series of characterization test. The overall steps in the synthesizing NSPs were illustrated in Figure 3.2. There were six samples produced with label S1T6, S2T6, S3T6, S1T8, S2T8, and S3T8. S1, S2, and S3 indicate the concentrations of the silver salt precursor which were 0.1 M, 0.5 M, and 1.0 M, respectively. Meanwhile, T6 and T8 mean the reaction temperature was 60 ℃ and 80 ℃, respectively. The summary of the synthesis parameters was shown in Table 3.1.

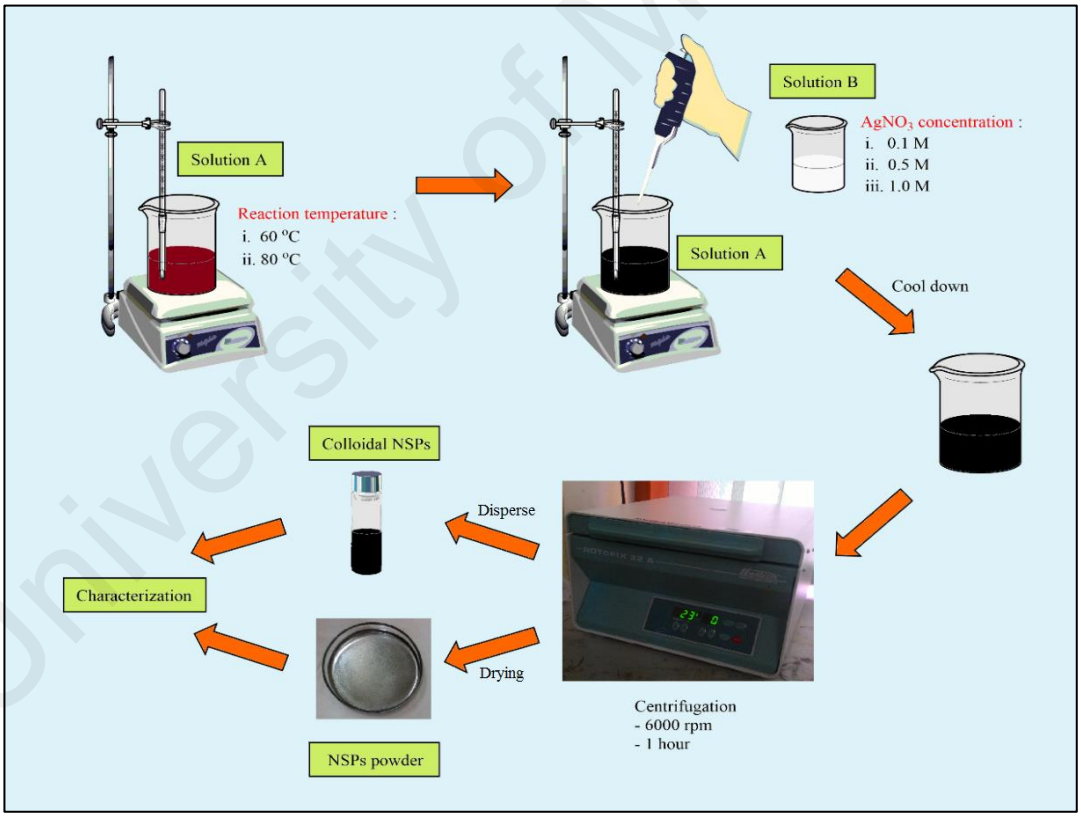

Figure 3.2: The procedure in the synthesizing of NSPs

Table 3.1: The studied parameters in the synthesizing NSPs

Sample	Temperature (°C)	Concentration of $AgNO_3$ [M]
S1T6	60	0.1
S2T6		0.5
S3T6		1.0
S1T8	80	0.1
S2T8		0.5
S3T8		1.0

3.2.1.2 Characterization of the Synthesized NSPs

A colloidal solution of NSPs was characterized using ultraviolet-visible spectrophotometer (UV-vis), transmission electron microscopy (TEM) and dynamic light scattering (DLS) analysis. UV-vis absorption spectra analysis was performed to confirm the formation of NSPs. The spectra were measured by UV-Vis spectrophotometer (Varian, USA, Cary 50 Scan) with a wavelength range of 300-600 nm using 1 cm path length disposable polystyrene cuvette at room temperature. The colloidal NSPs was diluted with distilled water 10x before taking a measurement. The structure and physical size of NSPs were studied using TEM (Carl Zeiss, Germany, LEO-Libra 120) operating at 120 kV with a magnification of 15K. A drop of diluted colloidal solution was placed onto a Lacey formvar/carbon film supported on a copper grid (ProSciTech Pty Ltd, Australia) and evaporated at room temperature. The average physical size and distribution of NSPs were measured based on a hundred single nanoparticles from TEM images that viewed under 80K magnification using Digimizer image analysis software (MedCalc, USA, Version 4.6.1). The mean hydrodynamic size (*Z-average*) and the zeta potential (*Zp*) of NSPs were measured by dynamic light scattering through the correlation function of the scattered intensity (cumulants analysis) and particles mobilities, respectively, using Zeta sizer (Malvern, UK, Nano ZS). Three measurements were taken using automated,

optimal measurement times and laser attenuation settings to obtain the average reading for each sample.

NSPs powder was characterized by X-ray diffractometer (XRD), vibrating-sample magnetometer (VSM) and Fourier transform infrared spectroscopy (FTIR). The crystalline structure of the produced nanoparticles was identified using XRD (PANalytical, Netherland, Empyrean) with Cu K-Alpha radiation at 1.5406 Å in a range of 2θ = 30-80 ° at a scan rate of 0.05 s^{-1}. The crystallite size of the NSPs was calculated from all prominent peaks in the diffraction pattern using Scherer's equation. Magnetic properties of NSPs was determined using VSM (Lake Shore Cryotronics, USA, 7400 Series) with applied fields of ± 8000 Oe at room temperature by mounting approximately 17-80 mg sample into the sample holder. FTIR analysis was performed to detect the presence of PVP on the NSPs surface. The infrared spectra were obtained using FTIR (Bruker, USA, Tensor 27) in the wavenumber range of 4000-500 cm^{-1}. NSPs were grounded with potassium bromide (KBr) powder (Sigma Aldrich, USA) and the mixture was pressed into platelets for the measurement.

3.2.2 Phase II: Fabrication of Electrospun PVDF/NSPs NFM via Electrospinning

In this phase, nanocomposite nanofibrous membrane was produced by incorporating as-synthesized NSPs into PVDF polymer matrix using the electrospinning process. The influence of weight percentage of NSPs on the properties of the electrospun nanofibrous membrane was investigated completely through a series of analysis.

3.2.2.1 Fabrication of Electrospun PVDF/NSPs NFM

Fabrication of electrospun NFM involves two main steps. The first step was the preparation of polymer solution. A certain amount of NSPs, depending on the weight percent (0.5 wt%, 1.0 wt% and 3.0 wt%) was dispersed in DMF with continuous stirring

for 15 mins before adding PVDF. After the addition of PVDF into the NSPs dispersion, the mixture was continuously stirred and heated up to 70 °C for overnight. After that, acetone was added into the solution and constantly stirred for another 24 h at 25 °C. For this polymer solution preparation, the weight percent of PVDF and the solvents ratio (DMF: Acetone) was fixed to 15 wt% and 7:3, respectively. Preparation of pure PVDF solution as a control has the similar procedure as mentioned above excluding the dispersion of NSPs.

The second step was the electrospinning of nanofibrous membrane. The polymer solution was drawn into a 15 ml syringe in which 0.5 inch long stainless steel needle was attached to it. The syringe together with a needle was mounted on a programmable syringe pump (New Era Pump Systems, New York) and the needle was connected to the positive terminal of the high voltage power supply (Leybold, 25 kV), while, the negative terminal was connected to the static collector (aluminium foil). The electrospinning process was carried out at room temperature using constant applied voltage (20 kV). The other parameters such as flow rate and the distance between needle tip to the collector, also fixed to 0.5 ml/h and 15 cm, respectively. In this phase, four samples with label PP, PS0.5, PS1.0 and PS3.0 were fabricated using electrospinning. PP indicates pure PVDF NFM, while, PS0.5, PS1.0 and PS3.0 indicate PVDF/NSPs NFM with a different weight content of NSPs. The overview of phase 2 was shown in Figure 3.3 and the information of the electrospun NFM was tabulated in Table 3.2.

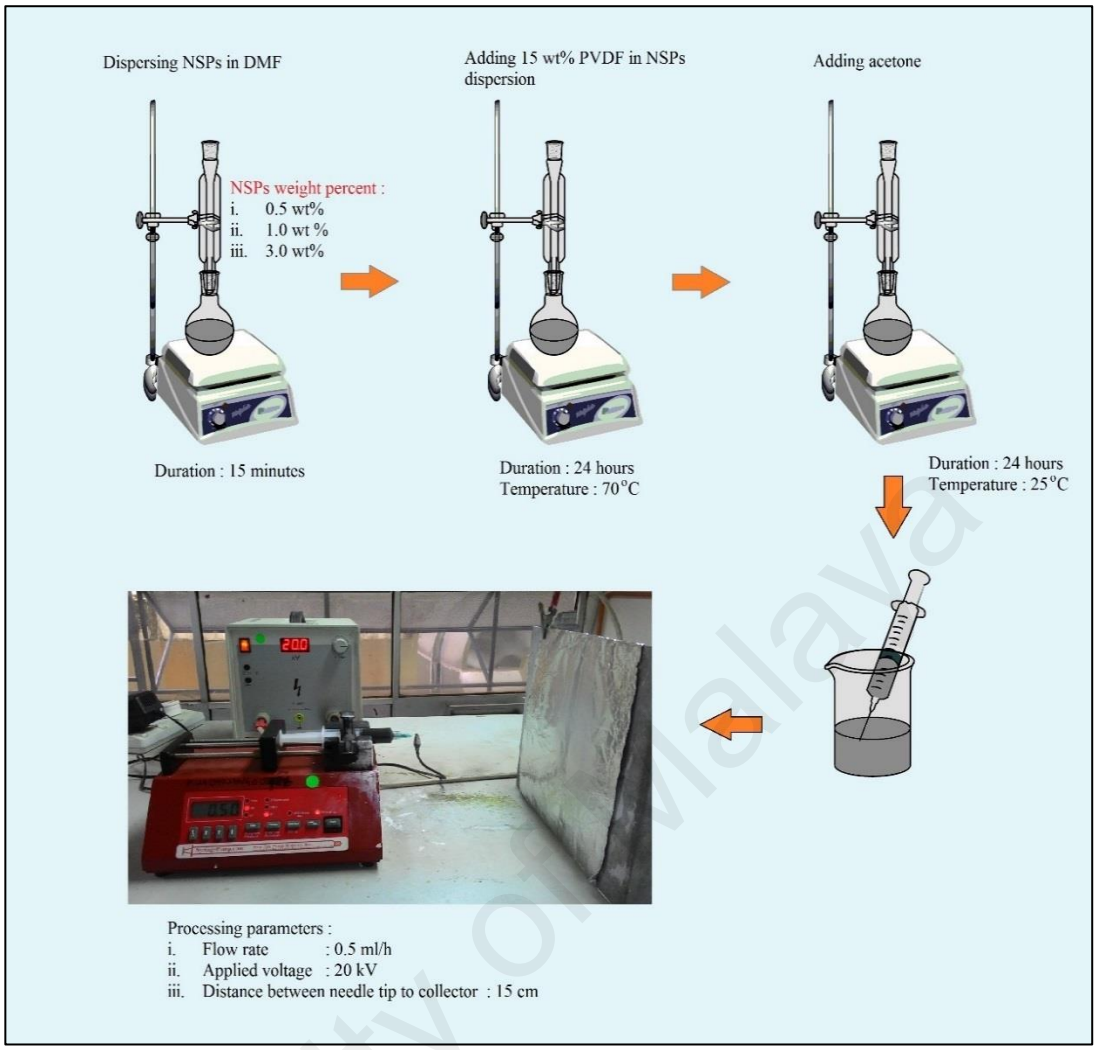

Figure 3.3: Overview of electrospun NFM fabrication

Table 3.2: Electrospun NFM information

Sample	Polymer solution			Processing parameter		
	Weight percent of PVDF (wt%)	Solvent ratio (DMF:Ace)	Weight percent of NSPs (wt%)	Applied voltage (kV)	Flow rate (ml/h)	Distance between needle tip to collector (cm)
PP	15	7:3	0.0	20	0.5	15
PS 0.5			0.5			
PS 1.0			1.0			
PS 3.0			3.0			

3.2.2.2 Characterization of Electrospun PVDF/NSPs NFM

Several analysis was performed to characterize the electrospun NFM using field emission scanning electron microscopy (FESEM), energy dispersive X-ray spectrometer (EDS), X-ray diffractometer (XRD) and porosimeter. FESEM (FEI, USA, Quanta 650) equipped with energy dispersive spectrometer (EDS; Oxford Instrument X, UK) was used to investigate the surface morphology, fiber diameter as well as an elemental of electrospun NFM. The electrospun NFM with a dimension of 1 cm x 1 cm was coated with the platinum coating before viewing under FESEM with a magnification of 50000x and operating voltage of 5 kV. Five different spots were observed to conclude the morphology and the average fiber diameter for each sample. The fiber diameter was determined by measuring over 100 fibers from the FESEM images using Digimizer image analysis software (MedCalc, USA, Version 4.6.1). For the elemental study, the analysis was performed using full-scan mapping technique under 1000x magnification and operated using applied voltage 5 kV. The microstructural analysis for the electrospun NFM was performed using XRD (PANalytical, Netherland, Empyrean), where the radiation of Cu K-Alpha = 1.5406 Å, the range of 2θ = 15-80 ° and the scan rate = 0.026 s^{-1}. Porosimeter (Thermo Finnigan, USA, Sorptomatic 1990 Series) was used to determine the specific surface area and the porosity of the NFM. For this analysis, 0.1-1 g of sample was placed into the sample tube and degassed for 8 h at 120 °C before measurement.

3.2.3 Phase III: Testing of the Membrane Effectiveness in Removing *E. coli* (ATCC 25922)

In this phase, an investigation was carried out to determine the capability of the membrane in removing *E. coli* from various contaminated water model by using membrane filtration technique, a standard method for examination of water and

wastewater. A non-pathogenic *E. coli* strain from American Type Cell Culture (ATCC 25922) was used as a reference strain because it was identified as a potential surrogate for pathogenic *E. coli* (Sauer & Moraru, 2009). The effectiveness of the membrane was evaluated by comparing the initial concentration of *E. coli* before filtration and the concentration of viable *E. coli* on the membrane after the incubation process.

3.2.3.1 Preparation of Contaminated Water Model and Filtration Process

E. coli (ATCC 25922) was grown for overnight in NB at 37 °C with a shaker. Two ml of overnight cultured was aliquoted into 100 ml of fresh NB and incubated for 6 h at 37 °C with a shaker. The growth of the bacteria was measured with an absorbance of approximately 1.0 at 600 nm using spectrophotometer (Hitachi, Japan, U-1900). *E. coli* was harvested from NB by centrifugation process at 3000 rpm for 10 min. The supernatant was discarded and the bacterial pellet was resuspended in 0.85 % saline water. The suspension of *E. coli* was then diluted until the absorbance value reach 1.0 at 600 nm (monitored by spectrophotometer), which is equivalent to 10^8 colony forming unit (CFU)/ml. This suspension was further diluted in sterile saline water to achieve the desired final concentration of *E. coli* suspension. The concentration of diluted *E. coli* suspension was double confirmed by the spread plate technique on MAC agar. In the filtration process (Figure 3.4), a saline sample containing *E. coli* was filtered through sterile electrospun NFM, the membrane was then placed onto MAC agar and incubated at 37 °C overnight. After incubation, the colonies growing on the electrospun NFM were enumerated and reported as colonies per 100 ml. The counted colonies on the control membrane were compared with the counted colonies on the nanocomposite membrane (PVDF/NSPs) to determine the effectiveness of NSPs addition on the membrane performance.

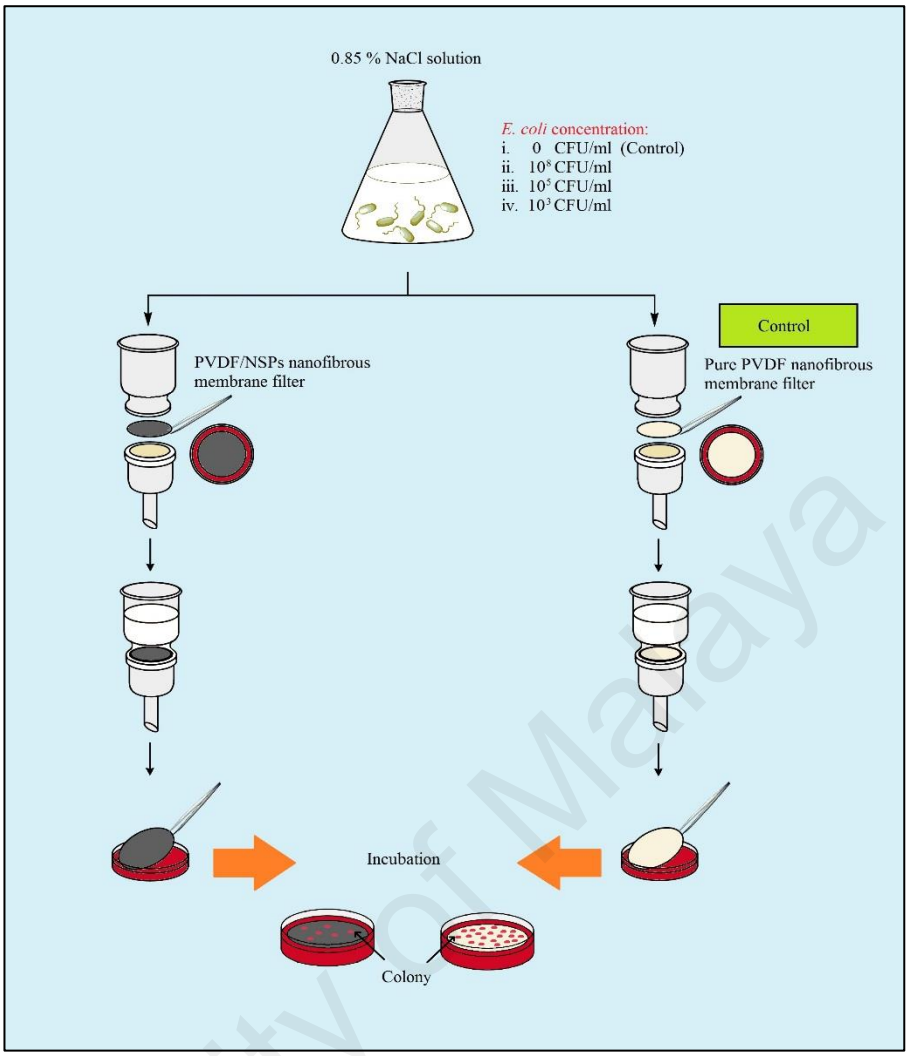

Figure 3.4: Filtration process in removing *E. coli*

3.2.3.2 Characterization and Analysis

A preliminary analysis was conducted on the heat sterilized electrospun PVDF/NSPs NFM using XRD (PANalytical, Netherland, Empyrean), where the Cu K-Alpha radiation = 1.5406 Å, the range of 2θ = 15-80 ° and the scan rate = 0.026 s^{-1}, to check the changes properties of NFM. The growth of *E. coli* on the electrospun PVDF/NSPs NFM surface was measured by counting the colony. Leaching analysis was performed to determine any presence of a silver element in the filtrate using UV-vis spectrophotometer (Varian, USA, Cary 50 Scan) with a wavelength range of 200-600 nm.

CHAPTER 4: RESULTS AND DISCUSSION

This chapter presenting overall results for this study. The results are shown and discussed according to the phases as follows: i) Synthesis of NSPs by chemical reduction method, ii) Fabrication of electrospun PVDF/NSPs NFM *via* electrospinning and iii) Removal of *E. coli* (ATCC 25922).

4.1 Phase I: Synthesis of NSPs by Chemical Reduction Method

In this phase, NSPs coated with PVP were produced by reducing $AgNO_3$ using glucose and the influence of $AgNO_3$ concentration and reaction temperature on the properties of NSPs especially size were investigated thoroughly.

4.1.1 Absorption Spectra Analysis

Figure 4.1 shows the UV-Vis spectra of the synthesized particles in water. All the colloidal dispersion exhibits strong absorption within a range of 350-460 nm, which is the characteristic absorbance band of the surface plasmon resonance (SPR) for NSPs (Sun et al. 2004; Bhui et al. 2009; Lu et al. 2011; Suwatthanarak et al. 2016). This UV-vis results confirmed the formation of NSPs.

The size of synthesized NSPs was predicted from the spectral based on the shifting of the absorption peak and the intensity of the absorbance. Jiang et al. (2006) reported that the absorption peak will shift to the longer wavelength when the particles become larger. These larger particles tend to form agglomeration or aggregation and cause the surface plasmon resonance shift to lower energy level that leads to the red-shift to a longer wavelength due to the delocalize and sharing of conduction electrons near each particle surface among neighboring particles. At 60 °C, the absorbance peak was shifted to longer wavelength as the concentration increased from 0.1 M to 0.5 M and shifted slightly to the

shorter wavelength as the concentration further increased to 1.0 M, implying the particles size can be predicted as S1T6 < S2T6 > S3T6. A narrow bandwidth with high intensity of S2T6 spectrum was clearly observed which indicated the formation of larger NSPs and increase of the number of nanoparticles (Suwatthanarak et al. 2016) which will be further verified with TEM image later. For the 80 °C reaction temperature, the particles size become larger as the concentration increases from 0.1 M to 1.0 M as can be seen from the peak shifting phenomena. When the concentration of $AgNO_3$ was increased, the existence of Ag^+ ions in the system will be higher, so it can promote the growth of NSPs and lead to the formation of larger particles (Jiang et al. 2006).

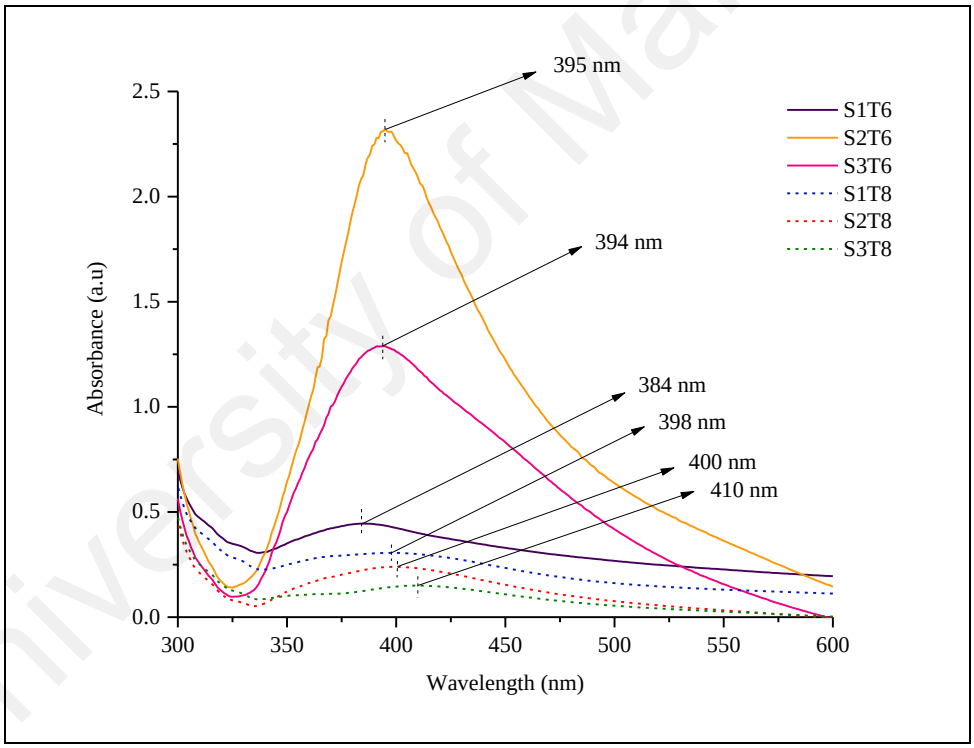

Figure 4.1: The UV-vis spectra of NSPs produced using different $AgNO_3$ concentration (0.1 M, 0.5 M and 1.0 M) at 60 °C and 80 °C

When the reaction temperature was increased from 60 °C to 80 °C, the absorbance peak was clearly showed red-shifting (shifting of the peak to the higher wavelength) for every precursor concentration (0.1 M, 0.5 M and 1.0 M). From this observation, the size

of NSPs produced at 60 °C was predicted smaller than the NSPs synthesized at 80 °C. At low temperature, the formation and growth reaction was slower and in order to complete the reduction, it usually took longer reaction time (Jiang et al. 2011). However, in this study, the reaction was immediately stopped once the dropping process of the precursor was complete. For this reason, the collision frequency may be lower due to a lower temperature. As a result, the tendency of Ag atoms to bind with each other is lesser and thus, forming smaller nanoparticles. Based on Figure 4.1, the broad absorption peaks with low intensity were observed for the NSPs that produced at a high temperature. The broadness of the bandwidth and reduction of the absorbance intensity might due to the agglomeration and the aggregation of NSPs (Singh et al. 2010; Hussain et al. 2011; Rashid et al. 2013).

4.1.2 Mechanism Prediction on the Formation of NSPs

From the observation, several reactions took place throughout the experimental work. The first reaction was observed during preparation of polymer solution containing glucose, PVP and NaOH. During constant stirring for 1 hour, the color of the solution was slowly changed from colorless to dark brown, which might due to the oxidation process of glucose. Previous researchers mostly reported that glucose directly oxidized to gluconic acid during the synthesis process (Wang et al. 2005; Darroudi et al. 2010; Amany et al. 2012). However, through this study the oxidation of glucose was obviously separated into two stages. The first oxidation process happened in the polymer solution. The presence of hydroxide ion (OH^-) from NaOH makes glucose easily oxidizes to gluconate ion as shown in Figure 4.2(a) due to the existence of hydrogen atom in the aldehyde group (-CHO).

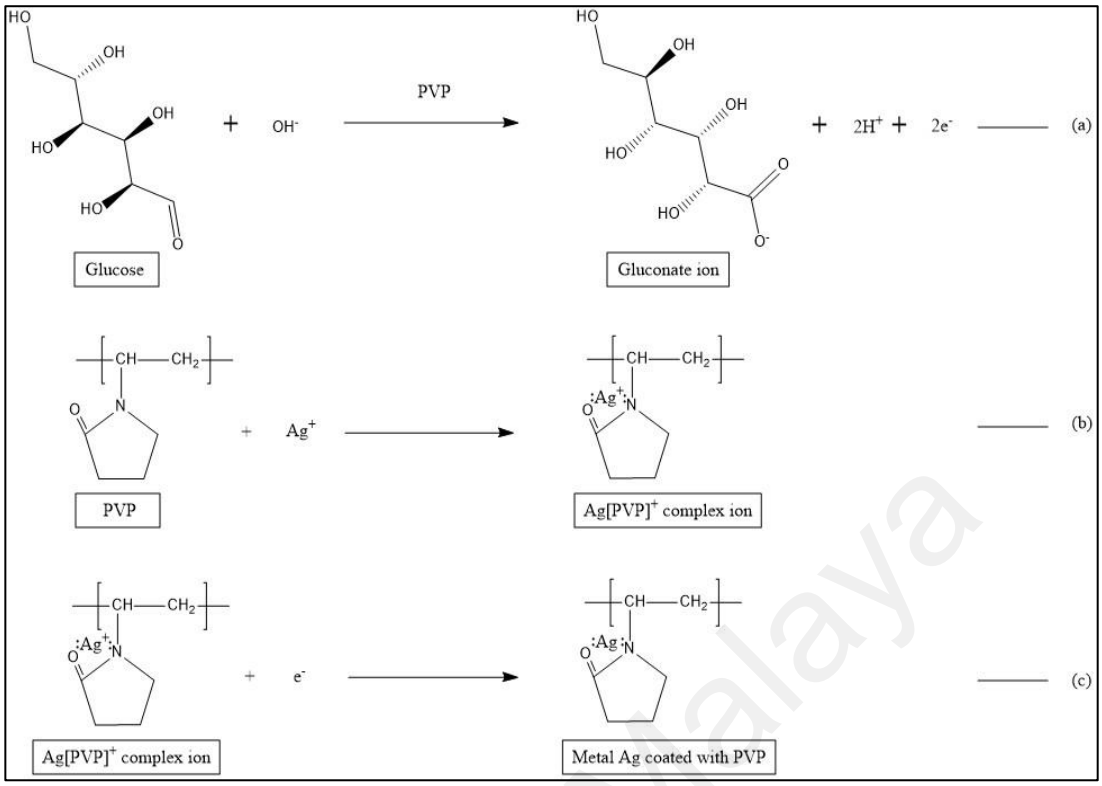

Figure 4.2: (a) Chemical reaction in the polymer solution (b) Coordinative bonding between PVP and Ag^+ (c) Reduction of $Ag[PVP]^+$ complex ion into coated Ag metal

The second reaction on the NSPs formation took place when the $AgNO_3$ solution was introduced into the polymer solution. As soon as the $AgNO_3$ solution was dropped into the solution, the color of the solution instantly changes from dark brown to black. This phenomenon due to the bonds occurrence between PVP and silver ions (Ag^+), which formed $Ag[PVP]^+$ complex ion (Figure 4.2(b)). The coordinative complex of Ag^+ and PVP are formed when PVP donates lone pair electrons of oxygen and nitrogen atoms to *sp* orbital of Ag^+ (Zhang et al. 1996). PVP promotes the nucleation of metallic silver because $Ag[PVP]^+$ complex ions are more easily reduced by gluconate ions than pure Ag^+ due to Ag^+ receiving more electronic cloud from PVP than from H_2O. During the reduction of $Ag[PVP]^+$ complex ions to metallic Ag (Figure 4.2(c)), the gluconate ions oxidized to gluconic acid. This generation of complex ions leads to the aggregates of Ag atoms, which defined as primary nanoparticles by Shin et al. (2004). The primary NSPs

combine with each other or interact with PVP and form larger aggregates known as secondary nanoparticles. The overall mechanism of NSPs formation was predicted as in Figure 4.3.

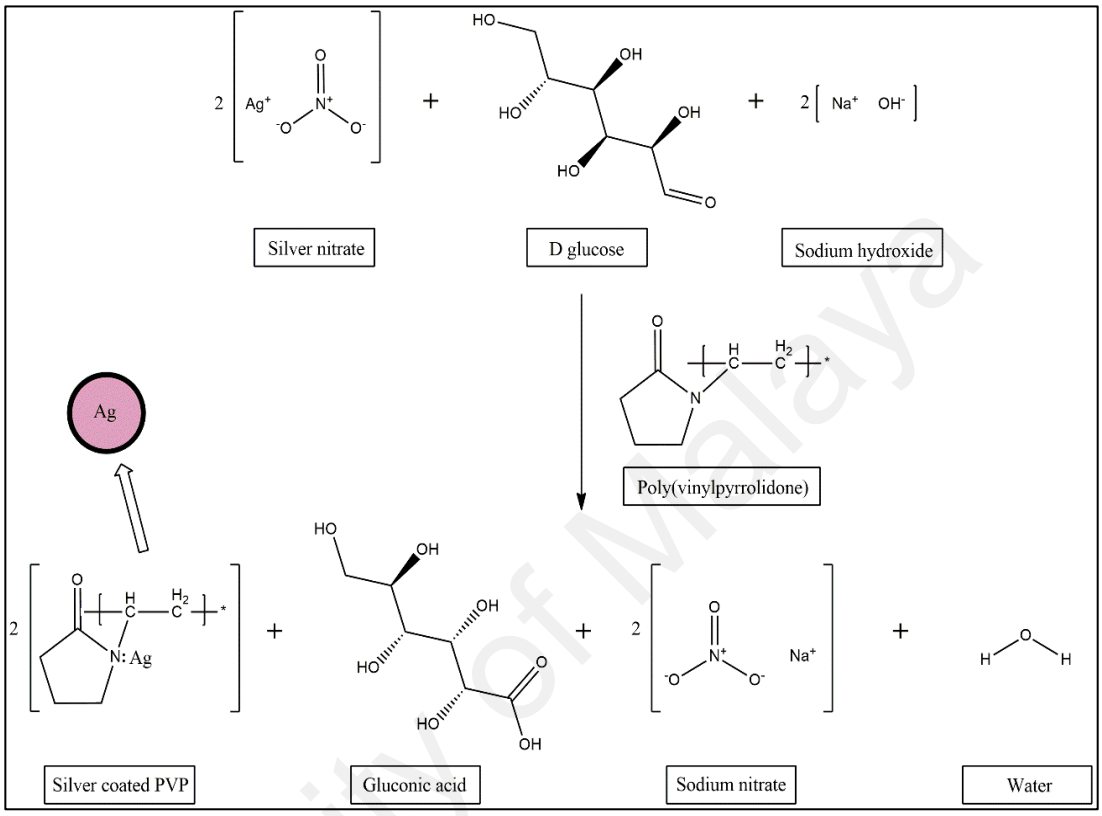

Figure 4.3: The prediction of NSPs formation

4.1.3 Microscopic Analysis on the Shape and Physical Size

Figure 4.4 represents the TEM images together with the particle distribution for all the produced NSPs using different $AgNO_3$ concentration at 60 °C and 80 °C, respectively. The figures clearly reveal the synthesized nanoparticles were spherical in shape and appear to be a little bit of aggregation. An increment in the number of larger nanoparticles was clearly observed when the concentration increases from 0.1 M to 0.5 M (Figure 4.4(a) and Figure 4.4(b)). When the concentration further increased to 1.0 M (Figure 4.4(c)), the produced NSPs were noticed have a smaller size. For the reaction temperature 80 °C, at a lower concentration of silver salt precursor (Figure 4.4(d)), the single spherical

nanoparticles still can be observed as compared to Figure 4.4(e) and Figure 4.4(f). When the concentration increased to 0.5 M, agglomeration obviously took place in the reaction (Figure 4.4(e)) and further increment of $AgNO_3$ concentration to 1.0 M (Figure 4.4(f)) caused the nanoparticles to aggregate further. At higher concentration of precursor, the agglomeration may be associated with the higher surface energy (Ahmad et al. 2014). Furthermore, the presence of a large amount of precursor created high attraction between atoms (Sibiya & Moloto, 2014), where the Ag atoms tend to attract to each other (Allen et al. 2001) that resulted in the agglomeration and aggregation of nanoparticles.

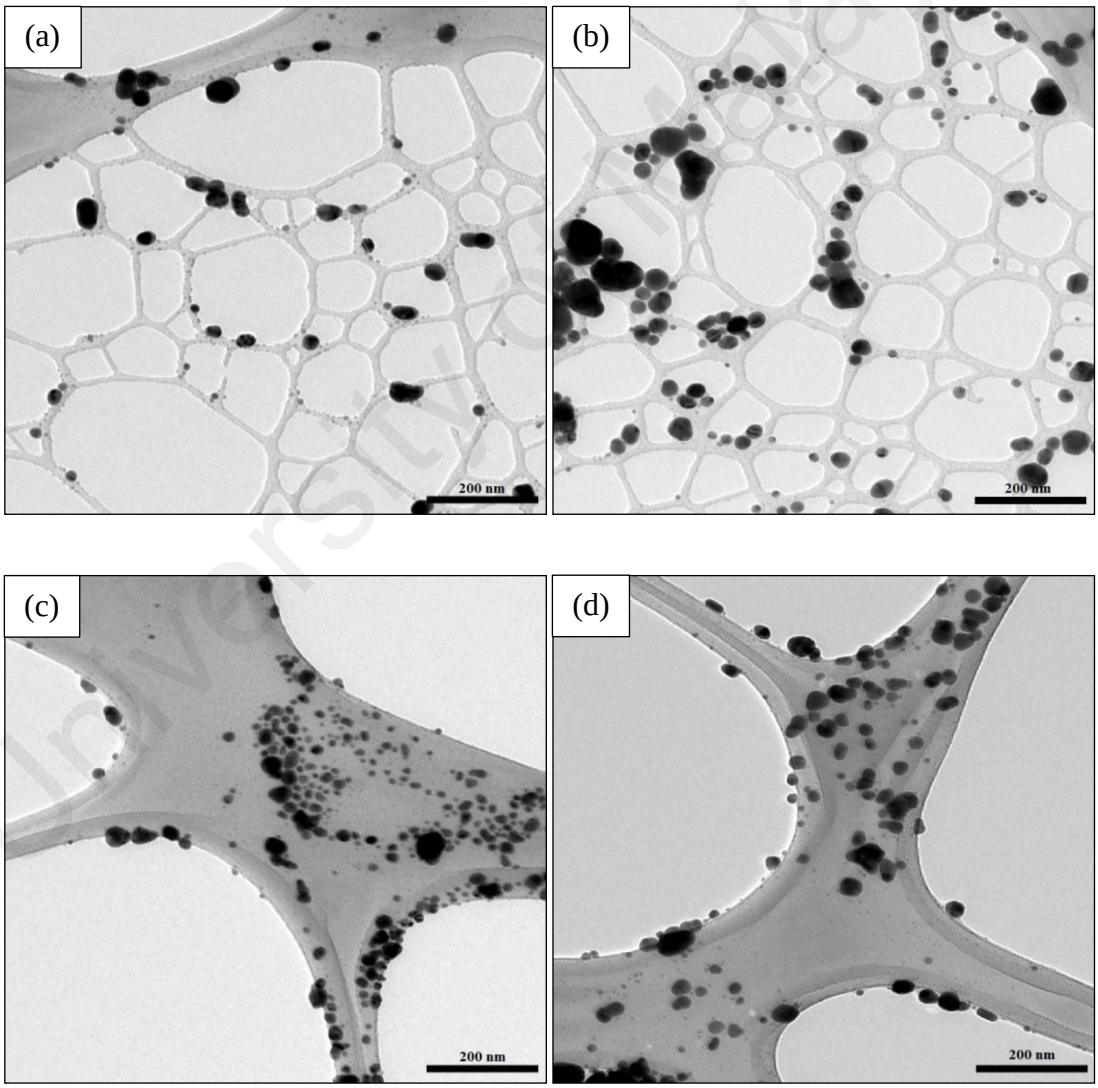

Figure 4.4: TEM images and particles size distribution of the synthesized NSPs (a) S1T6 (b) S2T6 (c) S4T6 (d) S1T8 (e) S2T8 (d) S3T8

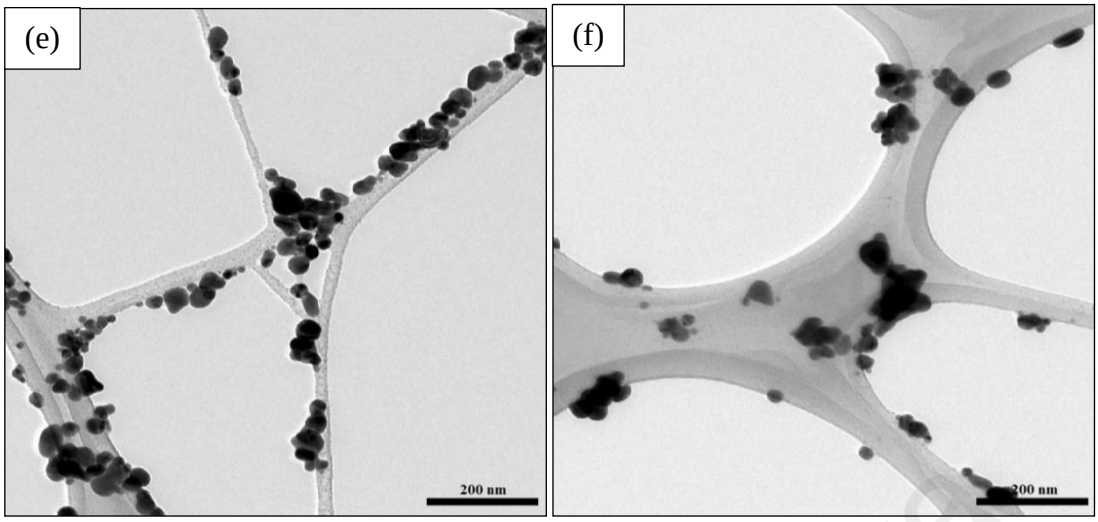

Figure 4.4: continued.

The physical size distribution of the NSPs was plotted in the box and whisker chart as shown in Figure 4.5. The black line in the middle of the box indicates the median value of 100 particles and the green line representing the mean value of the size. In both cases, S1T6 and S1T8 have the narrowest size distribution as compared to other samples, the particles lie in the range of ≈ 23-31 nm and ≈ 21-28 nm, respectively. The mean size of NSPs that produced at 60 °C using 0.1 M, 0.5 M and 1.0 M was 27.48 nm, 35.20 nm and 25.72 nm, respectively. The calculated mean size of synthesized NSPs at 80 °C was 25.34 nm, 30.79 nm and 39.13 nm, for S1T8, S2T8 and S3T8, respectively. This calculated size show identical trend as shown in UV-vis size prediction.

NSPs that prepared using 0.1 M and 0.5 M precursor concentration showed a reduction in the physical size as the temperature increases. When the temperature increases, the reaction take a shorter time to be completed and nuclei produced have fewer chance to grow into large particles by coagulation (Hee & Jinki, 2007), thus, smaller particles were produced at a higher temperature. In addition, an increase in the temperature allowed nanoparticle growth at a faster rate, the reaction for the particle formation may be incomplete in a short duration. Therefore, the observed particle size will be decreased

(Zhang et al. 2007). On contrary, when the $AgNO_3$ concentration fixed to 1.0 M, the nanoparticles display an increment in the physical size as the temperature increase. Even though temperature plays a major role in controlling size, the concentration of precursor is dominant in this situation. When the concentration of $AgNO_3$ is relatively high, the reducing agent might unable to reduce the Ag^+ completely. As a consequence, the excess Ag^+ will be deposited on the Ag nuclei that formed in the nucleation stage and thus, resulting in the formation of larger NSPs.

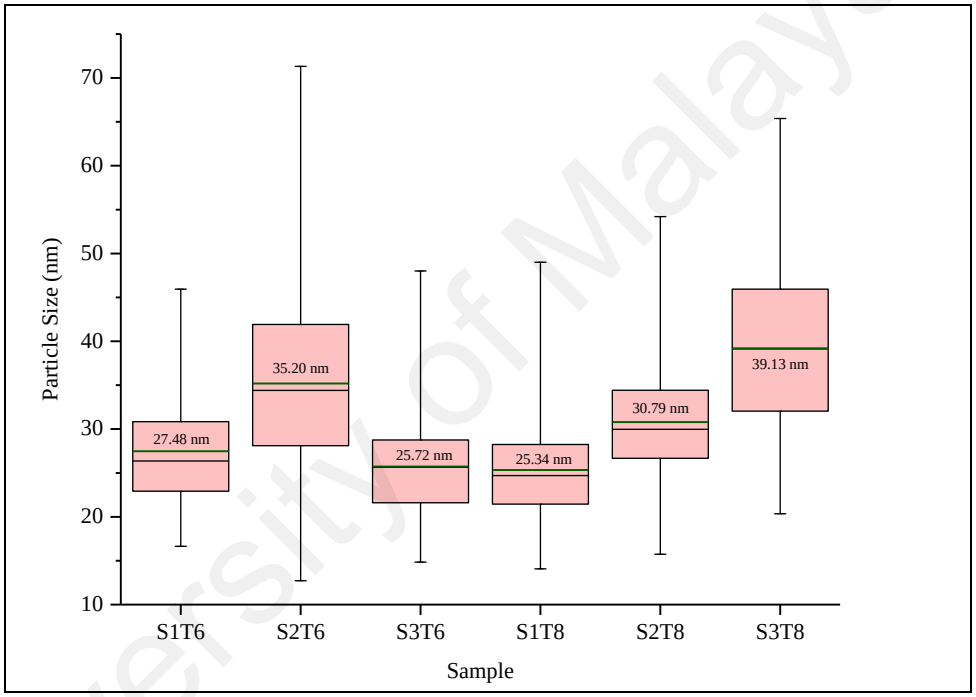

Figure 4.5: Particle size distribution for all sample

4.1.4 Particle Size Distribution and Zeta Potential Analysis

The average readings for the entire samples were summarized in Table 4.1. For both reaction temperature (60 °C and 80 °C), the mean hydrodynamic sizes were increased as the $AgNO_3$ concentration increases, except the nanoparticles that produced at 60 °C using 1.0 M of $AgNO_3$. The increasing trend of the NSPs hydrodynamic size is a good agreement with early size prediction by UV-Vis and also physical size from TEM. As the concentration of $AgNO_3$ increases, the hydrodynamic size becomes larger. When the

$AgNO_3$ concentration is relatively high, the stabilizer might find difficulty to fully coat the particles (Alahmad, 2014) and subsequently, increased the fraction of uncoated nanoparticles, leading to a higher tendency of the particles to interact with each other (Foliatini et al. 2015). Hence, larger NSPs will be formed. From the view of constant concentration, all the prepared NSPs have demonstrated an increment in the hydrodynamic size as the temperature increases. It has been known that increase in temperature allows a higher degree of the momentum of moving particles, resulting in higher probabilities of collisions between NSPs by Brownian motion (Chiad et al. 2013), hence causing particles aggregate to form larger particle size.

Table 4.1: The average hydrodynamic size and zeta potential for all NSPs

Sample	Hydrodynamic size (nm)	Zeta potential (mV)
S1T6	85.19	-30.87
S2T6	92.98	-25.17
S3T6	64.81	-30.03
S1T8	96.46	-27.83
S2T8	101.0	-30.37
S3T8	105.2	-28.47

The zetapotential (*Zp*) value was measured to estimate the electrostatic stabilization of the nanoparticles. The *Zp* value was discovered to be in the range from -25.17 to -30.87 mV (Table 4.1). Some of the colloidal NSPs was found have stable dispersion based on the *Zp* value which was taken at pH 8. According to Carneiro-da-Cunha et al. (2011), when the particles have a large positive or negative *Zp* (greater or lower than +30 mV and -30 mV), they will repel each other and the dispersion is stable. On contrary, when the particles have low *Zp* values, the particles tend to aggregate due to no sufficient force to prevent the aggregation. Based on this statement, nanosilver colloidal labeled as S1T6,

S3T6 and S2T8 can be classified as stable colloidal. The rest colloidal with the label of S2T6, S1T8 and S3T8 showed lower *Zp* values, indicating the solution are less stable. These lower *Zp* values were a good agreement to the TEM images as shown previously, where the particles obviously formed agglomeration and aggregation.

4.1.5 Microstructural Analysis

The XRD patterns of the synthesized nanoparticles are shown in Figure 4.6 the prominent peaks were detected at the angle of 2θ = 38.2°, 44.5°, 64.6° and 77.6° which correspond to the (111), (200), (220) and (311) Bragg's reflections respectively. All the detectable peaks can be indexed to face-centered cubic (FCC) silver crystal structure which is consistent with the JCPDS 04-0783 (Ajitha et al. 2013). No counterfeit diffraction pattern was observed, indicating the absence of impurities in all the sample. The absence of impurities in the samples prove the washing process was conducted perfectly.

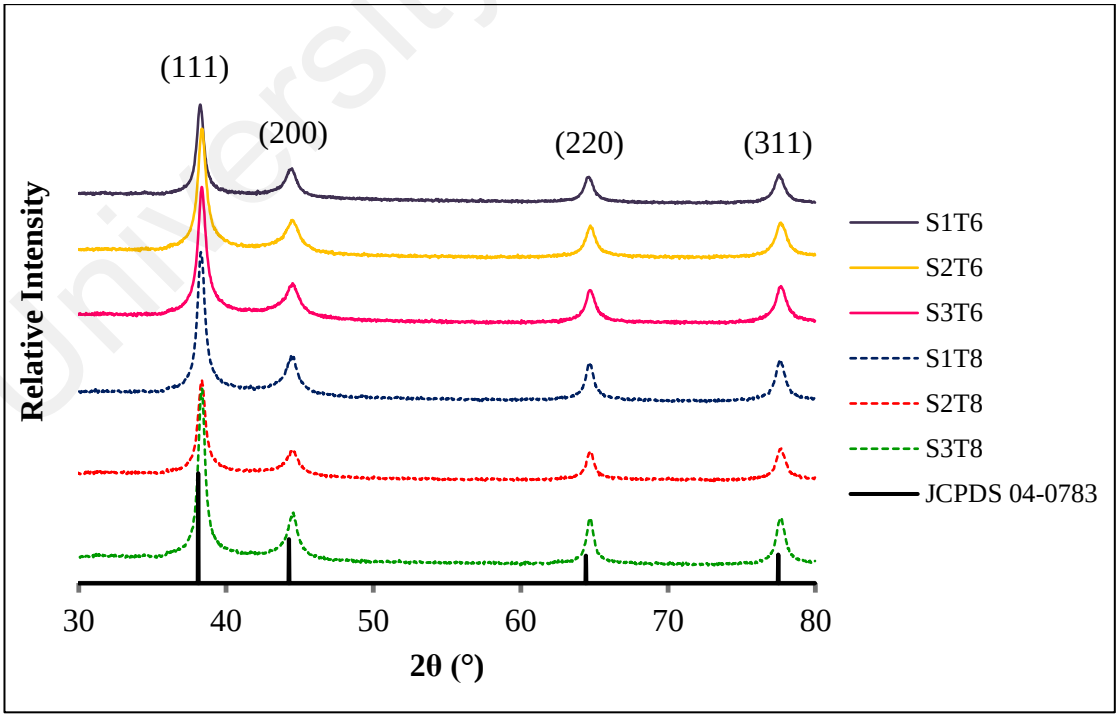

Figure 4.6: XRD patterns of produced NSPs at 60 °C and 80 °C for different $AgNO_3$ concentration (0.1 M, 0.5 M and 1.0 M)

The trend of the diffraction peak intensity and the peak width as shown in Figure 4.6 was used to predict the crystallite size of NSPs. Hassanien and Akl (2015) reported that an increment of intensity with the reduction of the peak width might due to the crystallite growth, increment of crystallinity degree or both. In order to prove the growth of crystallite, the average crystallite size of the NSPs was calculated from all prominent peaks from the diffraction pattern using Debye-Scherrer equation (Lanje et al. 2010; Ajitha et al. 2013; Agnihotri et al. 2014) as shown below.

$$D = \frac{0.94\lambda}{\beta \cos\theta} \tag{5.1}$$

where, λ is the wavelength of the source (1.54Å), β is a full half of maximum width (FHMW) of the peaks and θ is diffraction angle. The calculated average crystallite size was tabulated in Table 4.2.

Table 4.2: Calculated average crystallite size and lattice constant for all samples

Sample	Average crystallite size (nm)	Lattice constant (nm)
S1T6	3.30	0.4073
S2T6	5.57	0.4066
S3T6	5.54	0.4069
S1T8	2.53	0.4071
S2T8	3.72	0.4068
S3T8	6.96	0.4063

The calculated size displays a similar trend as UV-vis prediction in which the size increased and slightly decreased as concentration increases from 0.1 M to 1.0 M at 60 °C. Same goes for the NSPs that produced at 80 °C which recorded an increment of crystallite sizes with increasing of precursor concentration. This might due to the higher collision of particles with each other and thus, the stabilizer unable to prevent the particles from

aggregating. An et al. (2009) stated that the collision between particles become more frequent with further increasing of precursor concentration and the protection layer of nanoparticles was canceled out, resulting to the formation of particles aggregation.

At constant concentration (0.1 M and 0.5 M), the crystallite size of NSPs showed a decreasing trend when the temperature increases from 60 °C to 80 °C. Higher temperature will increase the rate of reaction, in which the reactants consume faster, hence reaction depletion takes place, leading to the formation of smaller nanoparticles and narrow size distribution (Fayaz et al. 2009). In contrast, at higher concentration (1.0 M), the crystallite size was found have an increasing trend as the physical size from TEM analysis.

Figure 4.7 displays the magnified view of the intense peak at the plane (111). The intense peak of NSPs that produced at 60 °C obviously shifted to the higher diffraction angle as the precursor concentration increase from 0.1 M to 0.5 M and slightly shifted to the lower angle as the concentration further increase to 1.0 M. For the produced NSPs at 80 °C, the peak was slightly shifted to higher angle as the concentration increase from 0.1 M to 1.0 M. At constant concentration (0.1 M and 1.0 M), the (111) peak was observed slightly shifted to higher angle, while, the intense peak for the produced NSPs using 0.5 M recorded reverse shifting as the temperature increase from 60 °C to 80 °C. These peaks shifting might due to the change of lattice, which closely related to the crystallite size. This shifting phenomenon was supported by the calculated lattice constant as tabulated in Table 4.2. The lattice constant was calculated using the following equation.

$$d_{hkl} = \frac{a}{\sqrt{h^2+k^2+l^2}} \tag{5.2}$$

In general, these peaks shifting directly proportional to the crystallite size and inversely proportional to the lattice parameter. The peaks position of (111) diffraction line shifted

to higher angles, with the increase of crystallite size and shrinkage the lattice/reduce the lattice parameter (Wei et al. 2007).

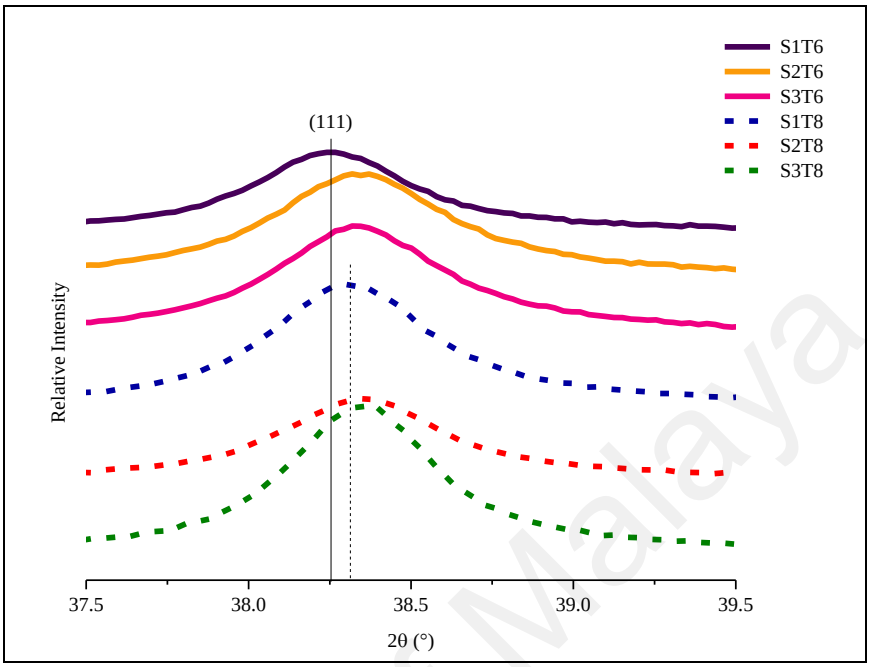

Figure 4.7: The magnified view of the shifting of XRD prominent peak at plane (111)

4.1.6 Chemical Composition Analysis

Figure 4.8 demonstrates the FTIR spectra for the synthesized NSPs (S1T8) and pure PVP. All the characteristic peaks of PVP were obviously detected in the S1T8 spectrum indicates the PVP molecules adsorbed on the NSPs surface, confirm the formation of complex ion. From the S1T8 spectrum, broad and weak bands were observed at 3433 cm^{-1} and 2976 cm^{-1} indicating the stretching vibration of OH from the intermolecular hydrogen bond and asymmetric CH from a methyl group, respectively. A sharp peak of amide carbonyl group (-N-C=O) appeared at 1616 cm^{-1} was red-shifted from 1648 cm^{-1} peak in the PVP spectrum. The wavenumber decrement for the C=O band may because of the bond weakening by means of an incomplete donation of oxygen to the silver, which

is predicted in the NSPs formation mechanism. This statement is supported by Zhang et al. (1996) and Liu et al. (2008) in their article journals.

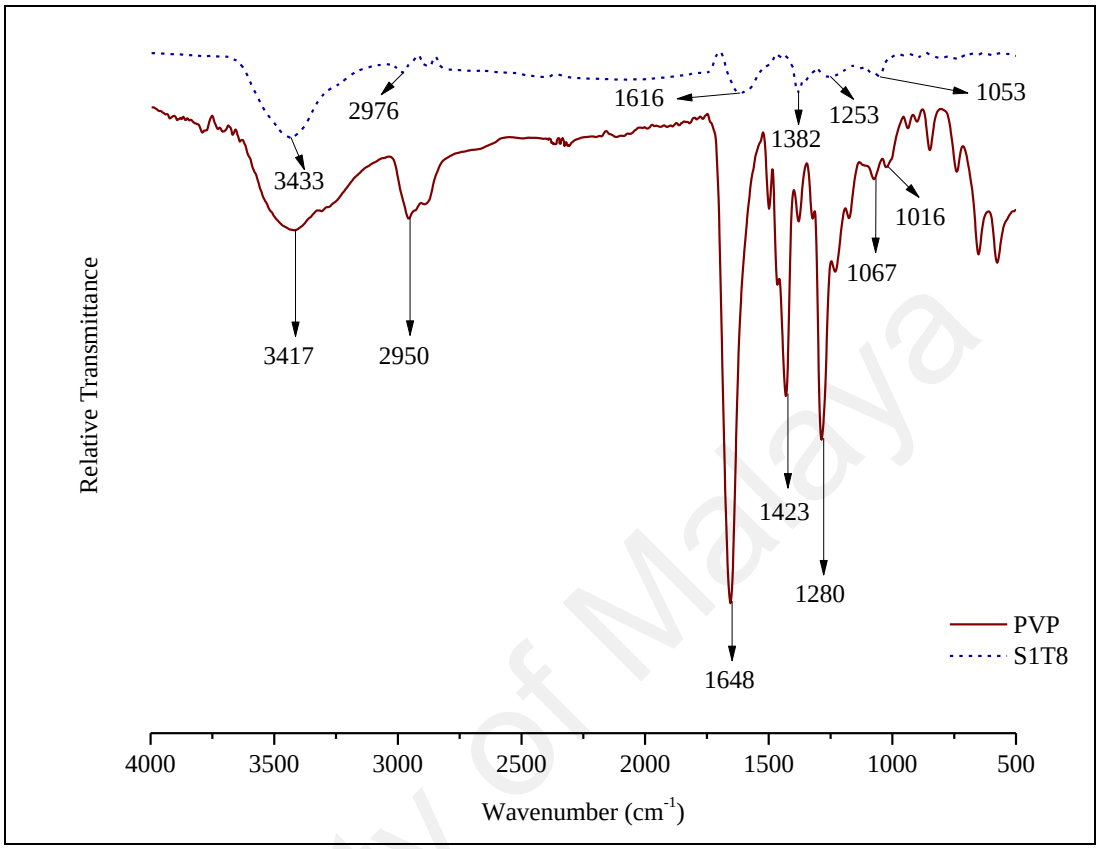

Figure 4.8: FTIR spectra of S1T8 and PVP

In the fingerprint region, a sharp and medium absorption band that detected at 1382 cm^{-1} might be attributed to the bending absorption of CH_3. At 1253 cm^{-1} and 1053 cm^{-1}, broad and weak absorption peaks were observed which attribute to –C-N stretching vibration. Both of these peaks were slightly shifted from the PVP peaks because of the bonding formation between Ag atom with PVP. The formation of coordinative bonding between Ag atoms and nitrogen or oxygen atoms from PVP units, leads to the peaks shifting phenomena (Bryaskova et al. 2011).

4.1.7 Magnetic Analysis

Bulk silver is well known as one of the diamagnetic materials, which shows a negative slope of the M-H curve (Jo et al. 2006) and produces negative magnetic susceptibility. However, silver in the nanosize range unexpectedly showed different magnetic properties. As shown in Figure 4.9, the magnetization curve of the produced NSPs shows the non-linear and hysteretic curve.

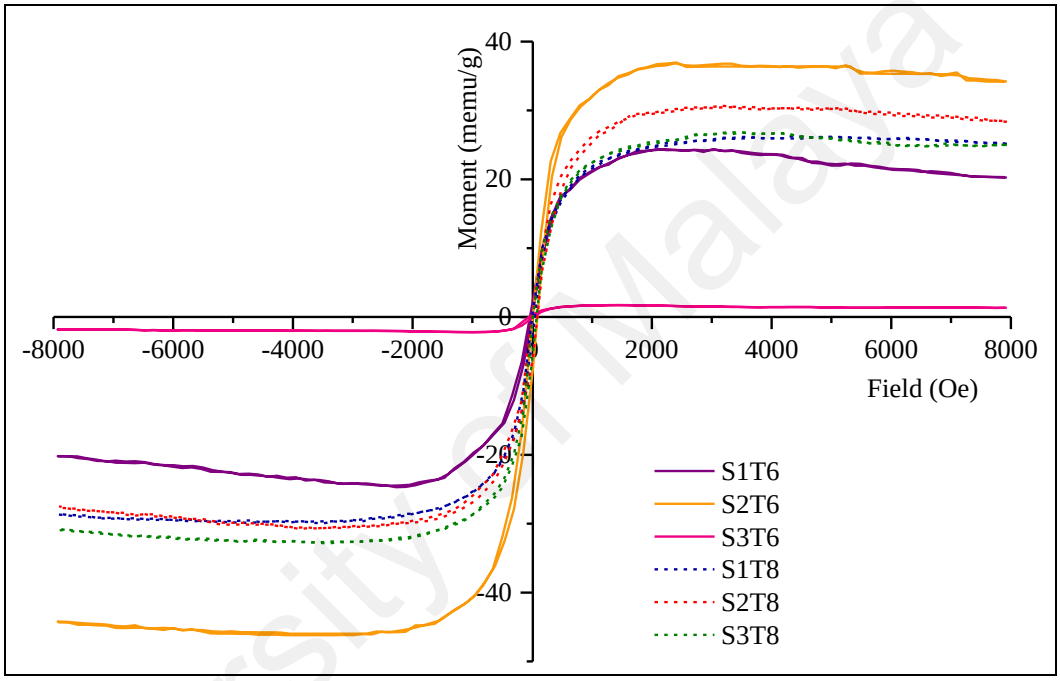

Figure 4.9: Magnetization curves for all samples measured at room temperature

The narrow loops were clearly observed for all the samples as shown in Figure 4.10, indicating the ferromagnetic-like behavior of the NSPs. The produced NSPs can be classified as soft magnetic particles due to the shape of the M-H curve which have a small loop with low coercive forces.

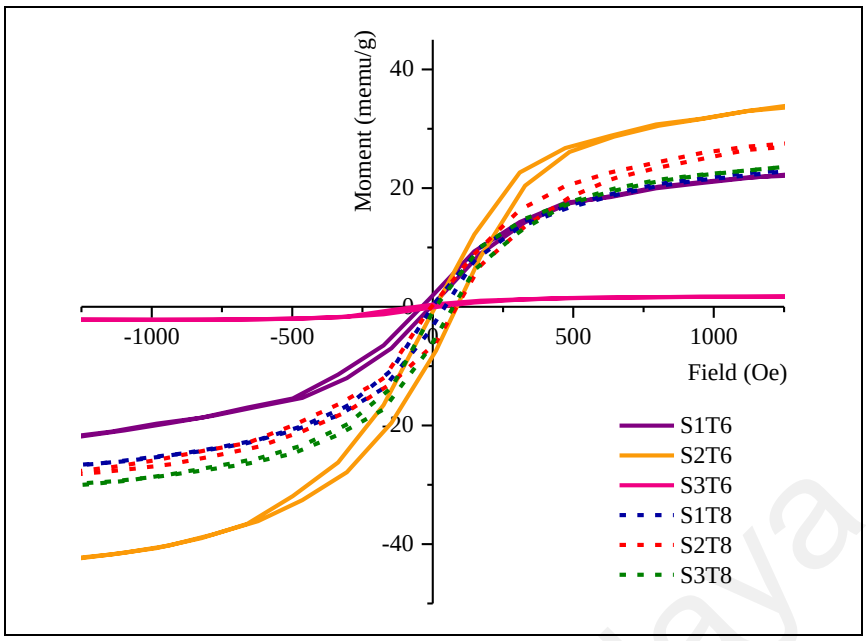

Figure 4.10: The magnified view of the curves at low magnetic fields

Table 4.3 summarizes the value of saturation magnetization (*Ms*), coercivity (*Hc*) and remanence (*Mr*) for all the sample. The changes in the *Ms* and *Hc* showed a similar trend for both reaction temperature, which the values increased when the precursor concentration increasing from 0.1 M to 0.5 M and as the concentration further increased to 1.0 M, the value shows decrement. This trend has a similar pattern as the changes in crystallite size of the prepared NSPs, except for sample S3T8. Generally, the saturation magnetization might relate to the size. The reduction in size causes an increment in surface area, leading to a higher surface to volume ratio and hence, reduces the saturation magnetization (Lanje et al. 2010). The inconsistency and randomness of the coercivity and remanence changes might due to the presence of particle aggregations which could influence the magnetic properties of the materials (Eid et al. 2015). To sum up, NSPs which behave as a ferromagnetic material was needed in the water filtration applications because if these nanoparticles leached and presented in the filtrate, separation of these nanoparticles can be performed by just applying an external magnetic field, thus, producing a clean water.

Table 4.3: The saturation magnetization, coercivity and remanence for all NSPs

Sample	Saturation magnetization (memu/g)	Coercivity (Oe)	Remanence (memu/g)
S1T6	24.57	22.80	1.10
S2T6	41.63	47.88	1.92
S3T6	1.97	18.24	1.30
S1T8	28.16	22.80	4.45
S2T8	30.75	41.04	0.0029
S3T8	29.90	36.48	2.12

4.1.8 Summary of Phase I

The comparison of size between hydrodynamic size, physical size as well as crystallite size was summarized in Table 4.4 and Figure 4.11. It can be concluded that at low temperature (60 °C), the size was increased when the $AgNO_3$ concentration increases from 0.1 M to 0.5 M, and as the concentration further increases to 1.0 M, the size become smaller. This might due to the reducing agent unable to reduce the precursor completely, leading to the decrement of the released Ag^+ ions, and hence, forms smaller nanoparticles. On contrary, the size gradually increased as the $AgNO_3$ concentration increases at a higher temperature (80 °C). Particles tend to aggregate at high temperature and high precursor concentration because more particles are available in the system and higher collision frequency between particles, that allow more nucleation and aggregation process took place.

In summary, the smallest nanoparticle can be obtained by producing nanoparticle at a higher reaction temperature using lowest precursor concentration. Therefore, S1T8 was selected as nanofiller to be incorporated into the polymer membrane in the next phase because it has the smallest physical and crystallite size, which is 25.34 nm and 2.53 nm,

respectively. The selection of the smallest nanoparticles is basically due to their largest surface area to volume ratio that will increase the effectiveness of the nanoparticles.

Table 4.4: Hydrodynamic, physical and crystallite size of samples

Sample	S1T6	S2T6	S3T6	S1T8	S2T8	S3T8
Hydrodynamic size (nm)	85.19	92.98	64.81	96.46	101.0	105.2
Physical size (nm)	27.48	35.20	25.72	25.34	30.79	39.13
Crystallite size (nm)	3.30	5.57	5.54	2.53	3.72	6.96

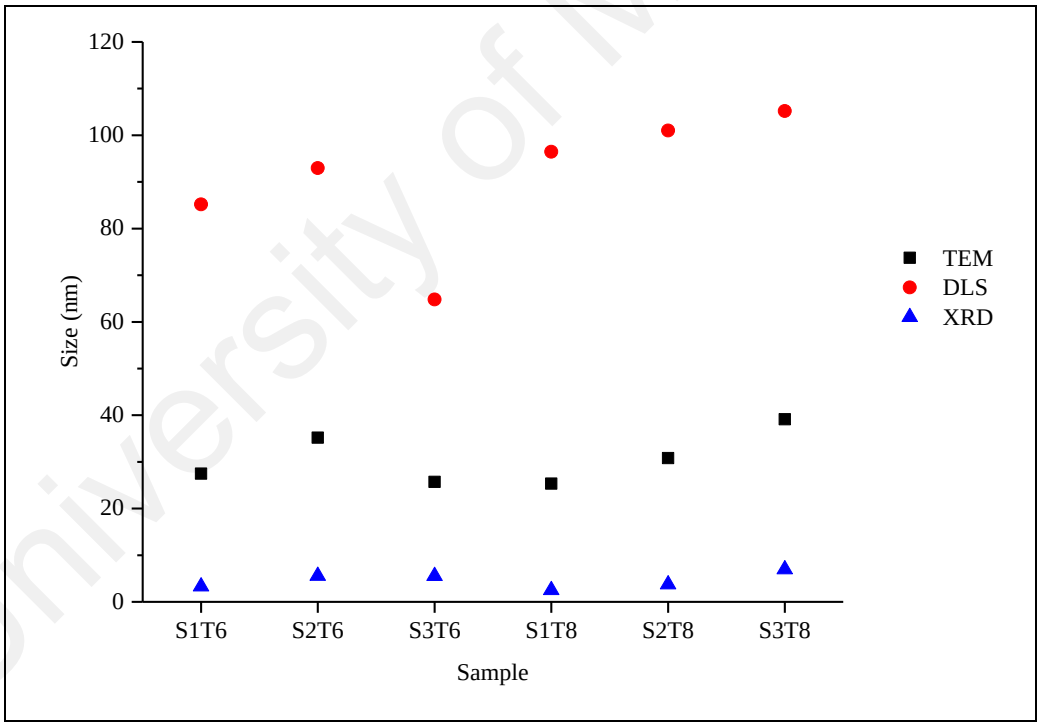

Figure 4.11: Summary of size from TEM, DLS and XRD analysis for all sample

4.2 Phase II: Fabrication of Electrospun PVDF/NSPs NFM via Electrospinning

In this phase, nanofibrous nanocomposite (PVDF/NSPs) membrane was fabricated using the electrospinning process. An investigation was carried out by varying the weight

percent of NSPs in the membrane to study the outcome of NSPs weight percent on the properties of electrospun nanofibrous membrane especially morphology, fiber diameter, elemental and porosity. Morphology, fiber diameter and porosity is an essential element for the membrane because they will determine the capability of the membrane to retain *E. coli* from penetration and to avoid leaching of NSPs from the membrane. Membrane elemental is another important part of this study because it will prove the functionality of NSPs toward *E. coli*.

4.2.1 Surface Morphology and Fiber Diameter Analysis

Figure 4.12 shows the morphology of electrospun NFM viewed under low and high magnifications. All sample were obviously composed of randomly oriented fibers as seen in the high magnification micrographs. Among the electrospun NFM, pure PVDF has the highest number of beads (Figure 4.12 (a)) and the formation of beads start to reduce when NSPs were added into the PVDF (Figure 4.12 (b)). When the NSPs loads further increased to 1.0 wt% (Figure 4.12(c)) and 3.0 wt% (Figure 4.12(d)), the electrospun NFM clearly showed fewer beads or almost bead-free and the distance between beads also further. The reduction of beads formation might due to high viscosity and conductivity of the polymer solution with the addition of NSPs. Incorporation of NSPs has indirectly raised the conductivity of a solution because the nanoparticles itself are highly conductive. NSPs may act as charge carriers that cause the solution conductivity to increase the charge density of the jet and, thereby, enhance instabilities. The addition of higher NSPs in the polymer matrix has produced electrospun NFM with fewer beads due to the upsurge of net charge density (conductivity) of the polymer solution, which suppresses the Rayleigh instability and enhances the whipping instability, leading to the formation of bead-free fibers (Heikkilä & Harlin, 2009).

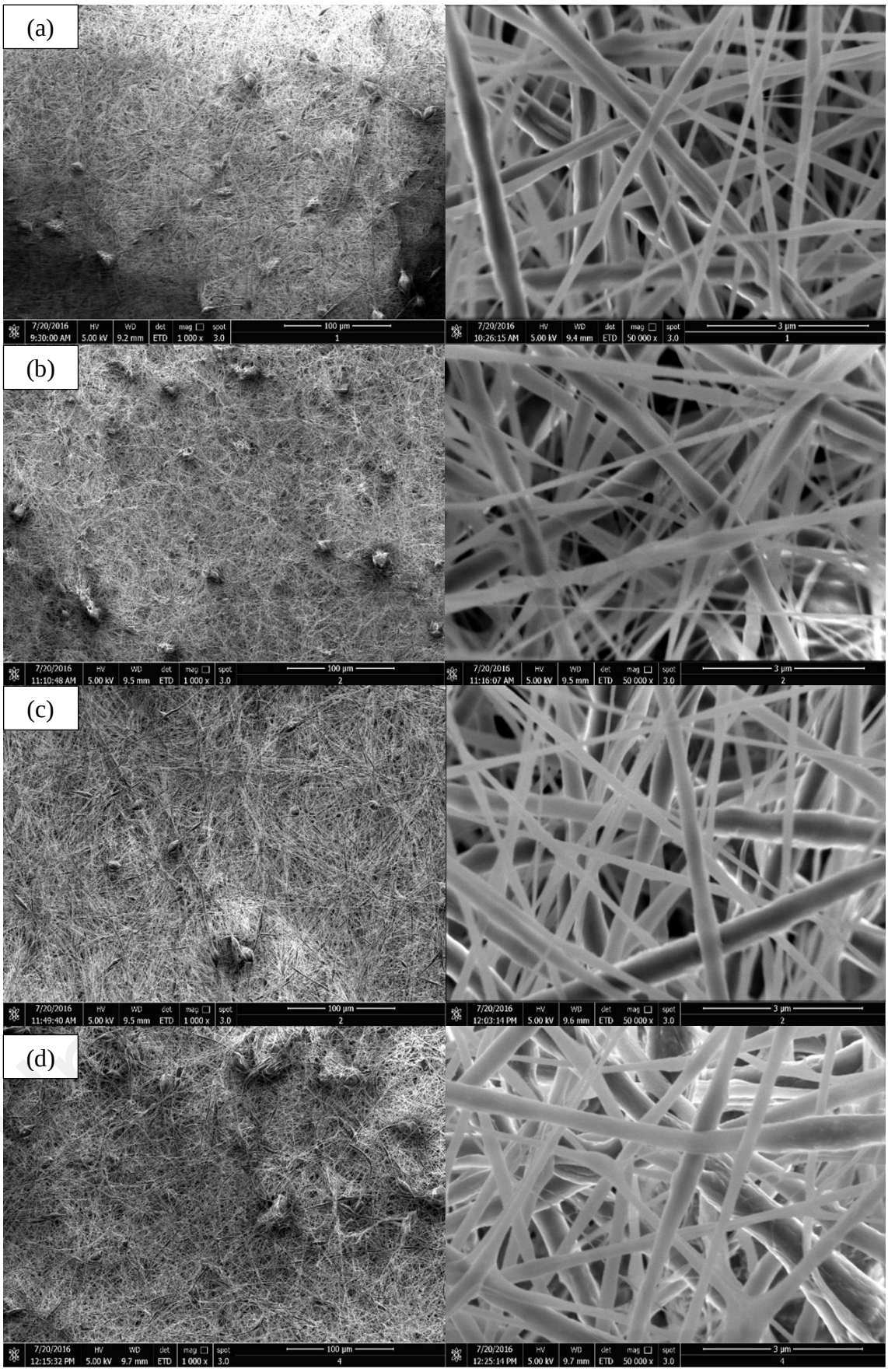

Figure 4.12: Low (1000x) and high (50000x) magnification FESEM micrograph of electrospun NFM (a) PVDF (b) PVDF-0.5 wt% NSPs (c) PVDF-1.0 wt% NSPs (d) PVDF-3.0 wt% NSPs

The fiber diameter distribution of NFM was plotted in the box plot and whisker chart as shown in Figure 4.13. The blue line indicates the average diameter of the fiber and the black line representing the median value of 100 fibers. The average diameter for sample PP, PS0.5, PS1.0 and PS3.0 was 150 ± 4.09 nm, 171 ± 7.65 nm, 223 ± 9.82 nm and 311 ± 14.28 nm, respectively. As expected, pure PVDF membrane have the narrowest fiber diameter distribution, where most of the fibers lie in the range of ≈ 115-176 nm and PS3.0 membrane have the broadest fiber diameter distribution which most of the fiber lies in the range of ≈ 216-359 nm.

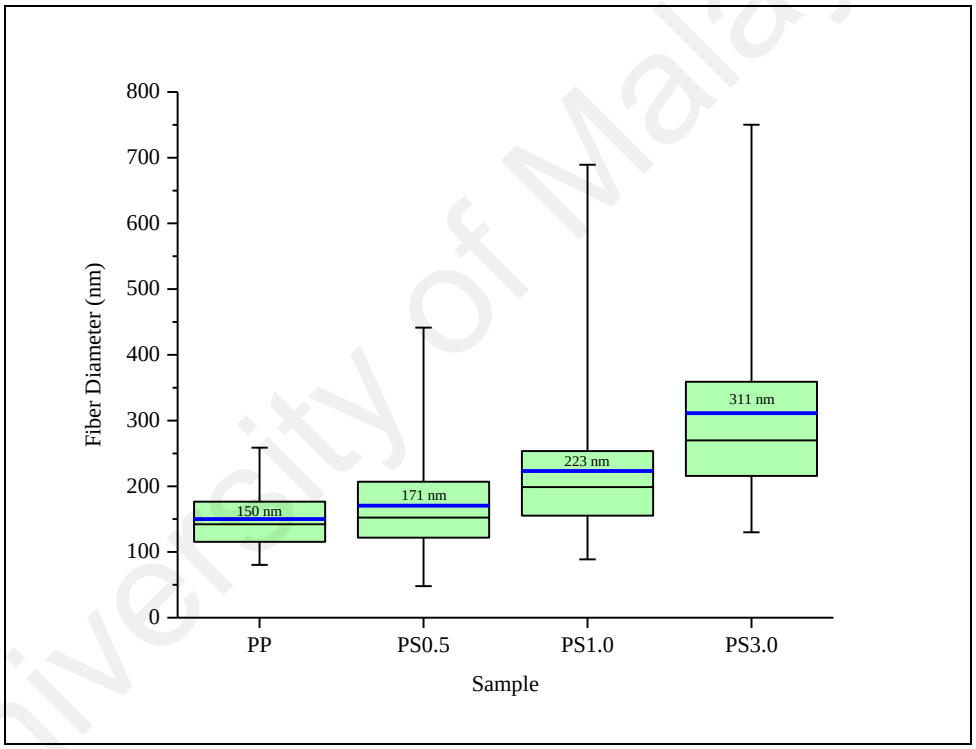

Figure 4.13: Fiber diameter distribution for all electrospun NFM

The calculated average fiber diameter was tabulated in Table 4.5. It was clearly observed that the average diameter increased when the NSPs weight percent increasing. As has been mentioned earlier, NSPs that used in this phase are coated with PVP and it is highly conductive. The characteristics of this nanoparticles caused the increases in

concentration and conductivity of polymer solution. Conductive NSPs may increase the flow rate and may affect the interactions in the solution, which can lead to larger fibers (Heikkilä & Harlin, 2009). The higher concentration will lead to the higher polymer viscosity and be resulting in the formation of larger fiber. This might be attributed to the greater resistance of the solution to be stretched by the charges on the jet (Souhaimi & Matsuura, 2011).

Table 4.5: Average fiber diameter for all sample

Sample	Fiber diameter (nm)		
	Min	**Max**	**Average**
PP	80.4	258.7	150.0 ± 4.09
PS 0.5	48.0	441.5	170.6 ± 7.65
PS 1.0	88.7	689.3	223.2 ± 9.82
PS 3.0	129.9	750.3	311.2 ± 14.28

4.2.2 Elemental Analysis

The presence and distribution of NSPs in the electrospun NFM was analyzed using EDS. From Figure 4.14, carbon (C) and fluoride (F) peaks were detected in every sample. The evolution of these peaks is due to the fact that PVDF as a matrix for the electrospun NFM and consists of these two molecular species at the elemental level (Sheikh et al. 2009). Figure 4.14(a) is an EDS spectrum for PVDF NFM and from this data, we can conclude that the membrane is not contaminated with other elements.

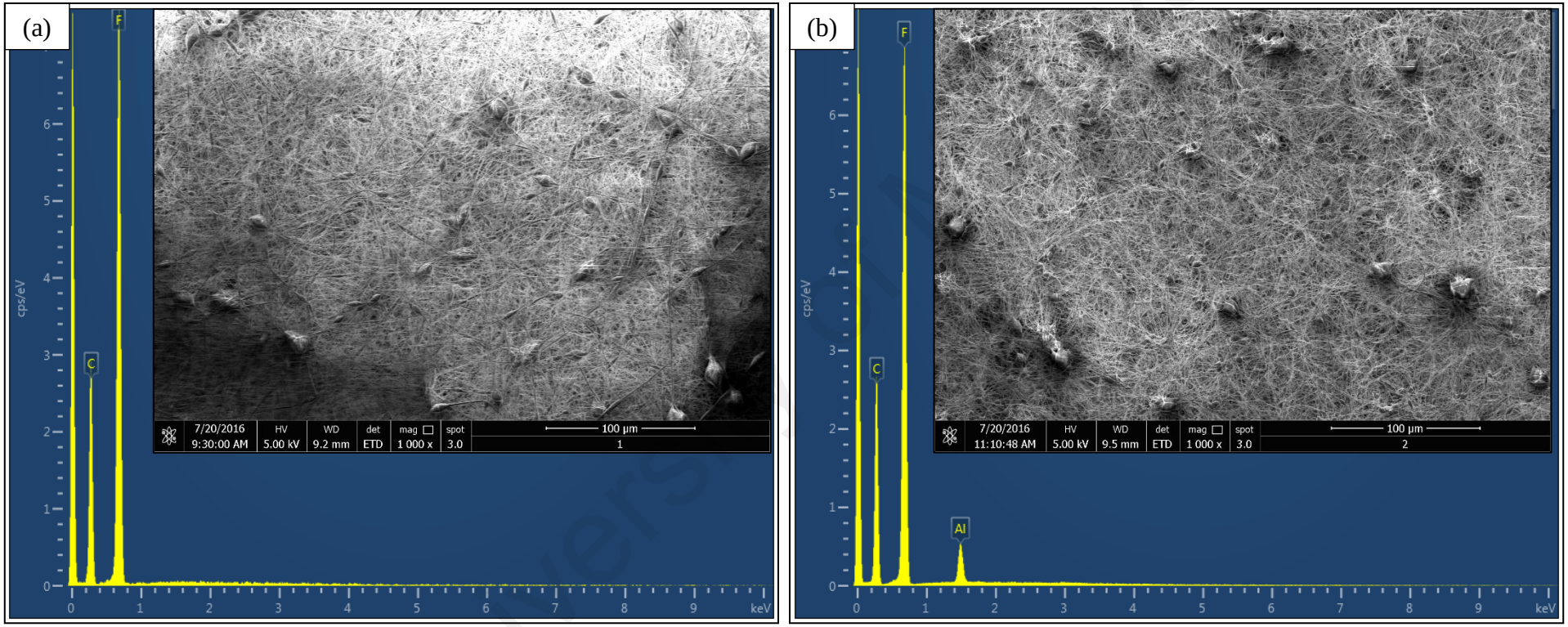

Figure 4.14: EDS spectrum ranging from 0 keV to 10 keV for all electrospun NFM (a) pure PVDF NFM (b) PVDF-0.5 wt% NSPs (c) PVDF-1.0 wt% NSPs (d) PVDF-3.0 wt% NSPs. Inset is map scanning area for elemental study for every sample

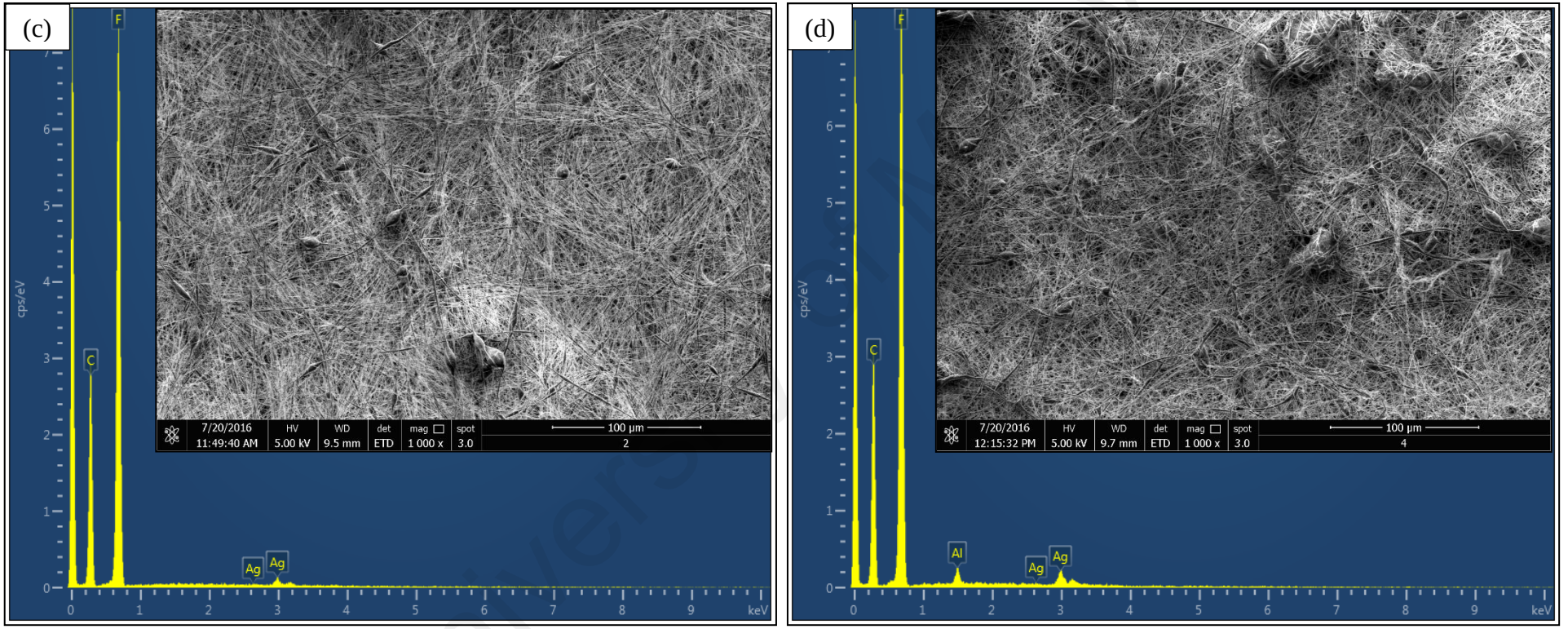

Figure 4.14: continued.

Silver peak was clearly observed in Figure 4.14(c) and Figure 4.14.(d) which proved the presence of NSPs in the NFM. While, in Figure 4.14(b) and Figure 4.14(d), aluminium peak was detected. The presence of this peak can be attributed to the underlying aluminium foil that used in collecting the fiber membrane.

Table 4.6 indicates the extracted data from the EDS spectrum for each sample. The amount of Ag was increased as the NSPs load increases, except for sample PS0.5 in which Ag was not detected. Since PS0.5 was produced using lowest NSPs load (0.5 wt%), the EDS machine unable to detect the Ag element due to the detection limit. As mentioned above, when the NSPs load increases, the detected Ag also increases. This might due to NSPs was successfully embedded into or/and on the surface of the membrane.

Table 4.6: Elemental analysis for all sample

Sample	Weight percent of elements (wt%)			
	F	C	Ag	Al
PP	60.0	40.0	-	-
PS 0.5	54.9	42.2	-	2.9
PS 1.0	57.8	39.9	2.2	-
PS 3.0	56.2	38.9	3.9	1.0

Figure 4.15 represents the distribution of NSPs on the NFM surface. Even though, the amount of Ag was unable to record for sample PS0.5, the distribution of NSPs was clearly observed on the surface of the membrane as shown in Figure 4.15 (a). Meanwhile, NSPs was uniformly distributed on the PS1.0 (Figure 4.15 (b)) and PS3.0 (Figure 4.15 (c)) surface with a little bit of aggregation that might occur during the preparation of polymer solution. In the preparation of polymer solution, NSPs was dispersed in DMF, heated up to 70 °C together with PVDF and stirred continuously for a long time. During this step,

nanoparticles might gain enough force to move vigorously in the system and the probability for the nanoparticles to collide and attach with each other is high, leading to the growth of the crystals.

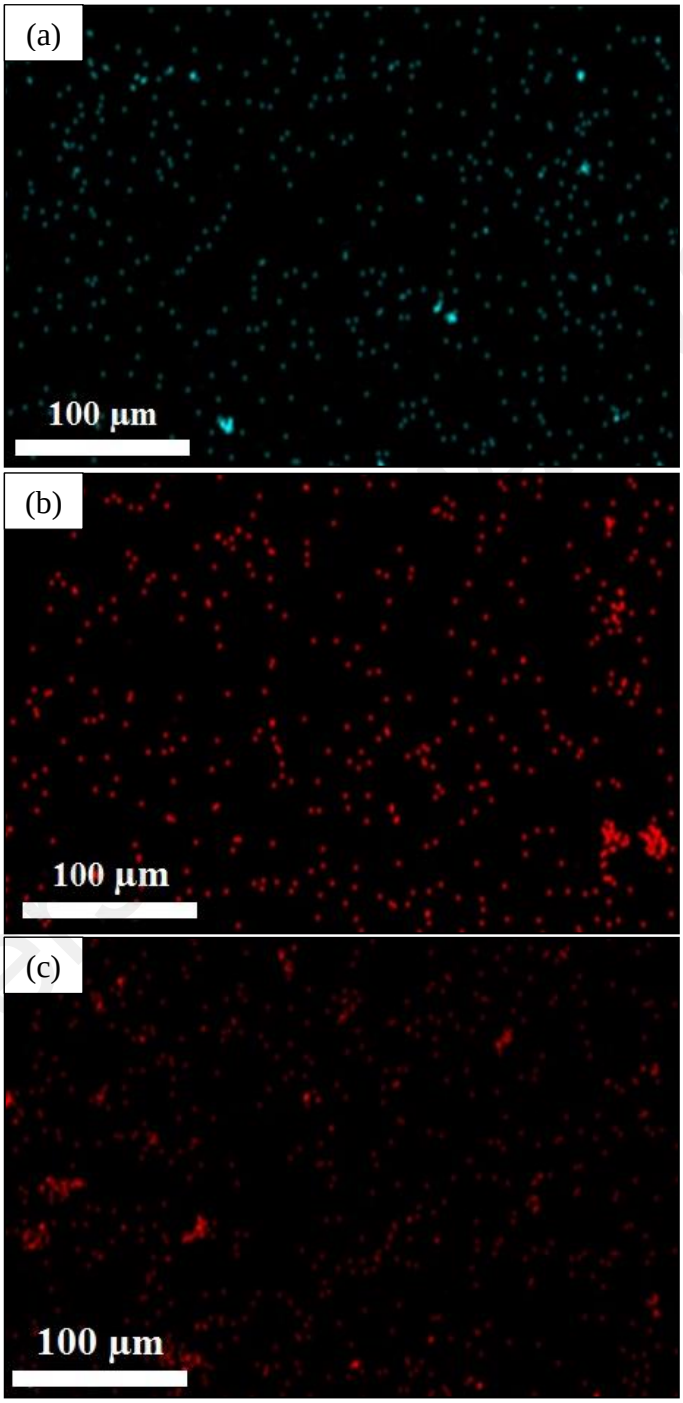

Figure 4.15: Distribution of NSPs on the nanofibrous membrane surface (a) PVDF-0.5 wt% NSPs (b) PVDF-1.0 wt% NSPs (c) PVDF-3.0 wt% NSPs

4.2.3 Microstructural Analysis

Figure 4.16 shows the XRD pattern of pure PVDF and all the electrospun PVDF/NSPs NFM. The characteristic peaks of PVDF crystal were recorded at around 2θ = (18.4°, 26.2°) and 20.7° that corresponding to the α-phase and β-phase, respectively (Sheikh et al. 2014; Agyemang et al. 2015). The formation of α-phase and β-phase in the diffraction pattern validated that PVDF has a semi-crystalline structure (Amouamouha & Badalians Gholikandi, 2017). For sample PS0.5, PS1.0 and PS3.0, in addition to the diffraction peaks of PVDF, four prominent peaks were observed at 2θ = 38.3°, 44.9°, 64.6° and 77.6° which can be respectively corresponded to the (111), (200), (220) and (311) Bragg's plane of silver crystal structure. These peaks were consistent with the reference file (JCPDS 04-0783). The existence of characteristic peaks of PVDF and silver verified that PVDF and NSPs coexist in the membrane.

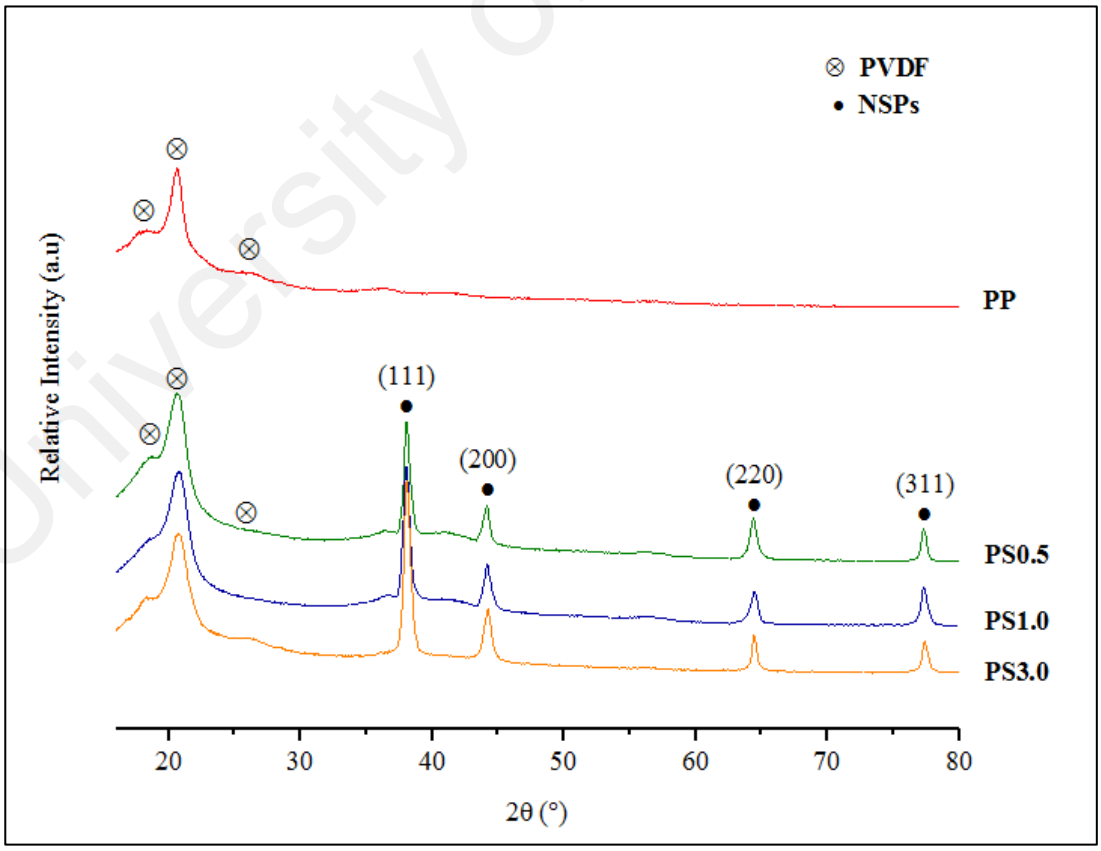

Figure 4.16: XRD diffraction patterns for PP, PS0.5, PS1.0 and PS3.0

From the diffraction pattern of PVDF/NSPs NFM, the diffraction peaks of silver become more intense especially peak at (111) plane after the addition of different NSPs loads. The increment of intensity might due to the crystallite growth or rise of degree crystallinity (Hassanien & Akl, 2015). As mentioned earlier in section 4.2.2, the continuous stirring process during the preparation of the polymer solution allows the nanoparticles to collide and stick together, and thus, lead to the growth of the crystals.

4.2.4 Pores Distribution and Specific Surface Area Analysis

In general, all electrospun NFM exhibit type IV adsorption desorption isotherm as shown in Figure 4.17(a) – (d). At the initial region ($P/P_o \rightarrow 0$), the adsorption value approximately equal to zero that indicates the absence of microporous structure in the membrane. A gradual rise in the absorbed volumes of nitrogen as the relative pressure increases and a sudden increased of nitrogen uptake at high relative pressure ($P/P_o = 1$) were noticed from the adsorption curve. However, sample PS0.5 does not show a flat region as compared to the other sample, which it might due to a larger specific surface area. The flat region on the curve corresponds to the monolayer formation, while, the acute increase of nitrogen uptake indicates the multilayer formation (Xavier & Banda, 2016). In addition, a hysteresis loop was clearly viewed in all isotherms which are evidence of mesopores structure, where the first order capillary condensation transition occurs (Bulgariu et al. 2007; Shornikova et al. 2008; Wang et al. 2016; Xavier & Banda, 2016).

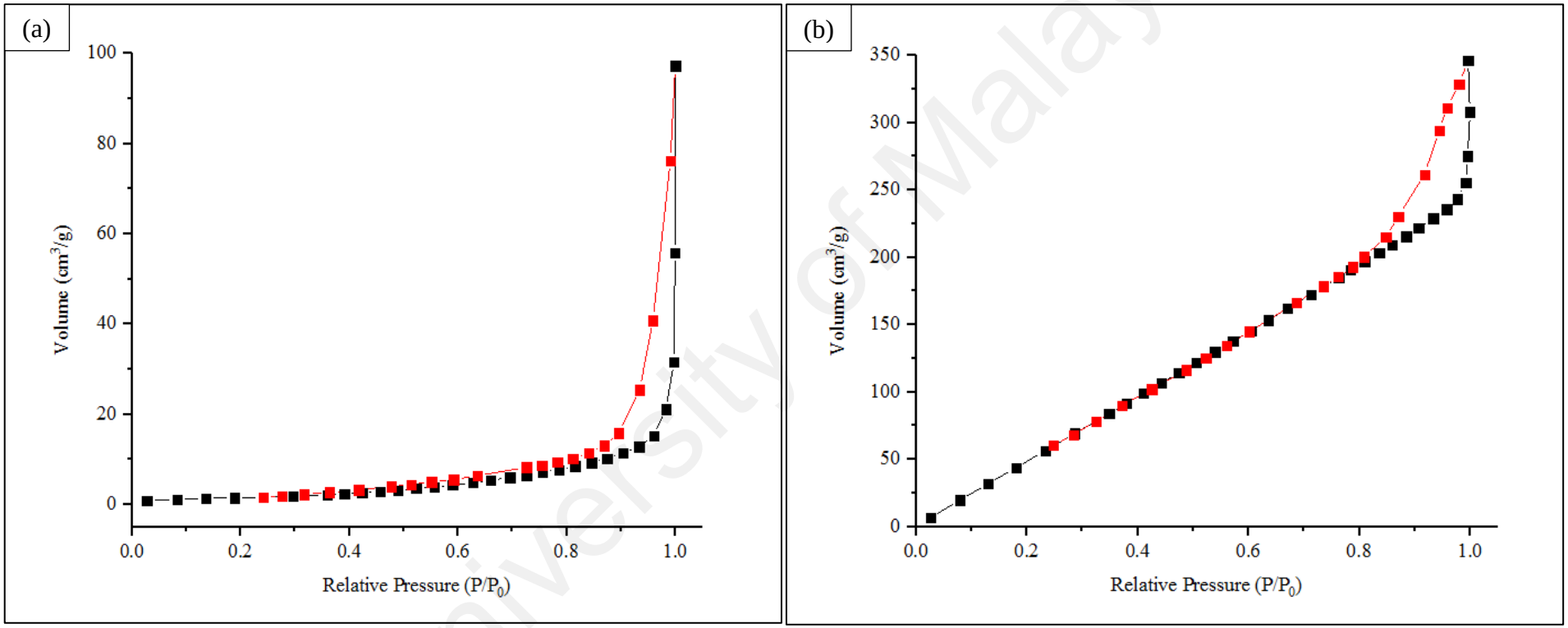

Figure 4.17: Nitrogen adsorption desorption isotherm for the electrospun nanofibrous membrane (a) PP (b) PS0.5 (c) PS1.0 (d) PS3.0

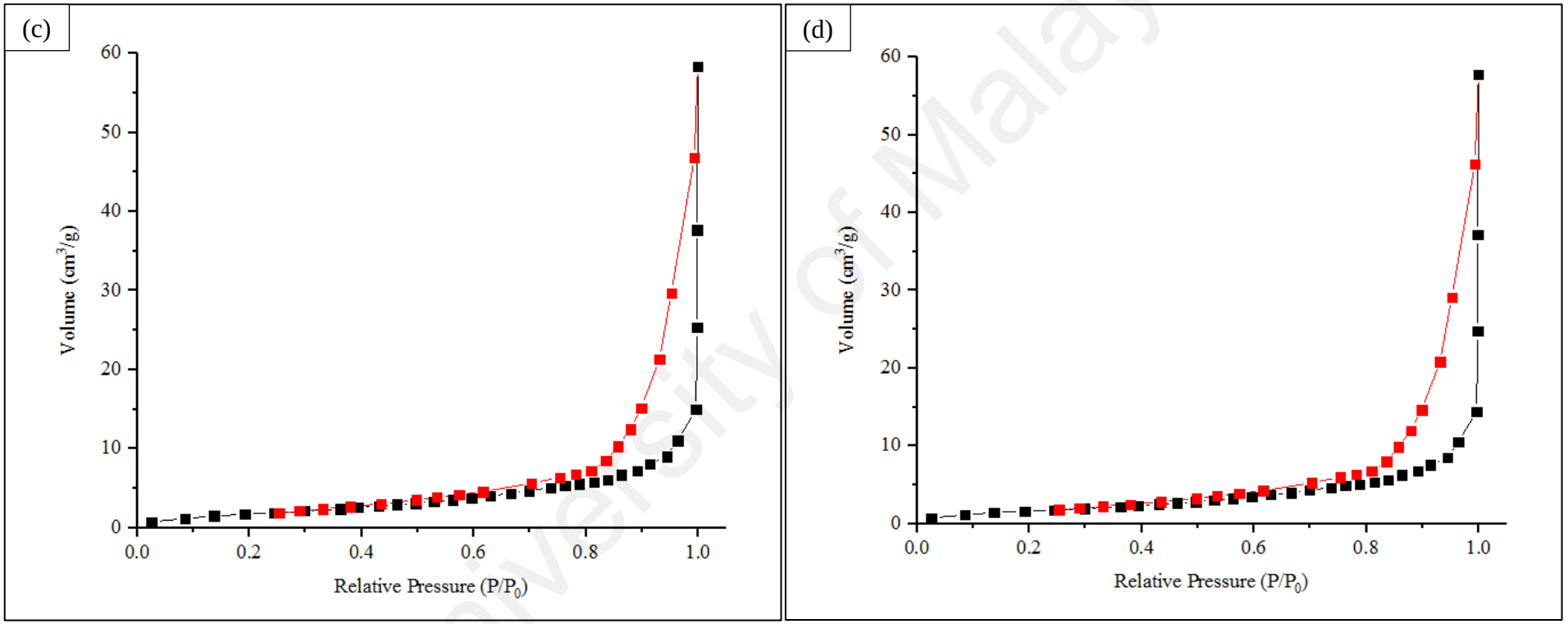

Figure 4.17: continued.

Table 4.7 shows the Brunauer-Emmett-Teller (BET) specific surface area, pore specific volume and average pore diameter of the sample. As can be seen, the specific surface area was directly proportional to the pore specific volume, where the surface area increased when the pore volume increasing and decreased with the decreases of pore volume. A significant increase in pore volume as well as the surface area was observed with the addition of 0.5 wt% NSPs and decline when the NSPs load further increase up to 3 wt%. The incorporation of highly porous NSPs (Average pore size = 148.30 nm) into the polymer matrix indirectly increased the overall pore volume of electrospun NFM. However, the further addition of NSPs in the polymer has decreased the total porosity, which might due to the agglomeration of nanoparticles (Rastgar et al. 2017). Besides that, the presence of pores in the electrospun NFM might be related to the intra-fiber formation. The higher formation of intra-fiber pores that created by the phase separation based on evaporation of the solvent or in the presence of a vapor during electrospinning and by electrospinning of the polymer composites followed by selective removal of a component (Greiner & Wendorff, 2007; Matsumoto & Tanioka, 2011) caused an increment of the electrospun NFM surface areas. In this analysis, the pore diameter of electrospun NFM is the main focus due to it helps in determining the capability of the membrane to retain *E. coli* on the membrane surface. The average pore diameter of the electrospun NFM was drop abruptly with the incorporation of 0.5 wt% NSPs into PVDF. The decrease of pore size with the addition of nanoparticles might due to the increased viscosity of the blend solution by the addition of nanoparticles. The increment of viscosity typically delays the exchange of solvent and nonsolvent and suppresses the formation of large pore size (Vatanpour et al. 2012). Yet, further addition of NSPs up to 3 wt% increased the pore size. This phenomenon might due to the atoms occupy the framework of the polymer as the nanoparticles content increases (Vinu et al. 2007). Overall, the pore size of the membrane less than the dimension of *E. coli* cell (0.25-1 μm in diameter and 2 μm long),

verified the membrane able to retain all the bacteria cells from passing through the membrane.

Table 4.7: Physisorption properties of the electrospun nanofibrous membrane

Sample	Specific surface area (m^2/g)	Pore specific volume (cm^3/g)	Average pore diameter (nm)
PP	5.58	0.049	34.93
PS 0.5	408.79	0.426	4.16
PS 1.0	7.21	0.023	12.83
PS 3.0	6.54	0.022	13.63

In summary, NFM that incorporated with NSPs were successfully produced by electrospinning. The presence of NSPs has great influence on the average fibers diameter, average pore diameter and other physical properties such as morphology, elemental and texture. The average fibers diameter, average pore diameter and amount of embedded NSPs obviously increased with the increment of NSPs load. NFM with random orientation fibers and the mesoporous structure was also able to produce by electrospinning. The pore size of the membrane which smaller than the dimension of *E. coli* has proved that the possibility of *E. coli* to passing through the membrane is very low.

4.3 Phase III: Testing of the Membrane Effectiveness in Removing *E. coli* (ATCC 25922)

In this phase, the efficiency of electrospun PVDF/NSPs NFM in removing *E. coli* was determined by comparing the initial concentration of *E. coli* before filtration (inlet) and the concentration of viable *E. coli* on the membrane surface after incubation (outlet). A

preliminary test by XRD was performed to ensure the heat sterilization will not affect the properties of electrospun NFM.

4.3.1 Microstructural Analysis

Figure 4.18 displays the XRD diffraction pattern for electrospun PVDF/NSPs NFM, before and after sterilization. The sterilization process is a process that involves high temperature (121 °C in 15 min) to eliminate transmissible agents or contamination, which is a crucial element in this phase. From the diffraction pattern, the characteristic peaks of PVDF at 2θ = 18.3° (α-phase), 20.5° (β-phase) and 26.4° (α-phase) as well as NSPs peaks at 2θ = 38.1°, 44.4°, 64.5° and 77.4°, that correspond to (110), (021), (111), (200), (220) and (311) planes were clearly observed remain at the same position after sterilization. A hypothesis that can be made is the electrospun PVDF/NSPs NFM having similar crystallinity even after experiencing high temperature during the sterilization process and also having high thermal stability with the incorporation of NSPs.

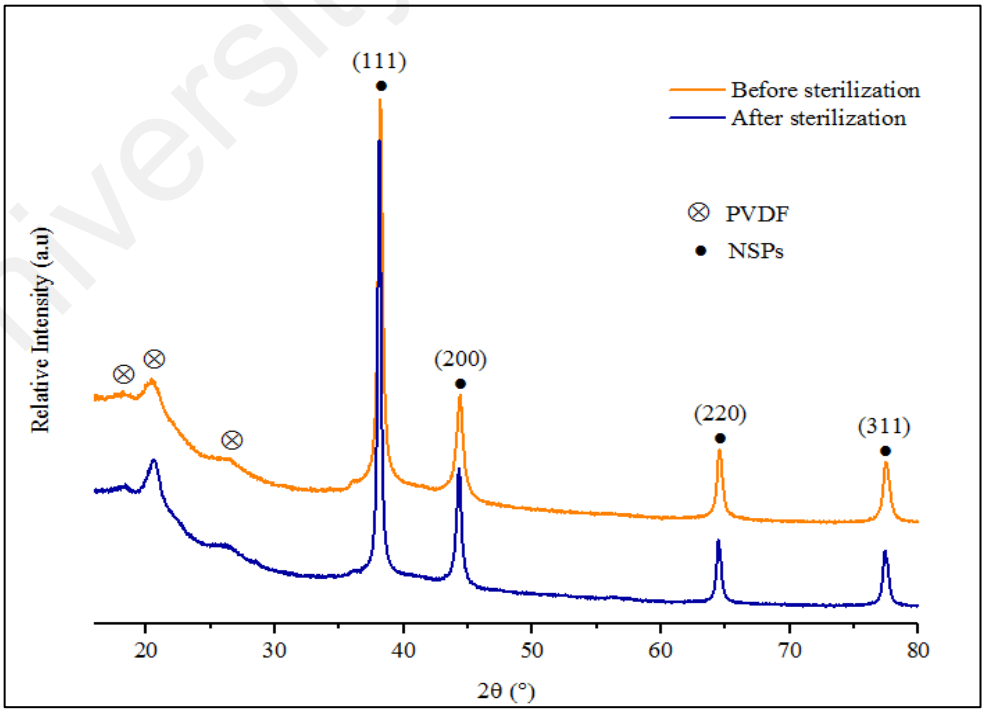

Figure 4.18: XRD pattern of electrospun PVDF/NSPs NFm before and after sterilization process

4.3.2 Enumeration of *E. coli*

Table 4.8 demonstrates the concentration of the viable *E. coli* on the membrane surface after the filtration and incubation process. Electrospun NFM without NSPs (Sample PP) that utilized as control membrane have high *E. coli* concentration as compared to the electrospun PVDF/NSPs NFM. An incorporation of the smallest-sized NSPs with the lowest weight percent (0.5 wt%) into the membrane has reduced the population of *E. coli* from $1x10^8$ to $1x10^7$ CFU/100ml and $6x10^4$ to $4x10^4$ CFU/100ml, which representing the sewage water and the surface water, respectively. The reduction phenomenon might due to the antibacterial properties of NSPs, in which, silver particles with size ranging between 1 to 100 nm have been reported to have an effect on the antibacterial activity of nanoparticles (Mpenyana-Monyatsi et al. 2012). In addition, the reduction of *E. coli* population because of the dissolution of NSPs, where the smaller size of NSPs leading to the higher dissolution rate of NSPs (Ivask et al. 2014) which generate more free Ag^+ and thus, more effective to kill the bacteria as compared to the larger-sized particles (Raza et al. 2016). On contrary, *E. coli* population for the groundwater sample recorded a slight increment from $1.36x10^4$ to $1.54x10^4$ CFU/100ml upon the addition of NSPs (0.5 wt%), which might due to a slight growth of *E.coli* cells. The *E. coli* population exhibited a similar trend for each type of water; sewage water, surface water and groundwater, when 1.0 wt% NSPs was incorporated into the membrane, where, the viable *E. coli* reduced to $4x10^5$, $1x10^3$ and less than 10 (Estimation) CFU/100ml, for the sewage water, surface water and groundwater, respectively. Further increase of NSPs weight percent to 3 wt% obviously lessen the population of *E. coli* up to $2.4x10^4$, $3x10^1$ and less than 10 (Estimation) CFU/100ml for the sewage water, surface water and groundwater, respectively. These results revealed that all the membranes inclusive the PP able to reduce the concentration of *E. coli*. In general, the highest *E. coli* removal efficiency (almost

100% removal) achieved by incorporating 3 wt% NSPs into the membrane. As expected, the efficiency of the membrane in removing *E. coli* depends on the loading of NSPs, where highest NSPs load on/in the membrane will reduce the formation of *E. coli* and increase the percentage of reduction. This might due to the higher amount of cationic Ag that released from the nanoparticles contribute to the higher penetration of Ag^+ into the cell (Franci et al. 2015) as well as the direct attachment of NSPs on the bacterial cells.

Table 4.8: Concentration of viable *E. coli* after filtration and incubation process

Samples	Concentration of viable *E. coli* (CFU/100 ml)		
PP	1.00×10^8	6.00×10^4	1.36×10^3
PS0.5	1.00×10^7	4.00×10^4	1.54×10^3
PS1.0	4.00×10^5	1.00×10^3	< 10 Est
PS3.0	2.40×10^4	3.00×10^1	< 10 Est

Note:
Est = Estimated count based on the non-ideal colony counts

The mechanism of NSPs antibacterial effect is not fully understood, but studies propose that NSPs took place on the cell membrane morphology, where the interaction between NSPs with *E. coli* caused the formation of pits on the cell wall (Kim et al. 2011; Praveena et al. 2016). These pits formation lead to a significant increase of cell permeability and when the Ag^+ ions successfully penetrate the cell wall, they start to accumulate in the cytoplasm and caused irreversible damage to the cellular membrane (Mpenyana-Monyatsi et al. 2012). Besides that, an interference of Ag cation in DNA replication by turning DNA into a condensed form, which at the same time reacts with proteins can lead to the damage or the cell death (Feng et al. 2000; Praveena et al. 2016), thus resulting in the reduction of *E. coli* population. In addition, the adherence of NSPs

on the cell membrane surface has disturbed the cell respiration as silver ions interact with enzymes of the respiratory chains of bacteria (Holt & Bard, 2005; Raffi et al. 2008).

4.3.3 Leaching Analysis

Figure 4.19 illustrates the absorption spectra of a standard solution of silver and the filtrate of contaminated water model from each electrospun NFM type. The important part of this test is to determine the presence of a silver element in the effluent, which can risk human health if exceeding the standard amount for drinking water. According to Malaysian Drinking-Water Quality Standards and United States Environmental Protection Agency standards, the maximum contaminant level of silver ions in drinking water must less than 0.1 mg/L (Praveena et al. 2016) and due to this fact, 0.1 ppm of silver standard solution, which is equivalent to 0.1 mg/L was used to verify the existence of the silver element in the filtrate. The leached out of silver ions or nanoparticles can be confirmed by the presence of a characteristic peak of silver in the range of 350-460 nm, and the figure obviously shows that no peak was detected in that range for every sample, which proves Ag^+ and NSPs does not leach from the membrane. This might due to the strong interaction between NSPs with the membrane that generated from the incorporation method (Reidy et al. 2013; Praveena et al. 2016). The continuous stirring during the preparation of polymer solution might be the reason NSPs well blended with PVDF, so, during the electrospinning, nanoparticles tend to strongly embed on/in the membrane and thus, hinder the release of NSPs. In addition, the absence of Ag^+ ions in the effluent might due to fully utilization of ions for the deactivation of *E. coli* cells.

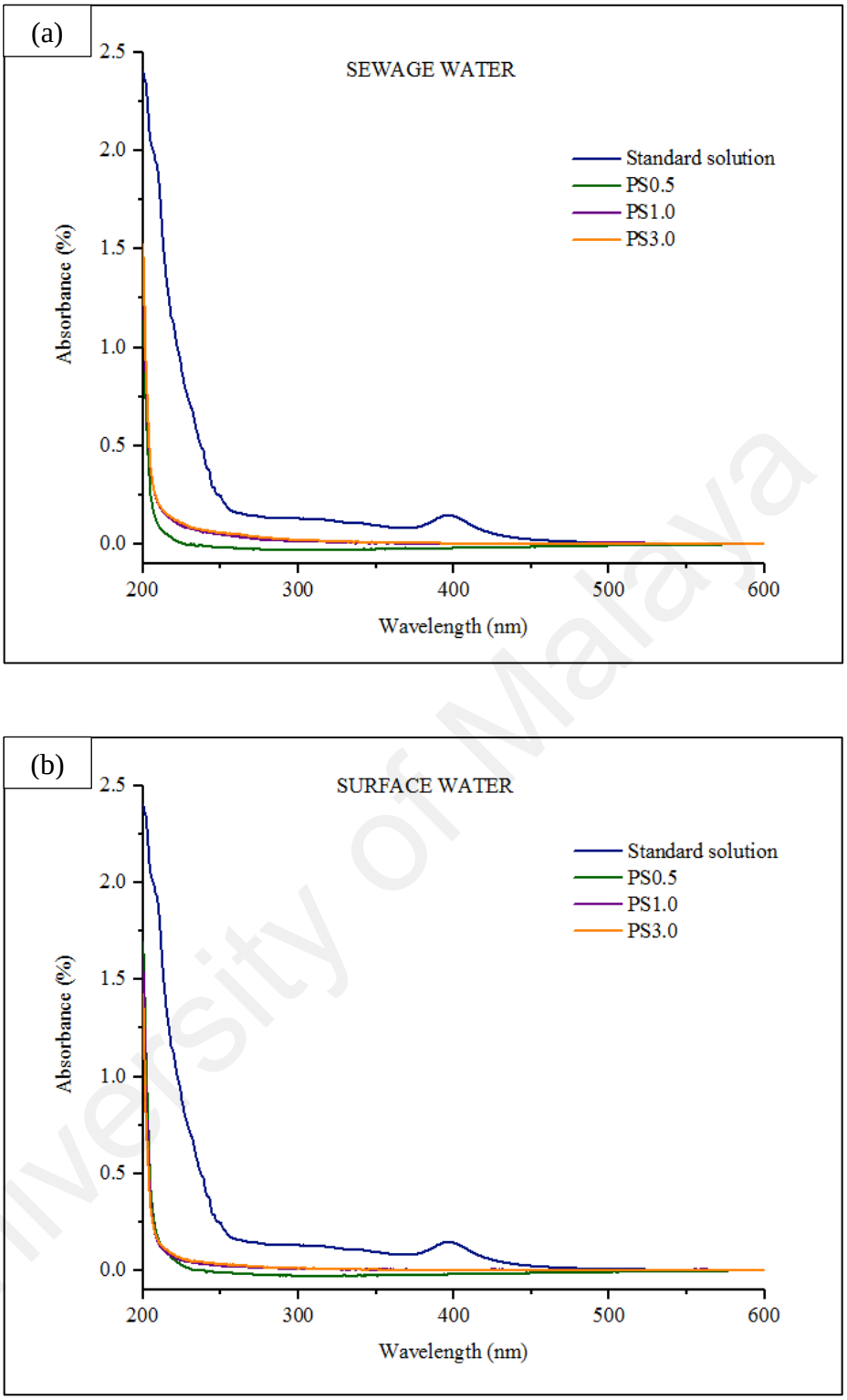

Figure 4.19: Absorption UV-vis spectra of filtrate from PVDF/NSPs NFM for different model of contaminated water (a) Sewage water (b) Surface water (c) Groundwater

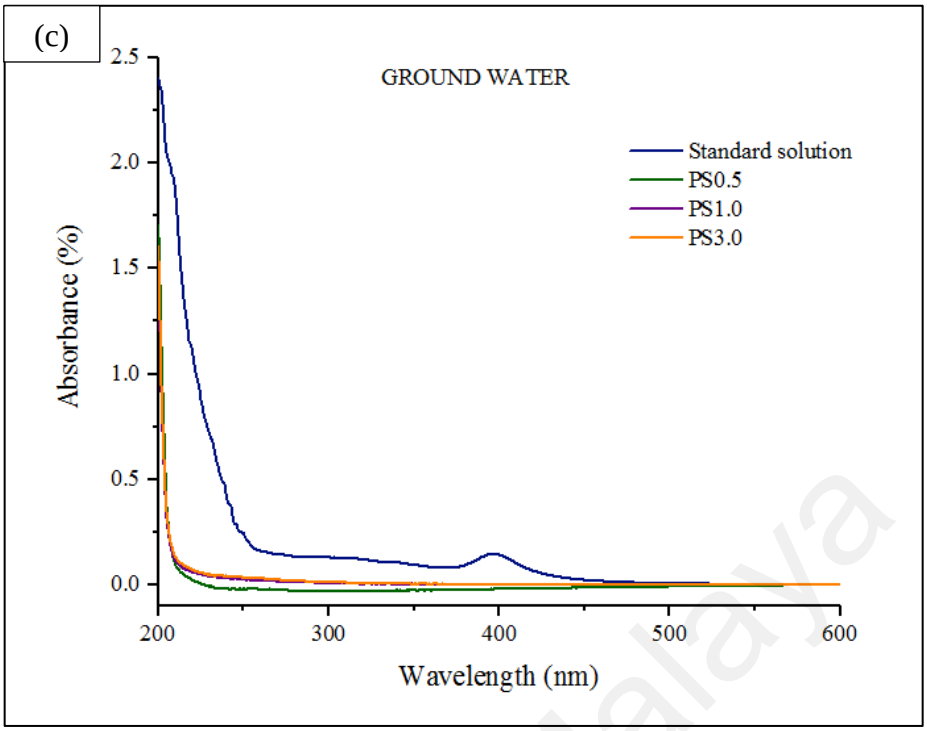

Figure 4.19: continued.

CHAPTER 5: CONCLUSION

Through the first phase of this study, we can deduce that NSPs without any presence of impurities were successfully produced by chemical reduction method using different parameters (precursor concentration and synthesis temperature). These synthesis parameters were investigated meticulously to obtain the optimal condition on the NSPs formation. The produced NSPs are confirmed coated with PVP based on the presence of PVP functional groups in the NSPs infrared spectrum, therefore, create a stable suspension with the zeta potential value of -30 mV. The physical size, crystallite size as well as the hydrodynamic size recorded the same trend when the parameter changed, either precursor concentration or reaction temperature. In general, the smallest nanoparticles can be obtained when the precursor concentration is lower and at constant precursor concentration, higher temperature able to produce the smallest nanoparticles. Briefly, the smallest nanoparticle was obtained at a higher reaction temperature using lowest precursor concentration, therefore, S1T8 was an optimum nanoparticle and chosen to be incorporated into PVDF polymer because of its smallest physical and crystallite size, which is 25.34 nm and 2.53 nm, respectively.

Nanocomposite NFM (PVDF/NSPs) was successfully fabricated *via* electrospinning technique, with, the applied voltage, flow rate and distance between needle tip to the collector are set to be 20 kV, 0.5 ml/h and 15 cm, respectively. Through the electrospinning process, the produced NFM have randomly oriented fibers and when the NSPs load increases up to 3 wt%, the electrospun membranes were almost bead-free and increasing average fiber diameter from 170.6 nm to 311.2 nm. In addition, the electrospun membranes have a mesoporous structure with a pore size range of 4.16 nm to 34.93 nm, in which should be able to retain *E. coli* from passing through the membrane. An increment of NSPs load in PVDF membrane resulting in the improvement of the

membrane performance in removing *E. coli*. The percentage of *E. coli* reduction achieved almost 100 % with the addition of a maximum load of NSPs (3 wt%) in the membrane. Leaching test revealed that the filtered water is safe to be consumed due to the absence of the silver element which can be toxic to the consumer.

In conclusion, the smaller pore size of the membrane that able to retain *E. coli*, together with the absence of the silver element in the filtrate has proved that the produced electrospun membrane was safe to be used as an ultrafiltration membrane. This PVDF/NSPs NFM not only showing its effectiveness in removing bacterial cells, cheap and easy to produce.

RECOMMENDATION FOR FUTURE WORKS

The following recommendations are made to broaden the study on the membrane performance in generating clean water.

1. The common problem in water filtration applications is the formation of biofilm on the membrane surface which will deteriorate the performance of the membrane especially water flux. In the future, an investigation can be performed to evaluate the influence of NSPs on the antifouling properties of PVDF/NSPs NFM.
2. Silver nanoparticles reportedly have an ability to decompose several metals. So, it is suggested to conduct a study on the capability of PVDF/NSPs NFM to remove heavy metals from contaminated water.

REFERENCES

Agnihotri, S., Mukherji, S., and Mukherji, S. (2014). Size-controlled silver nanoparticles synthesized over the range 5-100 nm using the same protocol and their antibacterial efficacy. *RSC Advances, 4*(8): 3974-3983.

Agyemang, F. O., Sheikh, F. A., Appiah-Ntiamoah, R., Chandradass, J., and Kim, H. (2015). Synthesis and characterization of poly (vinylidene fluoride)–calcium phosphate composite for potential tissue engineering applications. *Ceramics International, 41*(5): 7066-7072.

Ahmad, H. A., Saiden, N. M., Saion, E., Azis, R. S., Mamat, M. S., and Hashim, M. (2017). Effect of PVP as a capping agent in single reaction synthesis of nanocomposite soft/hard ferrite nanoparticles. *Journal of Magnetism and Magnetic Materials, 428*, 219-222.

Ahmad, T., Wani, I. A., Ahmed, J., and Al-Hartomy, O. A. (2014). Effect of gold ion concentration on size and properties of gold nanoparticles in TritonX-100 based inverse microemulsions. *Applied Nanoscience, 4*(4), 491-498.

Ahmed, F. E., Lalia, B. S., Hilal, N., and Hashaikeh, R. (2014). Underwater superoleophobic cellulose/electrospun PVDF–HFP membranes for efficient oil/water separation. *Desalination, 344*, 48-54.

Ahmed, M. B., Zhou, J. L., Ngo, H. H., Guo, W., Thomaidis, N. S., and Xu, J. (2017). Progress in the biological and chemical treatment technologies for emerging contaminant removal from wastewater: A critical review. *Journal of Hazardous Materials, 323*, 274-298.

Ajitha, B., Divya, A., Harish, G. S., and Sreedhara, R. D. (2013). The influence of silver precursor concentration on size of silver nanoparticles grown by soft chemical route. *Research Journal of Physical Sciences, 1*(7): 11-14.

Alahmad, A. (2014). Preparation and characterization of silver nanoparticles. *International Journal of ChemTech Research, 6*(1): 450-459.

Allen, E., Henshaw, J., and Smith, P. (2001). A review of particle agglomeration. U.S. Department of Energy: 1-42.

Amany, A., El-Rab, S. F. G., and Gad, F. (2012). Effect of reducing and protecting agents on size of silver nanoparticles and their anti-bacterial activity. *Der Pharma Chemica, 4*(1): 53-65.

Amin, M. T., Alazba, A. A., and Manzoor, U. (2014). A review of removal of pollutants from water/wastewater using different types of nanomaterials. *Advances in Materials Science and Engineering, 2014*.

Amouamouha, M., and Badalians Glodikandi, G. (2017). Characterization and antibiofouling performance investigation of hydrophobic silver nanocomposite membranes: A comparative study. *Membranes, 7*(4): 64.

An, J., Wang, D., and Yuan, X. (2009). Synthesis of stable silver nanoparticles with antimicrobial activities in room-temperature ionic liquids. *Chemical Research in Chinese Universities, 25*(4), 421-425.

Baji, A., and Mai, Y.-W. (2017). Engineering Ceramic Fiber Nanostructures Through Polymer-Mediated Electrospinning *Polymer-Engineered Nanostructures for Advanced Energy Applications* (pp. 3-30): Springer.

Baruah, S., K Pal, S., and Dutta, J. (2012). Nanostructured zinc oxide for water treatment. *Nanoscience & Nanotechnology-Asia, 2*(2): 90-102.

Basavaraj, U., Praveenkumar, N., Sabiha, T., Rupali, S., and Samprita, B. (2012). Synthesis and characterization of silver nanoparticles. *International Journal of Pharmacy and Biological Science, 2*(3), 10-14.

Bell, W. C., and Myrick, M. L. (2001). Preparation and characterization of nanoscale silver colloids by two novel synthetic routes. *Journal of Colloid and Interface Science, 242*(2): 300-305.

Benzinger, W., Parekh, B., and Eichelberger, J. (1980). High temperature ultrafiltration with Kynar® poly (vinylidene fluoride) Membranes. *Separation Science and Technology, 15*(4), 1193-1204.

Beyth, N., Houri-Haddad, Y., Domb, A., Khan, W., and Hazan, R. (2015). Alternative antimicrobial approach: nano-antimicrobial materials. *Evidence-Based Complementary and Alternative Medicine, 2015*.

Bhui, D. K., Bar, H., Sarkar, P., Sahoo, G. P., De, S. P., and Misra, A. (2009). Synthesis and UV–vis spectroscopic study of silver nanoparticles in aqueous SDS solution. *Journal of Molecular Liquids, 145*(1): 33-37.

Boutilier, M. S., Lee, J., Chambers, V., Venkatesh, V., and Karnik, R. (2014). Water filtration using plant xylem. *Plos One, 9*(2): 1-8.

Bryaskova, R., Pencheva, D., Nikolov, S., and Kantardjiev, T. (2011). Synthesis and comparative study on the antimicrobial activity of hybrid materials based on silver nanoparticles (AgNps) stabilized by polyvinylpyrrolidone (PVP). *Journal of Chemical Biology, 4*(4): 185-191.

Bulgariu, L., Cojocaru, C., Robu, B., and Macavenu, M. (2007). Equilibrium isotherm studies for the sorption of lead ions from the aqua solutions using Romanian peat samples. *Environmental Engineering Management Journal, 6*(5): 425-430.

Burlingame, G. A., Doty, R. L., and Dietrich, A. M. (2017). Humans as sensors to evaluate drinking water taste and odor: a review. *Journal Awwa, 109*(11): 13-24.

Carneiro-da-Cunha, M. G., Cerqueira, M. A., Souza, B. W. S., Teixeira, J. A., and Vicente, A. A. (2011). Influence of concentration, ionic strength and pH on zeta potential and mean hydrodynamic diameter of edible polysaccharide solutions envisaged for multinanolayered films production. *Carbohydrate Polymers, 85*(3): 522-528.

Chernnousova, S., and Epple, M. (2013). Silver as antibacterial agent:ion, nanoparticles, and metal. *Angewandte Chemie-International Edition, 52*(6): 1636-1653.

Chiad, B., Ali, N., Sadik, Z., and Al-Awadi, S. (2013). Study the optimum conditions of synthesis AgNP by chemical reduction method. *Journal of Kerbala University, 11*(4): 40-46.

Chili, M. M., Pullabhotla, V. R., and Revaprasadu, N. (2011). Synthesis of PVP capped gold nanoparticles by the UV-irradiation technique. *Materials Letters, 65*(17-18), 2844-2847.

Costa, L. M. M., Bretas, R. E. S., and Gregorio, R. (2010). Effect of solution concentration on the electrospray/electrospinning transition and on the crystalline phase of PVDF. *Materials Sciences and Applications, 1*(04), 247.

Dang, T. M. D., Le, T. T. T., Fribourg-Blanc, E., and Dang, M. C. (2011). The influence of solvents and surfactants on the preparation of copper nanoparticles by a chemical reduction method. *Advances in Natural Sciences: Nanoscience and Nanotechnology, 2*(2), 025004.

Darroudi, M., Ahmad, M. B., Abdullah, A. H., Ibrahim, N. A., and Shameli, K. (2010). Effect of accelerator in green synthesis of silver nanoparticles. *International Journal of Molecular Sciences, 11*(10): 3898-3905.

Deegan, A. M., Shaik, B., Nolan, K., Urell, K., Oelgemöller, M., Tobin, J., and Morrissey, A. (2011). Treatment options for wastewater effluents from pharmaceutical companies. *International Journal of Environmental Science & Technology, 8*(3), 649-666.

Department of the Environment, Malaysia. (2016). Malaysia environmental quality report. Department of the Environment, Ministry of Science, Technology and Environment, Malaysia.

Dhakras, P. (2011). *Nanotechnology applications in water purification and waste water treatment: a review*. Paper presented at the Nanoscience, Engineering and Technology (ICONSET), 2011 International Conference on.

Dizaj, S. M., Lotfipour, F., Barzegar-Jalali, M., Zarrintan, M. H., and Adibkia, K. (2014). Antimicrobial activity of the metals and metal oxide nanoparticles. *Materials Science and Engineering: C, 44*: 278-284.

Dong, X., Ji, X., Wu, H., Zhao, L., Li, J., and Yang, W. (2009). Shape control of silver nanoparticles by stepwise citrate reduction. *The Journal of Physical Chemistry C, 113*(16), 6573-6576.

Dong, Z.-Q., Ma, X.-h., Xu, Z.-L., You, W.-T., and Li, F.-b. (2014). Superhydrophobic PVDF–PTFE electrospun nanofibrous membranes for desalination by vacuum membrane distillation. *Desalination, 347*, 175-183.

Durán, N., Marcata, P. D., Conti, R. D., Alves, O. L., Costa, F. T. M., and Brocchi, M. (2010). Potential use of silver nanoparticles on pathogenic bacteria, their toxicity and possible mechanisms of action. *Journal of the Brazilian Chemical Society, 21*(6): 949-959.

Eid, C., Assaf, E., Habchi, R., Miele, P., and Bechelany, M. (2015). Tunable properties of GO-doped $CoFe_2O_4$ nanofibers elaborated by electrospinning. *RSC Advances, 5*: 97849-97854.

Esakkimuthu, T., Sivakumar, D., and Akila, S. (2014). Application of nanoparticles in wastewater treatment. *Pollution Research, 33*(03), 567-571.

Escherichia coli (13 November 2014). Retrieved 24 April 2017 from https://microbewiki.kenyon.edu/index.php/Escherichia_coli

Escherichia coli (E. coli) detections in drinking water (27 September 2017). Retrieved fromhttp://conditions.health.qld.gov.au/HealthCondition/condition/14/33/666/escherichia-coli-e-coli-detections-in-drinkin

Farkas, J., Peter, H., Christian, P., Urrea, J. A. G., Hassellöv, M., Tuoriniemi, J., . . . Thomas, K. V. (2011). Characterization of the effluent from a nanosilver producing washing machine. *Environment International, 37*(6), 1057-1062.

Fawell, J. and Nieuwenhuijsen, M. J. (2003). Contaminants in drinking water. *British Medical Bulletin, 68*: 199-208.

Fayaz, A., Balaji, K., Kalaichelvan, P., and Venkatesan, R. (2009). Fungal based synthesis of silver nanoparticles - An effect of temperature on the size of particles. *Colloids and Surfaces B: Biointerfaces, 74*(1): 123-126.

Feng, Q., Wu, J., Chen, G., Cui, F., Kim, T., and Kim, J. (2000). A mechanistic study of the antibacterial effect of silver ions on Escherichia coli and Staphylococcus aureus. *Journal of biomedical materials research, 52*(4): 662-668.

Foliatini, F., Yulizar, Y., and Hafizah, M. A. E. 2015. The synthesis of alginate-capped silver nanoparticles under microwave irradiation. *Journal of Mathematical and Fundamental Sciences* 47(1): 31-50.

Fong, H., Chun, I., and Reneker, D. H. (1999). Beaded nanofibers formed during electrospinning. *Polymer, 40*: 4585-4592.

Franci, G., Falanga, A., Galdiero, S., Palomba, L., Rai, M., Morelli, G., and Galdiero, M. (2015). Silver nanoparticles as potential antibacterial agents. *Molecules*, *20*(5): 8856-8874.

Gatoo, M. A., Naseem, S., Arfat, M. Y., Mahmood Dar, A., Qasim, K., and Zubair, S. (2014). Physicochemical properties of nanomaterials: implication in associated toxic manifestations. *BioMed Research International, 2014*.

Gelt, J. (1998). Microbes increasingly viewed as water quality threat. *Water Resources Research Center (WRRC)*. Retrieved from https://wrrc.arizona.edu/publications/arroyo-newsletter/microbes-increasingly-viewed-water-quality-threat.

Ghorbani, H. R. (2014). Chemical synthesis of copper nanoparticles. *Oriental Journal of Chemistry, 30*(2), 803-806

Ghorbani, H. R., Safekordi, A. A., Attar, H., and Sorkhabadi, S. (2011). Biological and non-biological methods for silver nanoparticles synthesis. *Chemical and Biochemical Engineering Quarterly, 25*(3), 317-326.

Gleick, P. H. (2002). *Dirty-water: Estimated deaths from water-related diseases 2000-2020*: Pacific Institute for Studies in Development, Environment, and Security.

Goel, G., and Kaur, S. (2012). A study on chemical contamination of water due to household laundry detergents. *Journal of Human Ecology-New Delhi, 38*(1): 65.

Gopal, R., Kaur, S., Ma, Z., Chan, C., Ramakrishna, S., and Matsuura, T. (2006). Electrospun nanofibrous filtration membrane. *Journal of Membrane Science, 281*(1): 581-586.

Grande, L. (2015). *Evolution of virulence in pathogenic Escherichia coli strains: impact on public health* (Doctoral thesis, Universita Degli Studi Roma Tre, Rome, Italy).

Greiner, A., and Wendorff, J. H. (2007). Electrospinning: a fascinating method for the preparation of ultrathin fibers. *Angewandte Chemie International Edition, 46*(30): 5670-5703.

Guzmán, M. G., Dille, J., and Godet, S. (2008). Synthesis of silver nanoparticles by chemical reduction method and their antibacterial activity. *World Academy of Science, Engineering and Technology, International Journal of Chemical, Molecular, Nuclear, Materials and Metallurgical Engineering, 2*(7), 91-98.

Hajipour, M. J., Fromm, K. M., Ashkarran, A. A., Aberasturi, D. J. D., Larramendi, I. R. D., Rojo, T.,… Mohmoudi, M. (2012). Antibacterial properties of nanoparticles. *Trends in Biotechnology, 30*(10): 499-511.

Hamzah, A., and Hattasrul, Y. (2007). *Water quality and bacterial study in Tasik Chini, Pahang.* Paper presented at the Proceedings of Taal2007: The 12th World Lake Conference.

Hassanien, A. S., and A. Akl, A. (2015). Crystal imperfections and Mott parameters of sprayed nanostructure IrO2 thin films. *Physica B: Condensed Matter, 473*: 11-19.

Hee, D. J., and Jinki, J. (2007). The effects of temperature on particle size in the gas-phase production of TiO_2. *Aerosol Science and Technology, 23*(4): 553-560.

Heikkilä, P., and Harlin, A. (2009). Electrospinning of polyacrylonitrile (PAN) solution: Effect of conductive additive and filler on the process. *Express Polymer Letters, 3*(7): 437-445.

Heydari Beni, A. (2014). *Screening of Microfiltration and Ultrafiltration Ceramic Membranes for Produced Water Treatment and Testing of Different Cleaning Methods.* (Master's Degree), University of Regina.

Holt, K. B., and Bard, A. J. (2005). Interaction of silver (I) ions with the respiratory chain of Escherichia coli: an electrochemical and scanning electrochemical microscopy study of the antimicrobial mechanism of micromolar Ag+. *Biochemistry, 44*(39): 13214-13223.

Hong, J., and He, Y. (2012). Effects of nano sized zinc oxide on the performance of PVDF microfiltration membranes. *Desalination, 302*, 71-79.

Huang, L., Arena, J. T., and McCutcheon, J. R. (2016). Surface modified PVDF nanofiber supported thin film composite membranes for forward osmosis. *Journal of Membrane Science, 499*, 352-360.

Hussain, J. I., Kumar, S., Hashmi, A. A., and Khan, Z. (2011). Silver nanoparticles: preparation, characterization, and kinetics. *Advanced Materials Letters, 2*(3), 188-194.

Inamori, Y., and Fujimoto, N. (2009). Water quality and standards-Vol. II, microbial/biological contamination of water. *Encyclopaedia of Life Support Systems (EOLSS).*

Inamori, Y., and Fujimoto, N. (2009). Water quality and standards-Vol. II, physical/mechanical contamination of water. *Encyclopaedia of Life Support Systems (EOLSS).*

Iravani, H. K., Mirmohammadi, S., and B Zolfaghari, S. (2014). Synthesis of silver nanoparticles: chemical, physical and biological methods. *Research in Pharmaceutical Sciences, 9*(6): 385-406.

Ivask, A., ElBadawy, A., Kaweeteerawat, C., Boren, D., Fischer, H., Ji, Z., ... Zink, J. I. (2014). Toxicity mechanisms in Escherichia coli vary for silver nanoparticles and differ from ionic silver. *Acs Nano, 8*(1): 374-386.

Jiang, H., Moon, K.-s., Zhang, Z., Pothukuchi, S., and Wong, C. (2006). Variable frequency microwave synthesis of silver nanoparticles. *Journal of Nanoparticle Research, 8*(1): 117-124.

Jiang, X., Chen, W., Chen, C., Xiong, S., and Yu, A. (2011). Role of temperature in the growth of silver nanoparticles through a synergetic reduction approach. *Nanoscale Research Letters, 6*(1), 32.

Jo, Y., Jung, M. H., Kyum, M. C., Park, K. H., and Kim, Y. N. (2006). Nano-sized effect on the magnetic properties of Ag clusters. *Journal of Magnetics, 11*(4): 160-163.

Johnson, G. (2015). *How E. coli bacteria become deadly: the making of a monster*. Retrieved from http://biologywriter.com/on-science/articles/deadlyecoli/

Johnson, J. R. (2002). Evolution of pathogenic Escherichia coli. In Donnenberg, M. S. (Eds). *Escherichia coli virulence mechanisms of a versatile pathogen* (pp. 55-77). USA: Academic Press.

Jung, W. K., Koo, H. C., Kim, K. W., Shin, S., Kim, S. H., and Park, Y.H. (2008). Antibacterial activity and mechanisms of action of the silver ion in Stahphylococcus aureus and Escherichia coli. *Applied and Environmental Microbiology, 74*(7): 2171-2178.

Kang, D. H., and Kang, H. W. (2016). Surface energy characteristics of zeolite embedded PVDF nanofiber films with electrospinning process. *Applied Surface Science, 387*, 82-88.

Kang, G. D., and Cao, Y. M. (2014). Application and modification of poly (vinylidene fluoride)(PVDF) membranes–a review. *Journal of Membrane Science, 463*, 145-165.

Keyser, S. L., and Johnson, B. T. (22 October 1997). *Microorganisms, bacteria and viruses.* Retrieved from http://extoxnet.orst.edu/faqs/safedrink/microorg.htm

Khan, Z., Al-Thabaiti, S. A., Obaid, A. Y., and Al-Youbi, A. (2011). Preparation and characterization of silver nanoparticles by chemical reduction method. *Colloids and Surfaces B: Biointerfaces, 82*(2), 513-517.

Kim, S.-H., Lee, H.-S., Ryu, D.-S., Choi, S.-J., and Lee, D.-S. (2011). Antibacterial activity of silver-nanoparticles against Staphylococcus aureus and Escherichia coli. *Korean Journal of Microbiology and Biotechnology, 39*(1): 77-85.

Kittler, S., Greulich, C., Diendorf, J., Köller, M., and Epple, M. (2010). Toxicity of silver nanoparticles increases during storage because of slow dissolution under release of silver ions. *Chemistry of Materials, 22*(16): 4548-4554.

Koczkur, K. M., Mourdikoudis, S., Polavarapu, L., and Skrabalak, S. E. (2015). Polyvinylpyrrolidone (PVP) in nanoparticle synthesis. *Dalton Transactions, 44*(41), 17883-17905.

Koseoglu-Imer, D. Y., Kose, B., Altinbas, M., and Koyuncu, I. (2013). The production of polysulfone (PS) membrane with silver nanoparticles (AgNP): physical properties, filtration performances, and biofouling resistances of membranes. *Journal of Membrane Science, 428*: 620-628.

Kumar, M., Devi, P., and Ghanshyam, C. (2014). Synthesis, characterization of PVP stabilized silver nanoparticles for gas sensing applications. *International Journal of Applied Engineering Research (Special Issue), 9*(15), 511-515.

Kwankhao, B. (2013). *Microfiltration membranes via electrospinning of polyethersulfone solutions.* (PhD), University of Duisburg-Essen.

Lah, N. A. C., and Johan, M. R. (2011). Facile shape control synthesis and optical properties of silver nanoparticles stabilized by Daxad 19 surfactant. *Applied Surface Science, 257*(17): 7494-7500.

Lai, C. Y., Groth, A., Gray, S., and Duke, M. (2014). Nanocomposites for improved physical durability of porous PVDF membranes. *Membranes, 4*(1), 55-78.

Lalia, B. S., Janajreh, I., and Hashaikeh, R. (2017). A facile approach to fabricate superhydrophobic membranes with low contact angle hysteresis. *Journal of Membrane Science, 539*, 144-151.

Lanje, A. S., Sharma, S. J., and Pode, R. B. (2010). Synthesis of silver nanoparticles: a safer alternative to conventional antimicrobial and antibacterial agents. *Journal of Chemical and Pharmaceutical Research, 2*(3): 478-483.

Lanje, A. S., Sharma, S. J., and Pode, R. B. (2010). Magnetic and electrical properties of nickel nanoparticles prepared by hydrazine reduction method. *Archieves of Physics Research, 1*(1): 49-56.

Lee, J., Rai, P. K., Jeon, Y. J., Kim, K. H., and Kwon, E. E. (2017). The role of algae and cyanobacteria in the production and release of odorants in water. *Environmental Pollution, 227*: 252-262.

Lei, G. (2007). *Synthesis of nano-silver colloids and their anti-microbial effects.* (Master's Degree), Virginia Tech.

Li, X., Hao, X., Xu, D., Zhang, G., Zhong, S., Na, H., and Wang, D. (2006). Fabrication of sulfonated poly(ether ether ketone ketone) membranes with high proton conductivity. *Journal of Membrane Science, 281*: 1-6.

Li, X., Xu, H., Chen, Z.-S., and Chen, G. (2011). Biosynthesis of nanoparticles by microorganisms and their applications. *Journal of Nanomaterials, 2011*: 16.

Lijesh, K. P., and Malhotra, R. (2016). Reduction of turbidity of water using Moringa Oleifera. *International Journal of Applied Engineering Reseacrh, 11*(2): 1414-1423.

Lindgren, A. L. (2014). The effects of silver nitrate and silver nanoparticles on Chlamydomonas reinhardtii: a proteomic approach. *Degree Project, Department of Biology and Environmental Sciences, University of Gothenburg, Germany*.

Liu, D., Lin, L., Ren, S., and Fu, S. (2016). Effect of polyvinyl pyrrolidone (PVP) molecular weights on dispersion of sub-micron nickel particles by chemical reduction process. *Journal of Materials Science, 51*(6), 3111-3117.

Liu, H., Zhang, B., Shi, H., Tang, Y., Jiao, K., and Fu, X. (2008). Hydrothermal synthesis of monodisperse Ag_2Se nanoparticles in the presence of PVP and KI and their application as oligonucleotide labels. *Journal of Materials Chemistry, 18*: 2573-2580.

Liu, F., Hashim, N. A., Liu, Y., Abed, M. M., and Li, K. (2011). Progress in the production and modification of PVDF membranes. *Journal of membrane science, 375*(1-2), 1-27.

Liu, J., Lu, X., and Wu, C. (2013). Effect of preparation methods on crystallization behavior and tensile strength of poly (vinylidene fluoride) membranes. *Membranes, 3*(4), 389-405.

Loeb, S., Andrews, S. A., and Hofmann, R. (2015). The effect of immobilized catalyst structure on the degradation of chemical and biological contaminants in simulated solar photocatalytic water purification. *Journal of Water Supply: Research and Technology-Aqua, 64*(8), 883-891.

Lu, W., Liao, F., Luo, Y., Chang, G., and Sun, X. (2011). Hydrothermal synthesis of well-stable silver nanoparticles and their application for enzymeless hydrogen peroxide detection. *Electrochimica Acta, 56*(5): 2295-2298.

Luo, Y., Guo, W., Ngo, H. H., Nghiem, L. D., Hai, F. I., Zhang, J., . . . Wang, X. C. (2014). A review on the occurrence of micropollutants in the aquatic environment and their fate and removal during wastewater treatment. *Science of The Total Environment, 473-474*, 619-641.

Malaysia-water & waste water treatment (12 June 2017). Retrieved 25 October 2017 from https://www.export.gov/article?id=Malaysia-Water-Industry

Malina, D., Sobczak-Kupiec, A., Wzorek, Z., and Kowalski, Z. (2012). Silver nanoparticles synthesis with different concentrations of polyvinylpyrrolidone. *Digest Journal of Nanomaterials and Biostructures, 7:* 1527-1534.

Maliszewska, I., Szewczyk, K., and Waszak, K. (2009). Biological synthesis of silver nanoparticles. In *Journal of Physics: Conference Series* (Vol. 146, No. 1, p. 012025). IOP Publishing.

Marambio-Jones, C., and Hoek, E. M. V. (2010). A review of the antibacterial effects of silver nanomaterials and potential implications for human health and the environment. *Journal of Nanoparticle Research, 12*(5): 1531-1551.

Matsumoto, H., and Tanioka, A. (2011). Functionality in electrospun nanofibrous membranes based on fiber's size, surface area, and molecular orientation. *Membranes, 1*(3): 249-264.

Mavani, K., and Shah, M. (2013). Synthesis of silver nanoparticles by using sodium borohydride as a reducing agent. *International Journal of Engineering Research & Technology, 2*(3).

Megelski, S., Stephens, J. S., Chase, D. B., and Rabolt, J. F. (2002). Micro- and nanostructured surface morphology on electrospun polymer fibers. *Macromolecules, 35*(22): 8456-8466.

Mittal, A. K., Chisti, Y., and Banerjee, U. C. (2013). Synthesis of metallic nanoparticles using plant extracts. *Biotechnology Advances, 31*(2): 346-356.

Mit-uppatham, C., Nithitanakul, M., and Supaphol, P. (2004). Ultrafine electrospun polyamide-6 fibers: effects of solution conditions on morphology and average fiber diameter. *Macromolecular Chemistry and Physics, 205*: 2327-2338.

Mohan, Y. M., Lee, K., Premkumar, T., and Geckeler, K. E. (2007). Hydrogel networks as nanoreactors: a novel approach to silver nanoparticles for antibacterial applications. *Polymer, 48*(1): 158-164.

Mohd Zainudin, F., Abu Hasan, H., and Sheikh Abdullah, S. R. (2018). An overview of the technology used to remove trihalomethane (THM), trihalomethane precursors, and trihalomethane formation potential (THMFP) from water and wastewater. *Journal of Industrial and Engineering Chemistry, 57*, 1-14.

Mollahosseini, A., Rahimpour, A., Jahamshahi, M., Peyravi, M., and Khavarpour, M. (2012). The effect of silver nanoparticle size on performance and antibacteriality of polysulfone ultrafiltration membrane. *Desalination, 306*: 41-50.

Monores, J. R., Elechiguerra, J. L., Camacho, A., Holt, K., Kouri, J. B., Ramirez, J. T., and Yacaman, M. J. (2005). The bactericidal effect of silver nanoparticles. *Nanotechnology, 16*: 2346-2553.

Moradi, R., Karimi-Sabet, J., Shariaty-Niassar, M., and Amini, Y. (2016). Air gap membrane distillation for enrichment of H218O isotopomers in natural water using poly (vinylidene fluoride) nanofibrous membrane. *Chemical Engineering and Processing: Process Intensification, 100*, 26-36.

Mpenyana-Monyatsi, L., Mthombeni, N. H., Onyango, M. S., and Momba, M. N. (2012). Cost-effective filter materials coated with silver nanoparticles for the removal of pathogenic bacteria in groundwater. *International Journal of Environmental Research and Public Health, 9*(1): 244-271.

Mohammed Fayaz, A., Balaji, K., Kalaichelvan, P. T., and Venkatesan, R. (2009). Fungal based synthesis of silver nanoparticles—An effect of temperature on the size of particles. *Colloids and Surfaces B: Biointerfaces, 74*(1), 123-126.

Muralimohan, N., Palanisamy, T., and Vimaladevi, M. N. (2014). Experimental study on removal efficiency of blended coagulants in textile wastewater treatment. *IMPACT International Journal of Research in Engineering & Technology, 2*(2): 15-20.

Nakata, K., Kim, S. H., Ohkoshi, Y., Gotoh, Y., and Nagura, M. (2007). Electrospinning of poly(ether sulfone)and evaluation of the filtration efficiency. *Society of Fiber Science and Technology Japan*, *63*(12): 307-312.

Nalawade, P., Mukherjee, T., and Kapoor, S. (2013). Green synthesis of gold nanoparticles using glycerol as a reducing agent. *Advances in Nanoparticles, 2*(02), 78

Nasreen, S. A. A. N., Sundarrajan, S., Syed Nizar, S. A., Balamurugan, R., and Ramakrishna, S. (2013). Advancement in electrospun nanofibrous membranes modification and their application in water treatment. *Membranes, 3*: 266-284.

Neiva, E. G., Bergamini, M. F., Oliveira, M. M., Marcolino Jr, L. H., and Zarbin, A. J. (2014). PVP-capped nickel nanoparticles: Synthesis, characterization and utilization as a glycerol electrosensor. *Sensors and Actuators B: Chemical, 196*, 574-581.

Ng, L. Y., Mohammad, A. W., Leo, C. P., and Hilal, N. (2013). Polymeric membranes incorporated with metal/metal oxide nanoparticles: A comprehensive review. *Desalination, 308*, 15-33.

Nurul Akma, R., Suriati, G., and Saidatul Shima, J. (2016). Effect of temperature and NaCl concentration on synthesis of silver nanoparticles prepared in aqueous medium. *ARPN Journal of Engineering and Applied Sciences, 11*(10), 6399-6404.

Obaid, M., Mohamed, H. O., Yasin, A. S., Yassin, M. A., Fadali, O. A., Kim, H., and Barakat, N. A. (2017). Under-oil superhydrophilic wetted PVDF electrospun modified membrane for continuous gravitational oil/water separation with outstanding flux. *Water Research, 123*, 524-535.

Odonkor, S. T., and Ampofo, J. K. (2013). Escherichia coli as an indicator of bacteriological quality of water: an overview. *Microbiology Research*, *4*(2): 5-11.

Oliveira, M. M., Ugarte, D., Zanchet, D., and Zarbin, A. J. (2005). Influence of synthetic parameters on the size, structure, and stability of dodecanethiol-stabilized silver nanoparticles. *Journal of Colloid and Interface Science, 292*(2), 429-435.

Oram, B. (2014). *Ozonation in water treatment*. Retrieved 20 August 2018 from https://www.water-research.net/index.php/ozonation.

Pantidos, N., and Horsfall, L. E. (2014). Biological synthesis of metallic nanoparticles by bacteria, fungi and plants. *Journal of Nanomedicine & Nanotechnology*, *5*(5), 1.

Park, H. (2005). *Fabrication of lanthanum copper oxide nanofibers by electrospinning*: (PhD), University of Florida.

Piñero, S., Camero, S., and Blanco, S. (2017). Silver nanoparticles: Influence of the temperature synthesis on the particles' morphology. *Journal of Physics: Conference Series, 786*(1), 012020.

Praveena, S. M., Han, L. S., Than, L. T. L., and Aris, A. Z. (2016). Preparation and characterisation of silver nanoparticle coated on cellulose paper: evaluation of their potential as antibacterial water filter. *Journal of Experimental Nanoscience, 11*(17): 1307-1319.

Pulit, J., Banach, M., and Kowalski, Z. (2011). Nanosilver-making difficult decisions. *Ecological Chemistry and Engineerings, 18*(2): 185-195.

Qu, X., Alvarez, P. J., and Li, Q. (2013). Applications of nanotechnology in water and wastewater treatment. *Water research, 47*(12): 3931-3946.

Rabuni, M., Nik Sulaiman, N., Aroua, M., and Hashim, N. A. (2013). Effects of alkaline environments at mild conditions on the stability of PVDF membrane: an experimental study. *Industrial & Engineering Chemistry Research, 52*(45), 15874-15882.

Raffi, M., Hussain, F., Bhatti, T., Akhter, J., Hameed, A., and Hasan, M. (2008). Antibacterial characterization of silver nanoparticles against E. coli ATCC-15224. *Journal of Materials Science and Technology, 24*(2): 192-196.

Rashed, H. H. (2016). Silver nanoparticles prepared by electrical arc discharge method in DIW. *Engineering and Technology Journal, 34*(2 Part (B) Scientific), 295-301.

Rashid, M. U., Bhuiyan, M. K. H., and Quayum, M. E. (2013). Synthesis of silver nano particles (Ag-NPs) and their uses for quantitative analysis of vitamin C tablets. *Dhaka University Journal of Pharmaceutical Sciences, 12*(1), 29-33.

Rastgar, M., Shakeri, A., Bozorg, A., Salehi, H., and Saadattalab, V. (2017). Impact of nanoparticles surface characteristics on pore structure and performance of forward osmosis membranes. *Desalination, 421*: 179-189.

Raza, M. A., Kanwal, Z., Rauf, A., Sabri, A. N., Riaz, S., and Naseem, S. (2016). Size- and shape-dependent antibacterial studies of silver nanoparticles synthesized by wet chemical routes. *Nanomaterials*, *6*(4): 74.

Reidy, B., Haase, A., Luch, A., Dawson, K. A., and Lynch, I. (2013). Mechanisms of silver nanoparticle release, transformation and toxicity: A critical review of current knowledge and recommendations for future studies and applications. *Materials*, *6*(6): 2295-2350.

Sarma, S. S. (2014). Fabrication of compound nanofibers for antibacterial applications in filtration. *International Journal of Emerging Technology and Advanced Engineering*, *4*(5), 832-836.

Sauer, A., and Moraru, C. I. (2009). Inactivation of Escherichia coli ATCC 25922 and Escherichia coli O157: H7 in apple juice and apple cider, using pulsed light treatment. *Journal of Food Protection*, *72*(5), 937-944.

Sheikh, F. A., Barakat, N. A., Kanjwal, M. A., Chaudhari, A. A., Jung, I. H., Lee, J. H., and Kim, H. Y. (2009). Electrospun antimicrobial polyurethane nanofibers containing silver nanoparticles for biotechnological applications. *Macromolecular Research*, *17*(9), 688-696.

Sheikh, F. A., Cantu, T., Macossay, J., and Kim, H. (2011). Fabrication of poly (vinylidene fluoride)(PVDF) nanofibers containing nickel nanoparticles as future energy server materials. *Science of Advanced Materials*, *3*(2): 216-222.

Sheikh, F. A., Kanjwal, M. A., Saran, S., Chuny, W. J., and Kim, H. (2011). Polyurethane nanofibers containing copper nanoparticles as future materials. *Applied Surface Science*, *257*: 3020-3026.

Sheikh, F. A., Zargar, M. A., Tamboli, A. H., and Kim, H. (2016). A super hydrophilic modification of poly (vinylidene fluoride)(PVDF) nanofibers: By in situ hydrothermal approach. *Applied Surface Science*, *385*, 417-425.

Shin, H. S., Yang, H. J., Kim, S. B., and Lee, M. S. (2004). Mechanism of growth of colloidal silver nanoparticles stabilized by polyvinyl pyrrolidone in γ-irradiated silver nitrate solution. *Journal of Colloid and Interface Science*, *274*(1): 89-94.

Shornikova, O. N., Kogan, E. V., Sorokina, N. E., and Avdeev, V. V. (2008). The specific surface area and porous structure of graphite materials. *Physical Chemistry of Surface Phenomena*, *83*(6): 1161-1164.

Sibiya, P., and Moloto, M. 2014. Effect of precursor concentration and pH on the shape and size of starch capped silver selenide (Ag2Se) nanoparticles. *Chalcogenide Letter* 11: 577-588.

Šileikaitė, A., Prosyčevas, I., Puišo, J., Juraitis, A., and Guobienė, A. 2006. Analysis of silver nanoparticles produced by chemical reduction of silver salt solution. *Journal of Materials Science: Materials in Medicine, 12*: 287-291.

Singh, G., Patankar, R. B., and Gupta, V. K. (2010). The preparation of polymer/silver nanocomposites and application as an antibacterial material. *Polymer-Plastics Technology and Engineering, 49*(13), 1329-1333.

Sloan, M., and Farnsworth, S. (2006). Testing and evaluation of nanoparticle efficacy on E. coli and Bacillus Anthracis Spores. *NSTI-Nanotechnology, 1*: 595-598.

Souhaimi, M. K., and Matsuura, T. (2011). *Membrane distillation: principles and applications*. Elsevier.

Sousa, C. P. (2006). The versatile strategies of Escherichia coli pathotypes: a mini review. *Journal of Venomous Animals and Toxins incl Tropical Diseases, 12*(3): 363-373.

Sreekanth, D., Sivaramakrishna, D., Himabindu, V., and Anjaneyulu, Y. (2009). Thermophilic treatment of bulk drug pharmaceutical industrial wastewaters by using hybrid up flow anaerobic sludge blanket reactor. *Bioresource Technology, 100*(9), 2534-2539.

Sun, X., Dong, S., and Wang, E. (2004). One-step preparation and characterization of poly (propyleneimine) dendrimer-protected silver nanoclusters. *Macromolecules, 37*(19): 7105-7108.

Sun, D., Yu, J., An, W., Yang, M., Chen, G., and Zhang, S. (2013). Identification of causative compounds and microorganisms for musty odor occurrence in the Huangpu River, China. *Journal of Environmental Sciences, 25*(3):460-465.

Sundaray, B., Bossard, F., Latil, P., Orgéas, L., Sanchez, J., and Lepretre, J. (2013). Unusual process-induced curl and shrinkage of electrospun PVDF membranes. *Polymer, 54*(17), 4588-4593.

Suwatthanarak, T., Than-ardna, B., Danwanichakul, D., and Danwanichakul, P. (2016). Synthesis of silver nanoparticles in skim natural rubber latex at room temperature. *Materials Letters, 168*: 31-35.

Tajkarimi, M., Iyer, D., Tarrannum, M., Cunningham, Q., Sharpe, I., Harrison, S. H., and Graves, J. L. (2014). The effect of silver nanoparticles size and coating on Escherichia coli. *JSM Nanotechnology & Nanomedicine, 2*(2): 1025.

Tan, K., and Obendorf, S. K. (2007). Fabrication and evaluation of electrospun nanofibrous antimicrobial nylon 6 membranes. *Journal of Membrane Science, 305*: 287-298.

Tang, Z., Qiu, C., McCutcheon, J. R., Yoon, K., Ma, H., Fang, D., … Chu, B. (2009). Design and fabrication of electrospun poly(ether sulfone) nanofibrous scaffold for high-flux nanofiltration. *Journal of Polymer Science Part B-Polymer Physics, 47*: 2288-2300.

Tarasova, E., Tamberg, K.-G., Viirsalu, M., Savest, N., Gudkova, V., Krasnou, I., . . . Krumme, A. (2015). Formation of uniform PVDF fibers under ultrasound exposure in presence of anionic surfactant. *Journal of Electrostatics, 76*, 39-47.

Templeton, M. R., and Butler, P. D. (2011). *Introduction to Wastewater Treatment*: Bookboon.

Tidy, C. (12 December 2014) *E. coli and VTEC O157*. Retrieved from https://patient.info/in/health/e-coli-and-vtec-o157

Tien, D., Liao, C., Huang, J., Tseng, K., Lung, J., Tsung, T., . . . Yu, B. (2008). Novel technique for preparing a nano-silver water suspension by the arc-discharge method. *Reviews on Advanced Materials Science, 18*: 750-756.

Tien, D.-C., Chen, L.-C., Van Thai, N., and Ashraf, S. (2010). Study of Ag and Au Nanoparticles Synthesized by Arc Discharge in Deionized Water. *Journal of Nanomaterials, 2010*, 9.

Tiwari, D. K., Behari, J., and Sen, P. (2008). Application of nanoparticles in waste water treatment 1.

United State Food and Drug Administration. (2010). US food and drug administration.

Varner, K., Sanford, J., El-Badawy, A., Feldhake, D., and Venkatapathy, R. (2010). State of the science literature review: everything nanosilver and more. *US Environmental Protection Agency, Washington DC, 363*.

Varkey, A. J. (2010). Antibacterial properties of some metals and alloys in combating coliforms in contaminated water. *Scientific Research and Essays, 5*(24): 3834-3839.

Vatanpour, V., Madaeni, S. S., Rajabi, L., Zinadini, S., and Derakhshan, A. A. (2012). Boehmite nanoparticles as a new nanofiller for preparation of antifouling mixed matrix membranes. *Journal of Membrane Science, 401*: 132-143.

Vinu, A., Krithiga, T., Gokulakrishnan, N., Srinivasu, P., Anandan, S., Ariga, K., . . . Mori, T. (2007). Halogen-free acylation of toluene over FeSBA-1 molecular sieves. *Microporous and Mesoporous Materials, 100*(1): 87-94.

Viruses can turn harmless E. coli dangerous (22 April 2009). Retrieved 25 October 2017 from https://www.sciencedaily.com/releases/2009/04/090417195827.htm

Wang, C., Hsu, C. H., and Lin, J. H. (2006). Scaling laws in electrospinning of polystyrene solutions. *Macromolecules, 39*(22): 7662-7672.

Wang, H., Qiao, X., Chen, J., and Ding, S. (2005). Preparation of silver nanoparticles by chemical reduction method. *Colloids and Surfaces A: Physicochemical and Engineering Aspects, 256*(2–3): 111-115.

Wang, H., Qiao, X., Chen, J., Wang, X., and Ding, S. (2005). Mechanisms of PVP in the preparation of silver nanoparticles. *Materials Chemistry and Physics, 94*(2): 449-453.

Wang, M., Yang, G., Jin, P., Tang, H., Wang, H., and Chen, Y. (2016). Highly hydrophilic poly(vinylidene fluoride)/meso-titania hybrid mesoporous membrane for photocatalytic membrane reactor in water. *Scientific Reports, 6*: 19148.

Wang, S.-H., Wan, Y., Sun, B., Liu, L.-Z., and Xu, W. (2014). Mechanical and electrical properties of electrospun PVDF/MWCNT ultrafine fibers using rotating collector. *Nanoscale Research Letters, 9*(1), 522.

Warsinger, D. M., Chakraborty, S., Tow, E. W., Plumlee, M. H., Bellona, C., Loutatidou, S., . . . Ghassemi, A. (2018). A review of polymeric membranes and processes for potable water reuse. *Progress in Polymer Science*.

Water pollution. (2006). Retrieved 20 August 2018 from http://www.filterwater.com/t-articles.water-pollution.aspx

Wei, Z., Xia, T., Ma, J., Feng, W., Dai, J., Wang, Q., and Yan, P. (2007). Investigation of the lattice expansion for Ni nanoparticles. *Materials characterization, 58*(10), 1019-1024

World Health Organization (2013). Water quality and health strategy 2013-2020.

World Health Organization and UNICEF. (2017). Progress on drinking water, sanitation and hygiene: 2017 update and SDG baselines.

Xavier, M. G., and Banda, S. F. (2016). Specific surface area and porosity measurements of aluminosilicate adsorbents. *Oriental Journal of Chemistry, 32*(5): 2401-2406.

Yao, C., Li, X., Neoh, K. G., Shi, I., and Kang, E. T. (2008). Surface modification and antibacterial activity of electrospun polyurethane fibrous membranes with quaternary ammonium moieties. *Journal of Membrane Science, 320*: 259-267.

Zahid, M., Rashid, A., Akram, S., Rehan, Z. A., and Razzaq, W. (2018) A comprehensive review on polymeric nano-composite membranes for water wreatment. *Journal of Membrane Science Technology, 8*, 179.

Zeng, J., Xu, X., Chen, X., Liang, Q., Bian, X., Yang, L., and Jing, X. (2003). Biodegradable electrospun fibers for drug delivery. *Journal of Controlled Release, 92*: 227-231.

Zhang, H. (2013). *Application of silver nanoparticles in drinking water purification*. (PhD). University of Rhode Island.

Zhang, H., Zou, G., Liu, L., Tong, H., Li, Y., Bai, H., and Wu, A. (2017). Synthesis of silver nanoparticles using large-area arc discharge and its application in electronic packaging. *Journal of Materials Science, 52*(6), 3375-3387.

Zhang, W., Qiao, X., and Chen, J. (2007). Synthesis of silver nanoparticles—Effects of concerned parameters in water/oil microemulsion. *Materials Science and Engineering: B, 142*(1): 1-15.

Zhang, X.-F., Liu, Z.-G., Shen, W., and Gurunathan, S. (2016). Silver nanoparticles: synthesis, characterization, properties, applications, and therapeutic approaches. *International Journal of Molecular Sciences, 17*(9), 1534.

Zhang, Z., Zhao, B., and Hu, L. (1996). PVP protective mechanism of ultrafine silver powder synthesized by chemical reduction processes. *Journal of Solid State Chemistry, 121*(1): 105-110.

Zodrow, K., Brunet, L., Mahendra, S., Li, D., Zhang, A., Li, Q., and Alvarez, P. J. (2009). Polysulfone ultrafiltration membranes impregnated with silver nanoparticles show improved biofouling resistance and virus removal. *Water research, 43*(3): 715-723.

Zong, X., Kim, K., Fang, D., Ran, S., Hsiao, B. S., and Chu, B. (2002). Structure and process relationship of electrospun bioabsorbable nanofiber membranes. *Polymer, 43*: 4403-4412.

Zook, J. M., MacCuspie, R. I., Locascio, L. E., Halter, M. D., and Elliott, J. T. (2011). Stable nanoparticle aggregates/agglomerates of different sizes and the effect of their size on hemolytic cytotoxicity. *Nanotoxicology, 5*(4), 517-530.

LIST OF PUBLICATIONS AND PAPERS PRESENTED

Ahmad, N., Ang, B. C., Amalina, M. A., and Bong, C. W. Influence of precursor concentration and temperature on the formation of nanosilver in chemical reduction method. Sains Malaysiana. (Accepted for publication on 8 June 2017).